AD 427769

ASD-TDR-63-776
VOLUME I

UNCONVENTIONAL METHODS FOR INFLUENCING FLUID FLOW

TECHNICAL DOCUMENTARY REPORT No. ASD-TDR-63-776, VOL. I

NOVEMBER 1963

AF AERO-PROPULSION LABORATORY
RESEARCH AND TECHNOLOGY DIVISION
AIR FORCE SYSTEMS COMMAND
WRIGHT-PATTERSON AIR FORCE BASE, OHIO

Project No. 8169, Task No. 816904

(Prepared under Contract No. AF 33(657)-9914 by the Carnegie Institute of Technology, Department of Mechanical Engineering, Pittsburgh, Pennsylvania)

NOTICES

When Government drawings, specifications, or other data are used for any purpose other than in connection with a definitely related Government procurement operation, the United States Government thereby incurs no responsibility nor any obligation whatsoever; and the fact that the Government may have formulated, furnished, or in any way supplied the said drawings, specifications, or other data, is not to be regarded by implication or otherwise as in any manner licensing the holder or any other person or corporation, or conveying any rights or permission to manufacture, use, or sell any patented invention that may in any way be related thereto.

Qualified requesters may obtain copies of this report from the Defense Documentation Center (DDC), (formerly ASTIA), Cameron Station, Bldg. 5, 5010 Duke Street, Alexandria 4, Virginia

This report has been released to the Office of Technical Services, U.S. Department of Commerce, Washington 25, D.C., in stock quantities for sale to the general public.

Copies of this report should not be returned to the Aeronautical Systems Division unless return is required by security considerations, contractual obligations, or notice on a specific document.

300 - January 1964 - 162-41-300

FOREWORD

This is volume I (of three volumes) of the Phase I Final Report supported by the Air Force under Contract No. AF 33(657)-9914. This volume contains the results of a number of studies made by the senior investigators on this project. The second and third volumes contain detailed studies in the form of doctoral theses supervised by the senior investigators.

In this volume eleven investigations of effects capable of affecting fluid behavior are summarized. A list of the personnel associated with each investigation is given below. The first name in each case is the senior investigator responsible for the content of the section and the names in parenthesis are his co-workers.

Section 1	J. F. Osterle
" 2	J. F. Osterle (S. W. Angrist)
" 3	J. F. Osterle
" 4	W. T. Rouleau (J. L. McElroy, G. Mott)
" 5	F. J. Young (J. N. Murphy)
" 6	F. J. Young
" 7	S. W. Angrist (S. C. Y. Kuo)
" 8	S. W. Angrist
" 9	S. W. Angrist (S. C. Y. Kuo)
" 10	W. T. Rouleau (F. J. Young)

The present status of each study and the action that we recommend be taken for the future in each case is summarized as follows:

Section	Present Status	Desired Action
1	theory complete	experimentation
2	complete	termination
3	theory complete	experimentation
4	incomplete	continuation
5	incomplete	continuation
6	incomplete	continuation
7	complete	termination
8	incomplete	continuation
9	incomplete	continuation
10	incomplete	continuation

ABSTRACT

A number of related problems concerning the utilization of unconventional effects for the purpose of affecting the behavior of fluids are investigated. Effects capable of directly converting thermal or electrical power into pumping power without the use of moving mechanical parts are studied. A means of improving the thermoelectric cooling of liquids is investigated. A way of decontaminating fluids by an electrical effect is studied. Finally, a scheme for suppressing pressure surges in flowing fluids is examined.

This technical documentary report has been reviewed and is approved.

Marc P. Dunnam
Chief, Technical Support Division
Air Force Aero Propulsion Laboratory

TABLE OF CONTENTS

LIST OF ILLUSTRATIONS

Section 1

THERMAL PUMPING

1-1 Introduction

In this section an investigation is made of the feasibility of utilizing several physical effects to convert thermal energy (heat) directly into mechanical pumping energy (flow work) in a device free of moving parts. These effects include capillarity, osmosis, and thermal convection. In all cases the energy input is a flow of heat and the energy output is represented by a flow of fluid leaving the convertor at a higher pressure than it enters. The process undergone by the fluid after it leaves the convertor need not be specified but in this study for the sake of uniformity in evaluating the power output and efficiency we will in all cases assume that the fluid is used to power a reversible adiabatic turbine. The fluid will undergo a cycle passing from the convertor to the turbine and back to the converter again. The power output of the convertor will be the mechanical power developed by the turbine. The power input will, of course, be the heat input rate to the convertor.

1-2 Capillarity

The energy convertor utilizing the effect of capillarity which will be studied here is shown schematically in Figure 1-1. The evaporator contains a bank of n fine bore capillary tubes in parallel each of diameter d and submergence Δ. Let the pressure and temperature in the condenser be p_o and T_o where T_o is the saturation temperature corresponding to p_o. If the liquid level in the evaporator is maintained the same as in the condenser, the pressure p' of the liquid in the capillaries just below the liquid-vapor interface is given by

$$P' = P_o - \frac{32\mu}{d^2}\frac{1}{A}v'm \qquad (1-1)$$

where μ is the viscosity of the liquid, A the "open" cross-sectional area of the tube bank, v' the specific volume of the liquid and m the mass flow around the cycle. The second term on the right accounts for the viscous pressure drop in the capillary bank which will dominate the pressure losses anywhere else in the cycle. The pressure p_1 just above the liquid-vapor interface is given by the capillary relation

$$P_1 = P' + \frac{4\sigma}{d} \qquad (1-2)$$

Manuscript released by the authors August 1963 for publication as an ASD Technical Documentary Report.

where σ is the surface tension of the liquid in the presence of the vapor. This equation assumes a zero contact angle between the meniscus and the tube wall and consequently represents an upper bound on the pressure rise across the interface. The pressure difference available to the turbine is thus

$$\Delta P = P_1 - P_o = (\Delta P)_{max} - \frac{32\mu}{d^2}\frac{l}{A}v'm \qquad (1\text{-}3)$$

where

$$(\Delta P)_{max} = \frac{4\sigma}{d} \qquad (1\text{-}4)$$

the pressure available to the turbine if there was no frictional pressure drop in the capillaries. Now, if the pressure difference is reasonably small relative to p_o, it can be related to the corresponding temperature difference $T_1 - T_o$ by the Clapeyron equation.

$$\Delta P = \frac{L_o}{T_o v''}\Delta T \qquad (1\text{-}5)$$

where ΔT is $T_1 - T_o$, L_o the heat of vaporization of the fluid at T_o and v'' is the specific volume of the vapor at this temperature. Equation (1-3) can now be written in a more useful form as follows

$$\Delta P = \frac{L_o}{T_o v''}(\Delta T)_{max} - \frac{32\mu}{d^2}\frac{l}{A}v'm \qquad (1\text{-}6)$$

where $(\Delta P)_{max}$ is the value of ΔP from equation (1-5) corresponding to $(\Delta T)_{max}$. The power output from the turbine consistent with the assumption that Δp is small relative to p_o is given by

$$P = m v'' \Delta p \qquad (1\text{-}7)$$

The required heat input rate q_i to the liquid-vapor interface in the capillary chamber is given with sufficient accuracy by

$$q_i = \lambda \frac{A}{l}(\Delta T)_{max} + L_o m \qquad (1\text{-}8)$$

where λ is the thermal conductivity of the liquid. The first term on the right accounts for the unavoidable heat loss down the capillary tubes neglecting the conductivity of the tubes themselves. Actually it overestimates this heat loss since the actual ΔT is less than $(\Delta T)_{max}$ but this

error will turn out to be unimportant. The second term on the right evaluates the heat required to raise the liquid from T_o to T_1 and then to vaporize it. It represents a slight underestimate by an amount which is entirely negligible.

The thermal efficiency of this convertor is defined by

$$\eta = \frac{P}{q_i} \tag{1-9}$$

which from equation (1-6, 1-7, 1-8) can be written

$$\eta = \frac{m\left(\alpha \frac{(\Delta T)_{max}}{T_o} - Rm\right)}{C \frac{(\Delta T)_{max}}{T_o} + \alpha m} \tag{1-10}$$

This equation has been written in a generalized form which as we will see can be applied to all of the convertors studied in this section. The quantity α is a generalized coupling coefficient, coupling the mechanical to the thermal effects (in this case L_v), and R and C are generalized resistance and conductance coefficients, in this case given by the following equations

$$R = \frac{32 \mu l}{d^4 A} \nu \nu'' \tag{1-11}$$

$$C = \frac{\lambda A T_o}{l} \tag{1-12}$$

The quantities α, R and C will take on different values for the different convertors to be examined in this section but the form of equation (1-10) will remain the same.

Considering $(\Delta T/T_o)_{max}$ fixed, the optimum value of m in terms of maximizing the efficiency works out to be

$$(m)_{opt} = \frac{C(\Delta T)_{max}}{\alpha T_o}\left\{\sqrt{1+\beta} - 1\right\} \tag{1-13}$$

with β the "figure of merit" given by

$$\beta = \frac{\alpha^2}{RC} \tag{1-14}$$

which in this case becomes

$$\beta = \frac{L_o^2 d^2}{32 \mu \lambda T_o v' v''} \tag{1-15}$$

The corresponding maximum efficiency is given by

$$(\eta)_{max} = \frac{\sqrt{1+\beta} - 1}{\sqrt{1+\beta} + 1} \quad \frac{(\Delta T)_{max}}{T_o} \tag{1-16}$$

and is seen, of course, to be Carnot limited.

To obtain some idea as to the possible magnitude of the efficiency for this capillary convertor, consider the following example using water at P_o = 1 atm as the working fluid with the following properties:

$T_o = 100^oC$	$v' = 10^{-3}$ m^3/kgm	$\mu = 0.284$ newton sec/m^2
$L_o = 2.26$ megajoules/kgm	$v'' = 1.67$ m^3/kgm	$\lambda = 0.686$ watt/m^oC

Equation (1-15) yields $\beta = 1.3 \times 10^{15} d^2$ with d in meters. Taking 10^{-5} as the smallest practical value for d, β becomes 1.3×10^5 a very large number. From Equation (1-16) the maximum efficiency is seen to be essentially $(\Delta T/T_o)_{max}$, the Carnot value. In other words the dissipations associated with flow resistance and heat conduction are negligible if the flow is at or near the optimum value. For this condition of near reversible conversion, Equations (1-7), (1-5) and (1-16) can be combined to yield the approximate relation

$$(\eta)_{max} = \frac{4 \sigma v''}{d L_o} \tag{1-17}$$

For the example data above and a σ value of 50×10^{-3} newton/m, $(\Delta P)_{max}$ works out to be 0.20×10^5 newton/m^2 (about 0.20 atm.) and the corresponding $(\Delta T)_{max}$ to be 5.5°C. The thermal efficiency works out to be 1.48%.

Recognizing that β is much greater than unity, Equation (1-13) for the optimum flow rate can be reduced to

$$\frac{(m)_{opt.}}{A} = \frac{\sigma}{2 L_o} \sqrt{\frac{\lambda T_o v''}{2 \mu v'}} \tag{1-18}$$

which for the data above and an ℓ of 10^{-2}m yields a value of 0.061 kgm/m^2 sec for the optimum flow rate per unit open cross-sectional area of the capillary bank.

The results of this example and two others using different working fluids are summarized in Table 1-I.

Table 1-I. Comparison of Several Fluids

Fluid	T_o (°C)	$p_o \times 10^{-5}$ (newt/m^2)	$(\Delta p)_{max} \times 10^{-5}$ (newt/m^2)	$(\Delta T)_{max}$ (°C)	η (%)	$(m)_{opt}/\ell$ (kgm/m^2 sec)
H_2O	100	1.01	0.200	5.5	1.48	0.061
NH_3	20	8.60	0.084	0.3	0.11	0.010
Freon - 114	30	2.53	0.052	0.7	0.22	0.019

It would appear that water is the best of the three working fluids compared here, but it has one drawback relative to the refrigerants, namely, the very low pressure which would be required if the convertor were to be operated at near atmospheric temperature.

Although the pressure developed by this device is rather small, it can be increased by connecting a number of them in series as shown in Figure 1-2. The same flow passes through each member of the series but the total pressure rise is increased roughly by a factor equal to the number of stages. A three stage pump is shown in Figure 1-2. The relevant heat flows are indicated with the first subscript on q designating whether the heat is an input (i) or an output (o) and the second subscript designating the stage. We note that the heat rejected from the third stage condenser can be used to supply the necessary heat input to the first stage evaporator. No matter how many stages there are there must be two heat inputs of magnitude equal to the heat of vaporization, contrary to the conventional vapor power cycle case in which the heat of vaporization, contrary to the conventional vapor power cycle case in which the heat of vaporization is added only once. Thus, roughly speaking, the efficiency of this power generator would only be one-half that of the conventional vapor power cycle (such as the Rankine cycle) with which it competes. However, this staged capillary power generator has one advantage over the conventional vapor cycle machines in that it does not involve a pump with moving parts. Its main disadvantage, in addition to its halved efficiency, is the small amount of power it can deliver (due to its small flow rate) unless a great number of capillaries are used.

As an example of staging, we will consider water as the working fluid and again a capillary diameter of 10^{-3} m. For simplicity we will assume a constant value of 50×10^{-3} newton/m for the surface tension and take T_o to be 30°C ($p_o = 0.04 \times 10^5$ newton/m^2). The results of staging are given in Table 1-II.

Table 1-II. Staged Pressures and Temperatures For Water

$p_0 = 0.0$ .. 10^5 newt/m^2, $T_0 = 30^\circ C$
$p_1 = 0.24$, $T_1 = 64$
$p_2 = 0.44$, $T_2 = 78$
$p_3 = 0.64$, $T_3 = 88$
$p_4 = 0.84$, $T_4 = 95$
$p_5 = 1.04$, $T_5 = 101$

Thus in five stages the pressure is increased almost 1 atm. The work output from the turbine is equal to the isentropic enthalpy drop through it which works out to be 197 Btu/lb. The heat inputs to the fourth and fifth evaporators work out to be 900 and 980 Btu/lb. respectively. The thermal efficiency is thus 10%. This efficiency figure neglects the dissipations in each stage due to viscous friction and heat conduction which as we have seen is valid only if the flow rate is optimum. Since the flow cannot be optimum in all stages this efficiency will be somewhat high. For a Rankine cycle operating between the same pressures the work output would be the same but the heat input would be 1098 Btu/lb. (greater than 980 since heat would now be added from 30°C rather than from 95°C), yielding an efficiency of about 18%.

A staged capillary pump operating on Freon - 114 was developed by the Jet Propulsion Laboratory[1] for pressurizing gas bearings. Instead of capillary banks they used 12 inch long glass tubes of 3/8 inch ID, compactly filled with 0.0005 inch D glass fibers. They present experimental evidence to prove that the device actually does pump.

1-3 Osmosis

The energy convertor utilizing the effect of osmosis which will be studied here is shown schematically in Figure 1-3. The evaporator contains at its base a membrane of thickness t permeable to the solvent but not the solute in a dilute solution. For example, the solvent might be water and the solute sugar. The solution is confined to the liquid space above the membrane in the evaporator. The fluid everywhere else is pure solvent. Again let the pressure and temperature in the condenser be p_0 and T_0. In the evaporator the pressure exceeds that in the condenser by the osmotic pressure less the pressure drop through the membrane due to flow. Thus Equation (1-3) applies here as well with t replacing δ and d now an effective pore diameter, and where now

$$(\Delta P)_{max} = c \bar{R} T_0 \qquad (1\text{-}19)$$

the osmotic pressure in dilute solutions. In Equation (1-19), c is the molarity of the solution (gm solute/liter solution), $\bar{R}$ is the gas constant (8.314 joule/gm mole °K) and T_0 is the temperature of the membrane. If we confine ourselves to reasonably small osmotic pressures relative to p_0 (which follows from the

dilute solution assumption), Δp can again be related to the corresponding ΔT by the Clapeyron equation (1-5) so that equation (1-6) follows as before. Continuing to parallel the previous development we see that Equation (1-7) for the power output, (1-8) for the heat input rate to the liquid-vapor interface in the evaporator (1-9) for the thermal efficiency, (1-10), (1-11) and (1-12) are valid for this convertor also except that t replaces ℓ in Equation (1-11) for the resistance coefficient. The figure of merit for this osmotic convertor now becomes

$$\beta = \frac{L_o^2 d^2}{32 \mu \lambda T_o v' v''} \left(\frac{\ell}{t}\right) \tag{1-20}$$

differing from the result for the capillary convertor by the factor (ℓ/t).

Considering again p_o to be 1 atm. and taking water as the solvent, Equation (1-20) yields $\beta = 1.3 \times 10^5 d^2 \ell/t$. This time, however, d is much smaller than before. A typical semi-permeable membrane suitable for a sucrose-water solution is cellophane coated with copper ferrocyanide ($Cu_2Fe(CN)_6$). Data on this membrane are available[2]. From these data it can be shown that the effective d based on taking A to be the total surface area of the membrane and not just the "open" area, is on the order of 10^{-9} m. Taking ℓ/t to be 10^2, β works out to be about 1.3 and the corresponding maximum efficiency to be about 20% of Carnot. Due to this very small β value the optimum flow rate would correspondingly be very small relative to the capillary convertor. Thus it appears that the osmotic convertor is greatly inferior to the capillary device in regards to efficiency and flow rate. The only advantage the osmotic device has over the capillary convertor is its ability to develop substantial pressures in a single stage. For example a $(\Delta p)_{max}$ of 1 atm. can be developed with a concentration of only 0.03 gm mole/liter.

1-4 Free Convection

The phenomenon of free or natural convection is widely utilized (for example, in steam generators) to promote natural flow circulation in liquids. Our intention here is to determine the feasibility of using this phenomenon to pump liquids. The convertor to be studied is sketched in Figure 1-4. The tank on the left is maintained at a higher temperature (T_1) than the one on the right (T_2). By free convection the liquid will circulate clockwise. A hydraulic turbine is connected as shown to make use of the pressure differential and flow between the upper and lower downcomer tanks. The riser tank is connected to the two downcomer tanks by horizontal tubes of diameter d and length ℓ separated by a vertical distance H. The diameter of the tanks is much greater than d so that the dominant frictional pressure drop will occur in the tubes. There will also be heat transfer by conduction through these tubes from the riser tank to the downcomer tanks.

Considering laminar flow in the tubes since this will involve the least friction, the pressure differential available to the turbine is

$$\Delta P = \left(\frac{1}{v_0} - \frac{1}{v_1}\right) g H - \frac{64\mu}{d^2} \frac{l}{A} v_0 m \tag{1-21}$$

where v_0 and v_1 are the specific volumes of the liquid at T_0 and T_1 respectively, g is the acceleration of gravity, and again A is taken to be the cross-sectional area of the tube (or tubes if a bank of conduits in parallel is used). The second term on the right accounts as before for the frictional pressure drop in the tubes, the factor 64 a result of accounting simultaneously for the upper and lower tubes. The specific volume difference can conveniently be expressed in terms of the expansivity ϵ of the fluid as follows

$$\epsilon = \frac{1}{v}\left(\frac{\partial v}{\partial T}\right)_p \doteq \frac{1}{v_0} \frac{v_1 - v_0}{T_1 - T_0} \tag{1-22}$$

so that Equation (1-21) can be written

$$\Delta P = \frac{g H \epsilon}{v_0} \Delta T - \frac{64\mu}{d^2} \frac{l}{A} v_0 m \tag{1-23}$$

where, of course, $\Delta T = T_1 - T_0$.

The necessary heat exchanges are as indicated in the figure. The heat fluxes q' and q" are equal in magnitude; and if we assume a regenerator of effectiveness e operating between these conduits, the input heat q' is given by

$$q' = m \bar{c} (1 - e) \Delta T \tag{1-24}$$

where $\bar{c}$ is the specific heat of the fluid. The heat flux q_i is necessary even though the temperature remains constant in the riser tank due to conduction through the tubes and the fact that the enthalpy of the fluid changes with pressure. It can be shown that

$$q_i = g H \epsilon T_1 m + 2\lambda \frac{A}{l} \Delta T \tag{1-25}$$

where the first term accounts for the enthalpy change with pressure and the second term accounts for conduction.

If, for the time being, we assume the regenerator mentioned above to be perfectly effective (e = 1), the total required heat input rate is q_i and the efficiency becomes

$$\eta = \frac{m v_0 \Delta P}{q_4} \tag{1-26}$$

which by Equations (1-23) and (1-25) can be written in the generalized form of Equation (1-10)

$$\eta = \frac{m\left(\alpha \frac{\Delta T}{T} - Rm\right)}{C \frac{\Delta T}{T} + \alpha m} \tag{1-27}$$

where, in this case,

$$\alpha = g H \epsilon T_1 \tag{1-28}$$

$$R = \frac{64 \mu}{d^2} \frac{l}{A} v_0^2 \tag{1-29}$$

$$C = 2 \frac{\lambda A T_1}{l} \tag{1-30}$$

The efficiency is again given by Equation (1-16)

$$\eta = \frac{\sqrt{1+\beta} - 1}{\sqrt{1+\beta} + 1} \frac{\Delta T}{T_1} \tag{1-31}$$

where now

$$\beta = \left(\frac{g H \epsilon d}{v_0}\right)^2 \frac{T_1}{128 \mu \lambda} \tag{1-32}$$

To obtain some idea as to the possible magnitude of the efficiency for this convection converter we will consider water and mercury as representative working fluids. The appropriate properties and data are listed in Table I-III.

Table 1-III. Properties of Water and Mercury

	water	mercury
expansivity ($^\circ K^{-1}$)	0.20×10^{-3}	0.19×10^{-3}
density (kgm/m^3)	10^3	13.6×10^3
viscosity (newt sec/m^2)	10^{-3}	1.5×10^{-3}
thermal conductivity (watt/$m^\circ K$)	0.6	8.0
high temperature ($^\circ K$)	373	450
low temperature ($^\circ K$)	273	300

The resulting expressions for B are

$$B = 18{,}700\ H^2 d^2 \quad \text{for water}$$

$$B = 188{,}000\ H^2 d^2 \quad \text{for mercury}$$

It appears, therefore, that a large H would be desirable (which is to be expected) and also a large tube diameter. The tube diameter, however, is limited to values for which the flow will be laminar. The flow in the tubes will be laminar only if the Reynolds number is appropriately small. The Reynolds number is defined by $Re = md/A\mu$ and will have its greatest value when m has its greatest value. From Equation (1-23) we see that the maximum m corresponds to vanishing pressure differential and thus is given by

$$(m)_{max} = \frac{g H \epsilon d^2 A \Delta T}{64 \mu l v_0^2} \tag{1-33}$$

The corresponding Reynolds number which is now really a Grashoff number becomes

$$Gr = \frac{G H \epsilon d^3 \Delta T}{64 l \mu^2 v_0^2} \tag{1-34}$$

For our representative fluids

$$Gr = 3 \times 10^4\ Hd^3/l \quad \text{for water}$$

$$Gr = 3.6 \times 10^{11}\ Hd^3/l \quad \text{for mercury}$$

In the interest of reasonable physical size we will arbitrarily set H and l equal to 1 meter. Letting d equal 10^{-2} m for water and 2×10^{-3} m for mercury the Grashoff numbers become 3000 and 2880 respectively. We will assume that at these Grashoff numbers the flow in the tubes is still laminar but just barely so. Thus the diameter figures quoted above represent the maximums allowable for our assumed operating conditions. It appears then that very small tubes are necessary which will necessitate tube banks if a practical amount of flow is to be provided.

The figures of merit for these dimensions are 1.37 for water and 0.752 for mercury and the corresponding thermal efficiencies work out to be 0.9% for water and 4.6% for mercury. Unfortunately, these figures are not realistic since they are based on the regenerator effectiveness being unity and it turns out that even small deviations from unity result in drastic reductions in thermal efficiency. For example, even if ϵ is as high as 0.99 the q_1 term completely dominates the q_i term and the thermal efficiencies assume the form

$$\eta = \frac{v_0 \Delta P}{\bar{c}(1-\epsilon)\Delta T} \tag{1-35}$$

which from Equation (1-23) neglecting friction entirely reduces to

$$\eta = \frac{g H \epsilon}{\bar{c}(1-\epsilon)} . \tag{1-36}$$

Now, the specific heats of water and mercury are about 4200 and 140 joule/kg-m°K respectively, resulting in efficiencies of roughly 5×10^{-5} and 10^{-3} respectively for an ϵ of 0.99.

Thus, it appears that pumping by the mechanism of free convection is completely impractical from an efficiency point of view and could only become practical if some form of artificial gravity of very high intensity (say, 10^4 g) were available. The conclusion with respect to pumping gases by this means is the same.

1-5 Conclusions

It is our feeling that of the three effects considered in this section only one, the capillarity convertor, is worth further consideration. We would like to extend our theoretical analysis of this device and to undertake an experimental investigation of it.

References

1. Research Summary No. 36-10, Jet Propulsion Laboratory, Pasadena, California, September 1, 1961.

2. R. Haase, "Thermoosmose in Flussigkeiten," Zeitschrift fur Physikalische Chemie Frankfurt, 21-22, p. 244 (1959).

Nomenclature

A = open cross-sectional area of tube bank, m^2

c = molarity of solution, gm solute/liter solution

$\bar{c}$ = specific heat of fluid, joule/kgm$^\circ$K

C = thermal conductance of fluid, joule/sec

d = tube diameter, m

e = effectiveness of regenerator

g = acceleration of gravity, m/sec^2

Gr = Grashoff number

H = height of riser tank, m

L = length of tubes or depth of solution, m

L = heat of vaporization of fluid, joule/kgm

m = mass flow rate, kgm/sec

n = number of tubes in tube bank

p = fluid pressure, newt/m^2

P = power output of turbine, joule/sec

q = heat flux rate, joule/sec

R = viscous resistance of fluid, joule sec/m^3

$\bar{R}$ = gas constant, joule/kgm mole$^\circ$K

Re = Reynolds number

t = thickness of membrane, m

T = fluid temperature, $^\circ$K

v = specific volume of fluid, m^3/kgm

α = coupling coefficient, joule/kgm

β = figure of merit of convertor

ϵ = expansivity of fluid, $^\circ F^{-1}$

η = thermal efficiency of convertor

λ = thermal conductivity of fluid, watt/$m^{o}K$

μ = viscosity of fluid, newt sec/m^2

σ = surface tension of liquid, newt/m

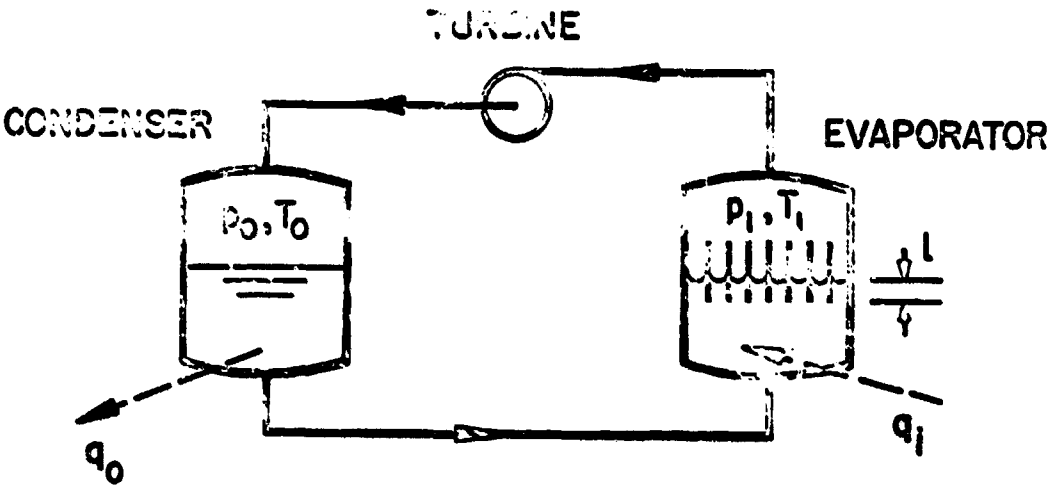

Figure 1-1. Schematic of Single-Stage Capillary Convertor

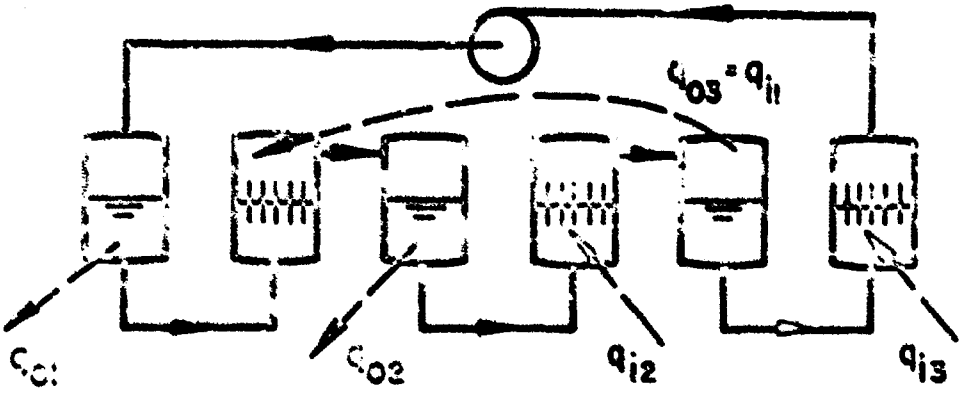

Figure 1-2. Schematic of Triple-Stage Capillary Convertor

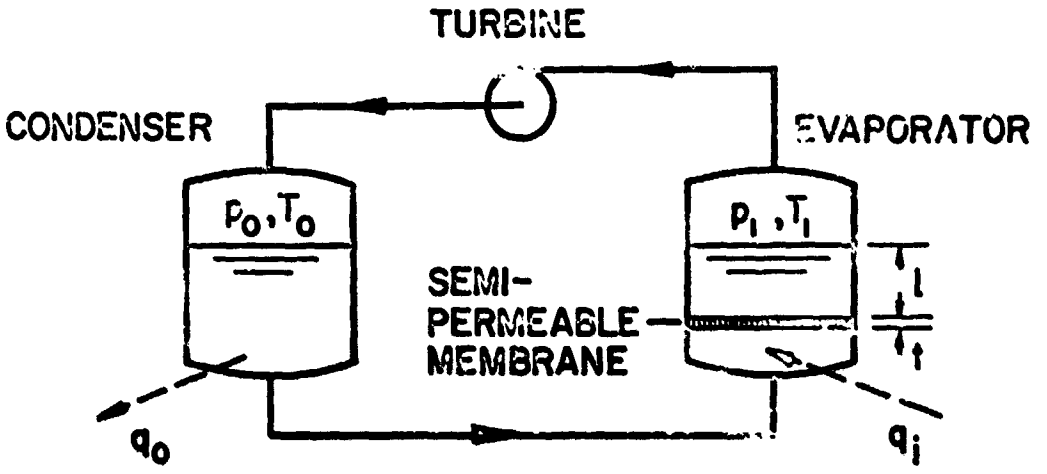

Figure 1-3. Schematic of Osmosis Convertor

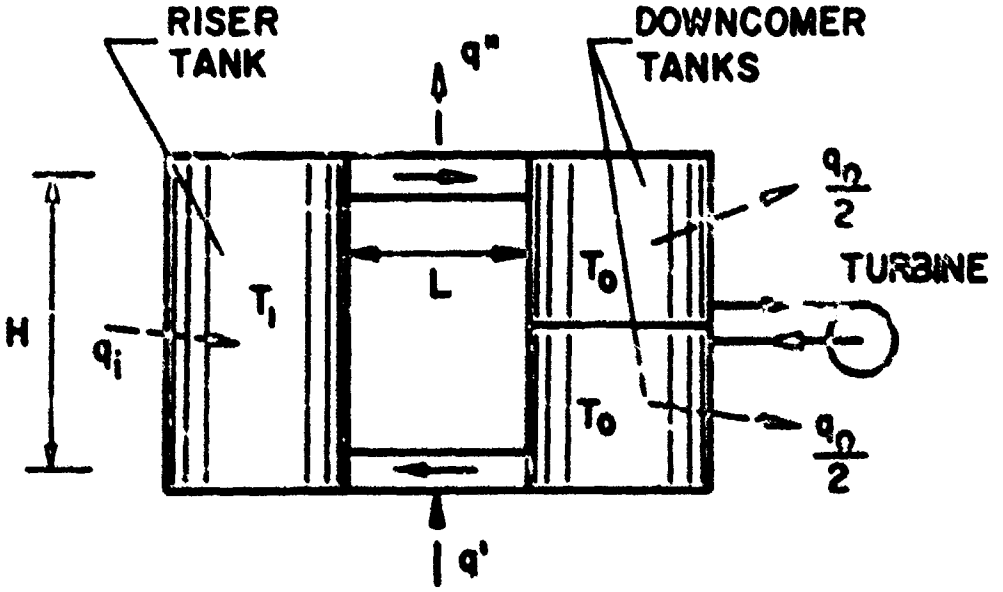

Figure 1-4. Schematic of Convection Convertor

Section 2

THERMOELECTRIC-HYDROMAGNETIC PUMPING

2-1 Introduction

By maintaining the junctions of a circuit made up of two dissimilar materials at different temperatures, a current is caused to flow in the circuit by the thermoelectric effect. In a recent publication[1] Rex proposed using this effect to pump liquid metals hydromagnetically. In his proposal, the walls of a channel of rectangular cross-section constitute one leg of a thermoelectric circuit and the liquid flowing in the channel the other. Two opposite walls of the channel are insulated from the field while the other two walls are not. If one of these latter two walls is heated and the other cooled, a thermoelectric current is generated which would pass through the fluid across the channel between the heated and the cooled walls. If now a magnetic field is impressed across the channel between the insulated walls, it will interact with the thermoelectric current to produce a Lorentz body force on the fluid directed along the channel. Thus, a thermoelectrically powered hydromagnetic pump has been constructed. This pump differs from conventional hydromagnetic pumps in that the current is obtained from a thermoelectric circuit composed of the channel walls and the fluid being pumped rather than from an external power supply. The energy input is thus thermal rather than electrical. It is obvious from the brief description given above that the merits of such a pump will be greatly dependent on the materials selected for its construction and on the fluid which is pumped. The performance of Rex's pump was particularly poor because he selected iron for the pump walls. In addition to leading the magnetic lines of force around the fluid and thus diminishing the Lorentz force to a negligible value, iron has a very small Seebeck coefficient. The low Seebeck coefficient will produce a small current further reducing the pump's output.

We will extend Rex's work by deriving an expression for pump efficiency which he did not do, and by optimizing pump geometry. Furthermore we will show the importance of material selection on pump performance by considering both metal and semiconducting walls.

2-2 The analysis of the Pump

Figure 2-1 shows a schematic of a hydromagnetic pump. For the moment we assume that the transverse electric current is supplied by an external current source. The transverse magnetic field is in the $+y$ direction and the electric current is in the z direction. Flow is in $+x$ direction. In our analysis of the hydromagnetic pump we assume the following:

(1) The Hall effect is negligible.
(2) There is no frictional pressure drop in the pump.
(3) The horizontal walls of the pump channel are electrically conducting
(4) The inner vertical walls of the pump channel are electrically insulated.

We now write Ohm's law for a conducting fluid in a magnetic field as

$$j_z = \sigma (E_z + u B) \tag{2-1}$$

and the electric current may be expressed in terms of the current density as

$$I = - j_z w l \tag{2-2}$$

while the electric field is given by

$$E_z = - \frac{\Delta V}{h} \tag{2-3}$$

The volume rate of flow through the pump is simply the velocity times the cross sectional area

$$Q = w h u \tag{2-4}$$

Combining Equations (2-1), (2-2), (2-3) and (2-4) we obtain an expression for the electric current where we have replaced the conductivity with its reciprocal, the resistivity

$$I = \frac{l w}{\rho h} \Delta V - \frac{l B}{\rho h} Q \tag{2-5}$$

which may be rearranged in favor of the voltage to yield

$$\Delta V = R_i I + \left(\frac{B}{w}\right) Q \tag{2-6}$$

where $R_i = h\rho_i/(lw)$ the electrical resistance of the fluid.
We may now write the force equation which balances the pressure rise per unit length in the pump against the Lorentz force as

$$- \Delta P / l - j_z B = 0$$

or

$$\Delta P = \left(\frac{B}{w}\right) I \tag{2-7}$$

Let us now consider the thermoelectrically powered hydromagnetic pump. We replace the battery with a heat source along the bottom of the channel and

a heat sink along the top. The thermoelectric current now passes through the fluid and the walls as is shown in Figure 2-2. We make two further assumptions:

(5) The Peltier heat is negligible.
(6) The Joule heat generated in both the walls and the fluid is dissipated to the atmosphere.

The voltage impressed on the fluid by the thermoelectric effect is the Seebeck voltage minus the voltage drop in the walls, thus

$$\Delta V = \alpha \Delta T - I R_o \tag{2-8}$$

where the wall resistance is $R_o = h\rho_o/(2t\ell)$. The heat transfer across the device is

$$q = K \Delta T \tag{2-9}$$

where K is the thermal conductance of the fluid plus the thermal conductance of the walls. The fluid thermal conductance is $K_i = \lambda_i w\ell/h$ and the wall thermal conductance is $K_o = \lambda_o 2t\ell/h$.

The voltage across the fluid required by the hydromagnetic effect (Equation 2-6) in the fluid must match the voltage due to the thermoelectric effect (Equation 2-8), thus

$$R_i I + \left(\frac{B}{w}\right) Q = \alpha \Delta T - I R_o$$

or in terms of the current

$$I = \frac{\alpha \Delta T - \left(\frac{B}{w}\right) Q}{R} \tag{2-10}$$

where $R = R_o + R_i$. We may now substitute Equation (2-10) into Equation (2-7)

$$\Delta P = \frac{B}{w}\left\{\frac{\alpha \Delta T - \left(\frac{B}{w}\right) Q}{R}\right\} \tag{2-11}$$

The pumping power output is the product of the pressure rise and the volume flow rate, thus

$$P = Q \Delta P = \frac{BQ}{wR}\left\{\alpha \Delta T - \left(\frac{B}{w}\right) Q\right\} \tag{2-12}$$

we may now find the flow rate that maximizes the power output by taking the derivative of Equation (2-12) with respect to Q and setting it equal to zero to obtain

$$Q^* = \frac{\alpha \Delta T w}{2 B} \tag{2-13}$$

Upon substituting Equation (2-13) into Equation (2-12) we obtain the maximum pumping power for a given value of R

$$P_{max} = \frac{(\alpha \Delta T)^2}{4 R} \tag{2-14}$$

and the corresponding thermal efficiency is obtained by combining Equation (2-14) and Equation (2-9)

$$\eta = \frac{P_{max}}{q} = \frac{\alpha^2 \Delta T}{4 R K} \tag{2-15}$$

This is the same result that is obtained for a thermoelectric generator operating at maximum power. This is to be expected as the hydromagnetic part of the pump adds no additional dissipation and we have neglected friction. We may further increase the thermal efficiency by making the RK product as small as possible. We form the RK product as follows:

$$RK = \left(\frac{h \rho_0}{2 t l} + \frac{l \rho_1}{l w}\right)\left(\frac{2 \lambda_0 t l}{h} + \frac{\lambda_1 w l}{h}\right) \tag{2-16}$$

and take the derivative of it with respect to $(2t/w)$ and set the result equal to zero to obtain

$$\left(\frac{2t}{w}\right)^* = \sqrt{\frac{\lambda_1 \rho_0}{\lambda_0 \rho_1}} \tag{2-17}$$

so that

$$(RK)_{min} = \left\{(\lambda_0 \rho_0)^{\frac{1}{2}} + (\lambda_1 \rho_1)^{\frac{1}{2}}\right\}^2 \tag{2-18}$$

We may now find the optimum values for the electrical resistance and thermal conductance by starting with their definitions

$$R = R_i \left(1 + \frac{R_o}{R_i}\right) \quad , \qquad K = K_i \left(1 + \frac{K_o}{K_i}\right)$$

and then substituting the definitions for R_i, R_o, K_i and K_o. The optimum value of (2t/w) can then be placed in the results to obtain

$$R^* = R_i \left(1 + \sqrt{\frac{\lambda_o \rho_o}{\lambda_i \rho_i}}\right) \tag{2-19}$$

and

$$K^* = K_i \left(1 + \sqrt{\frac{\lambda_o \rho_o}{\lambda_i \rho_i}}\right) \tag{2-20}$$

The maximum efficiency may now be found by substituting the minimum value for the RK product in the efficiency expression for maximum pumping power

$$\eta_{max} = \frac{\alpha^2 \Delta T}{(RK)_{min}} = \frac{\alpha^2 \Delta T}{4\left\{\sqrt{\lambda_o l_o} + \sqrt{\lambda_i \rho_i}\right\}^2} \tag{2-21}$$

The shut-off or zero flow pressure rise can be found by setting Q = 0 in Equation (2-11) to obtain

$$(\Delta P)_{Q=0} = \frac{B \alpha \Delta T}{w R} \tag{2-22}$$

and the short circuit or zero pressure rise flow can be found by setting $\Delta p = 0$ in equation (2-11)

$$(Q)_{\Delta p=0} = \frac{w \alpha \Delta T}{B} \tag{2-23}$$

The pressure rise that is obtained at maximum efficiency is obtained by setting $R = R^*$ in Equation (2-22) as defined by Equation (2-19).

We note that the pressure rise is linearly dependent on B while the flow rate is inversely dependent. Thus the maximum pumping power and hence

efficiency is independent of B under our assumptions. We further note that optimum pressure rise for maximum power output is one-half the zero flow pressure rise while the optimum flow rate is one-half the zero pressure rise flow rate.

2-3 A Metal Wall Pump

For our first example we choose a pump that uses walls made of constantan (60 Cu, 40 Ni) which is used to pump sodium. We assume a temperature difference of 300°C (100°C to 400°C). The constantan has the following properties[2] evaluated at the average temperature 250°C:

$$\alpha_o = -60 \times 10^{-6} \text{ volts/°C}$$
$$\rho_o = 44 \times 10^{-6} \text{ ohm-cm}$$
$$\lambda_o = 0.27 \text{ watts cm}^{-1}\text{-°K}^{-1}$$

This yields a thermoelectric figure of merit ($\alpha^2/\lambda\rho$) of 3.0×10^{-4} $(°K)^{-1}$ at 250°C.

The sodium is assumed to have the following properties:

$$\alpha_i = \text{negligible}$$
$$\rho_i = 10 \times 10^{-6} \text{ ohm-cm}$$
$$\lambda_i = 0.83 \text{ watts cm}^{-1}\text{-°K}^{-1}$$

For our pump geometry and magnetic flux density we assume the following

$$w = 1 \text{ cm}$$
$$h = 3 \text{ cm}$$
$$\ell = 5 \text{ cm}$$
$$B = 3 \text{ kilogauss}$$

For the assumed properties the pump has an optimum resistance of 13.2×10^{-6} ohms and an optimum thermal conductance of 3.05 watt/°K. Using these values we find a zero flow pressure rise of 0.40 atmosphere (5.8 psi) and a zero pressure rise flow of 0.6 liters/sec (1.27 ft³/min). The maximum pumping power is 6.2 watts and the energy supplied is 915 watts. The thermal efficiency for this device is 0.67 per cent. The optimum wall thickness, t, is 1.84 cm (0.72 inches). This pump represents at least a 50 per cent improvement in performance over the one proposed by Rex.

2-4 A Semiconductor Wall Pump

Considerable improvement in pump performance can be made by choosing a material with even better thermoelectric properties than constantan. Those semiconductors which have found application in power generation appear to be the most likely candidates to contribute to more efficient pumps. A material which appears promising in this respect is the ternary compound $AgSbTe_2$ which

has been examined by Rosi, Hockings and Lindenblad[3]. Using the same temperature difference as in the metal wall case the material has the following average properties.

$$\alpha_o = +240 \times 10^{-6} \text{ volts/}^\circ\text{C}$$
$$\rho_o = 4.5 \times 10^{-3} \text{ ohm-cm}$$
$$\lambda_o = 7.1 \times 10^{-3} \text{ watts-cm}^{-1}\text{-}^\circ\text{K}^{-1}$$

This gives a thermoelectric figure of merit $(\alpha^2/\lambda\rho)$ of 1.8×10^{-3} $(^\circ\text{K})^{-1}$ at 250°C.

Using the same geometry, magnetic flux density and properties for the sodium we may now calculate the performance of this pump. We begin by calculating the optimum wall thickness to channel width ratio. In this case it is

$$\left(\frac{2t}{w}\right)^* = 230$$

which is a completely unrealistic answer. This would require a wall thickness of 115 cm on each side of a 1 cm channel! Nevertheless if we could build such a pump, we would find a shut off pressure of 1.22 atm (18 psi) and a zero pressure rise flow of 7.2 liters/sec (15.2 ft³/min). The thermal efficiency is 5.89 per cent. We examine the effect of wall thickness on shut off pressure, pumping power and thermal efficiency in Figure 2-3. We note that performance becomes particularly poor when wall thickness drops down to a centimeter or so. It is interesting to note that if we make the walls 1.84 cm thick which is the same thickness as was found to be optimum in the constantan case, the semiconductor pump is less efficient and has a lower shut off pressure. Regardless of wall thickness, however, the flow rate is greatly improved by going to a semiconductor wall, in fact it improves in our example nearly 1200 per cent. Lower $(2t/w)^*$ ratios would be obtained if the fluid and the pump wall material did not have such disparate properties. This situation would exist, for example, if we were to consider the pumping of liquid semiconductors such as molten salts.

As in the case of the thermoelectric generator the pump efficiency is also directly related to the overall figure or merit of the fluid-wall combination.

2-5 Conclusion

Pump performance is improved considerably by choosing materials with high indexes of performance such as a metal like constantan or a semiconductor. When the fluid properties are greatly different from the wall properties then unrealistic values for the optimum wall thickness to channel width ratio are obtained. This type of pump might find application in a situation where contamination of the pump or the fluid must be avoided and where large heat fluxes are economically available such as around nuclear reactors. Because it has no moving parts, it would always be available for pumping the heat transfer fluid in case of a reactor emergency.

References

1. Von Dietrich Rex, "Thermoelektrische Pumpen für flüssige Metalle," VDI-Z, Vol. 103, No. 1, 1961, p. 17.

2. Handbook of Physics and Chemistry, 40th ed., Chemical Rubber Publishing Co., Cleveland, Ohio, 1958.

3. F. D. Rosi, E. F. Hockings, and N. E. Lindenblad, "Semiconducting Materials for Thermoelectric Power Generation," RCA Review, Vol. XXII, No. 1, March, 1961, p. 82.

Nomenclature

B = magnetic flux density, gauss

E = electric field, volts/cm

h = pump channel height, cm

I = electric current, amps

j = electric current density, amps/cm^2

K = thermal conductance, watts/deg C

ℓ = pump channel length, cm

p = pressure, dynes/cm^2

P = pumping power, watts

q = heat transfer, watts

Q = flow rate, liters/sec

R = electrical resistance, ohms

t = channel wall thickness, cm

T = temperature, deg C

u = fluid velocity, cm/sec

V = voltage

w = pump channel width, cm

x = coordinate in the direction of fluid flow

y = coordinate in direction of magnetic field

z = coordinate in direction of electric current flow

α = Seebeck coefficient, volts/deg C

Δ = increment

η = thermal efficiency

λ = thermal conductivity, watts/cm-deg C

ρ = electrical resistivity, ohm-cm

σ = electrical conductivity, $(ohm\text{-}cm)^{-1}$

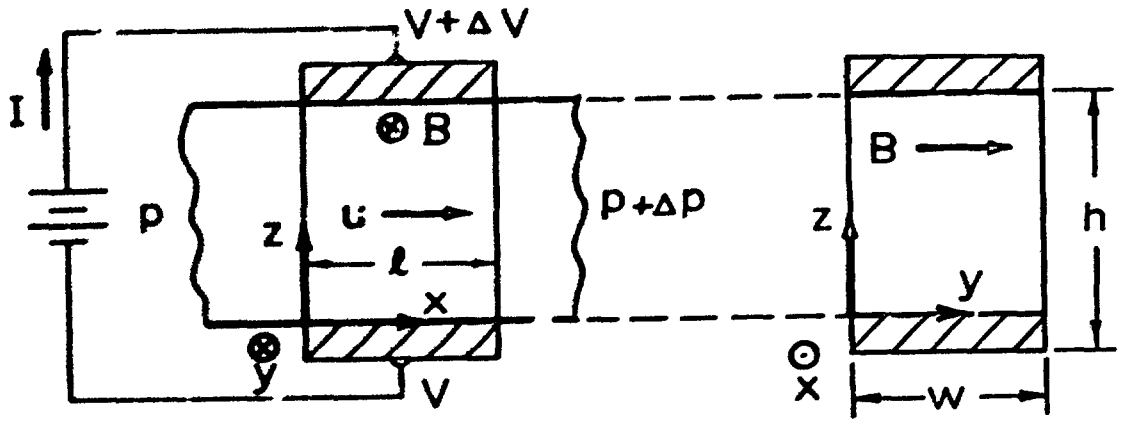

Figure 2-1. The Hydromagnetic Pump

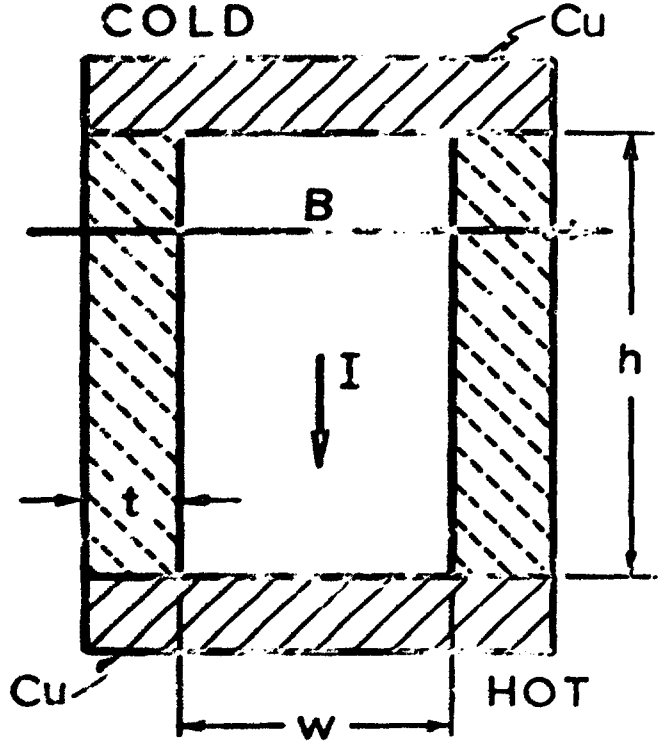

Figure 2-2. The Thermoelectric-Hydromagnetic Pump

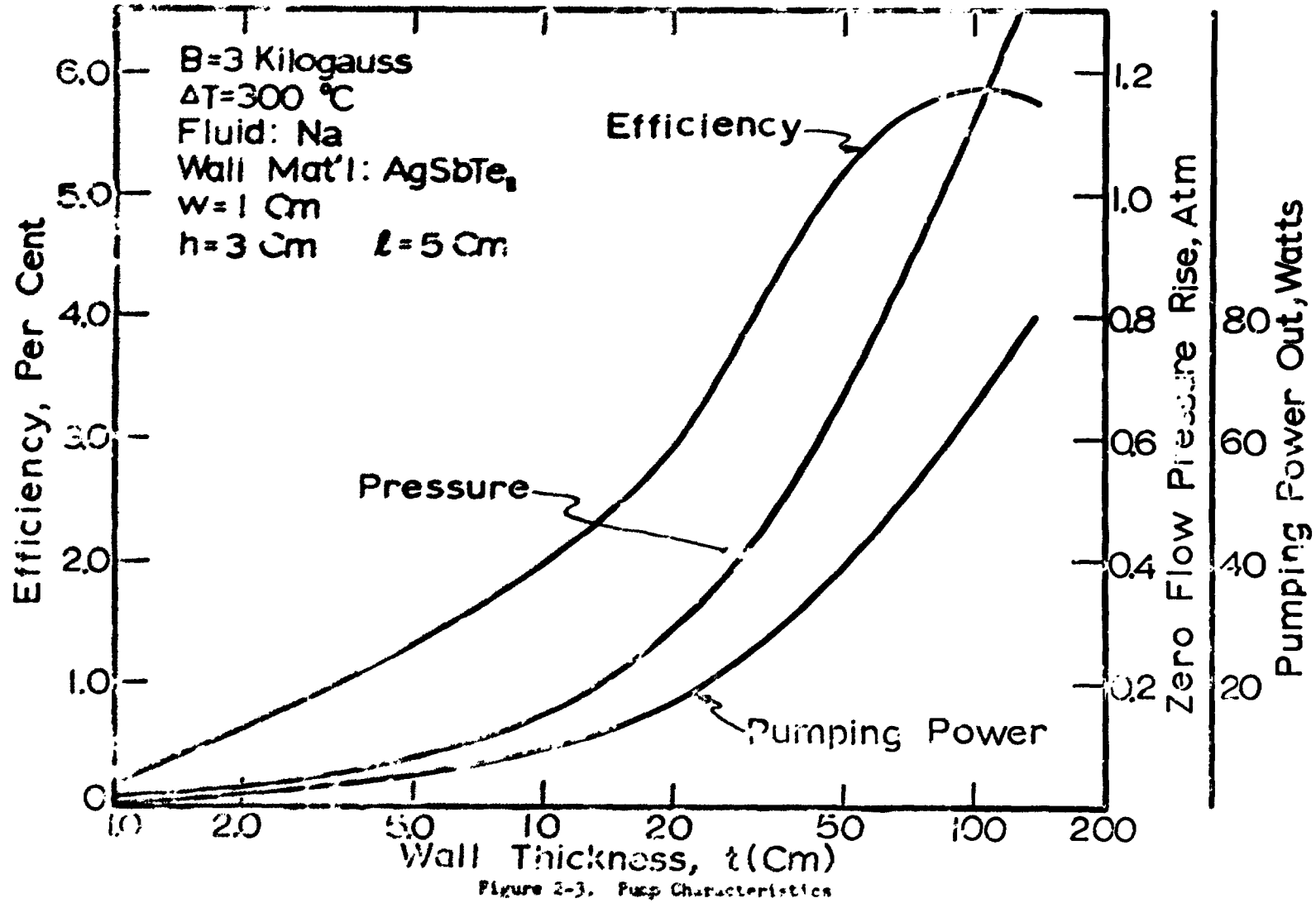

Figure 2-3. Pump Characteristics

Section 3

ELECTROKINETIC ENERGY CONVERSION

3-1 Introduction

When an electric field is impressed on a fluid electrolyte in a fine capillary tube and no flow is permitted, a pressure differential appears between the ends of the tube. Conversely, when a pressure gradient is impressed on the fluid and no electrical current is permitted, an electrical potential difference appears. These are the so-called electrokinetic effects first studied in any detail by Helmholtz in 1879[1]. In the first of these effects if flow is permitted, a conversion of electrical into pumping power can occur and in the second if current is permitted, the reverse conversion of pumping into electrical power can occur. We are interested in the thermodynamics of these energy conversions.

The electrokinetic effects are believed to be brought about by the mechanism of selective ion absorption on the tube wall leaving a net charge density in the bulk fluid. The electric field acting on this net charge develops a body force which acts counter to the pressure force. In this mechanism the applied voltage "induces" a pressure differential in the pumping mode and the applied pressure "induces" a voltage differential in the generation mode.

It is the purpose of this section to present an analysis of electrokinetic energy conversion to establish the feasibility of operating devices on this principle to either pump fluids or generate electrical power.

3-2 The Pumping Mode

A schematic of the electrokinetic energy convertor to be studied (in steady-state operation) in this section is shown in Figure 3-1. It is shown converting electrical power to pumping power (the pumping mode). The reverse conversion (generation mode) will be considered later.

The tube bank consists of n parallel fine bore capillary tubes of length ℓ and inside radius r_o. Porous electrodes are placed at either end of the tube bank and connected externally to a power supply (perhaps a d.c. generator as shown) which maintains a higher voltage on the left electrode than on the right. In the reverse conversion, of course, the generator would act as a motor. Fluid flows through the tube bank from left to right at a volume flow rate v; leaving at a higher pressure than it enters.

Let the selective ion absorption mechanism establish a charge density ρ within the tubes all of which are assumed to behave identically. The charge density will be a function of r the radial position within the individual tubes. If the tube walls remove more negative ions than positive, the charge density will be positive and vice versa.

If laminar flow is assumed in the tubes (to be verified later), the following momentum equation must be satisfied

$$-\frac{dP}{dx} + \rho E + \frac{1}{r}\frac{d}{dr}\left(\mu r \frac{du}{dr}\right) = 0 \tag{3-1}$$

where x is the axial position in the tube (measured from the left end of the tube bank), r the radial position, p the fluid pressure, E the electric field, μ the fluid viscosity, and u the fluid velocity in the x direction.

The charge density is related to the electrical potential φ in the fluid by Poisson's equation

$$\rho = -\epsilon \nabla^2 \varphi \tag{3-2}$$

where ϵ is the permittivity of the fluid. If ρ is assumed independent of x, then φ must be of the form

$$\varphi = \frac{l - x}{l} \Delta\varphi + \psi(r) \tag{3-3}$$

which stipulates a linear variation of φ with x but does not restrict its r variation. Equation (3-2) now yields

$$\rho = -\epsilon \frac{1}{r}\frac{d}{dr}\left(r \frac{d\psi}{dr}\right) \tag{3-4}$$

The electric field is given by

$$E = -\frac{\partial\varphi}{\partial x} = \frac{\Delta\varphi}{l} \tag{3-5}$$

Substituting equations (3-4) and (3-5) into equation (3-1) there results

$$\frac{d}{dr}\left\{r\frac{d}{dr}\left(\mu u - \frac{\epsilon\Delta\varphi}{l}\psi\right)\right\} = r\frac{dP}{dx} \tag{3-6}$$

Integrating equation (3-6) once with respect to r and using the fact that u and ψ are both radially symmetric to eliminate the integration constant we obtain

$$\frac{d}{dr}\left(\mu u - \frac{\epsilon\Delta\varphi}{l}\psi\right) = \frac{r}{2}\frac{dP}{dx} \tag{3-7}$$

Integrating again with respect to r there results

$$\mu u - \frac{\epsilon \Delta\varphi}{l}\psi = \frac{r^2}{4}\frac{dP}{dx} + C_1 \tag{3-8}$$

The integration constant C_1 can be evaluated from the condition that the velocity on the wall is zero. Thus

$$u = \frac{r^2 - r_0^2}{4\mu}\frac{dP}{dx} + \frac{\epsilon \Delta\varphi}{\mu l}(\psi - \psi_0) \tag{3-9}$$

where ψ_0 is the value of ψ on the tube wall.

The flow rate through the tube bank is found by integrating Equation (3-9) according to the definition

$$v \equiv 2\pi n \int_0^{r_0} r u \, dr \tag{3-10}$$

There result

$$v = 2\pi n \left\{ \frac{\epsilon \Delta\varphi}{\mu l}\left(\int_0^{r_0} r\psi \, dr - \frac{\psi_0 r_0^2}{2} \right) - \frac{r_0^4}{16\mu}\frac{dP}{dx} \right\} \tag{3-11}$$

Since v must be independent of x by continuity it is evident that

$$\frac{dP}{dx} = \frac{\Delta P}{l} \tag{3-12}$$

Inserting Equation (3-12) into Equation (3-11) and rearranging we obtain

$$\Delta P = \frac{16\epsilon}{r_0^2}\left\{ \int_0^{r_0} r\psi \, dr - \frac{\psi_0 r_0^2}{2} \right\}\Delta\varphi - \frac{8\mu l}{r_0^2 A} v \tag{3-13}$$

where A is the total cross-sectional area πr_0^2 available to the flow. Equation (3-13) indicates that the pressure rise through the electromagnetic

converter is equal to the pressure "induced" by the applied voltage less the pressure drop due to viscous friction in the tube bank.

We now need to relate the current to the same two variables, $\Delta\varphi$ and v. The following form, expressing the fact that the current is the sum of a conduction and a convection component, is appropriate

$$i = C\,\Delta\varphi + \alpha v \tag{3-14}$$

where C is the electrical conductance of the fluid (measured, of course, under conditions of zero flow) given by

$$C = \frac{\sigma A}{l}\left(1 + \frac{2\sigma_0}{r_0\sigma}\right) \tag{3-15}$$

with σ the electrical conductivity of the bulk fluid and σ_0 the surface conductivity of the tube walls. The factor α can be found most directly from the Onsager relation[2]

$$\left(\frac{\Delta P}{\Delta\varphi}\right)_{v=0} = \left(\frac{i}{v}\right)_{\Delta\varphi=0} \tag{3-16}$$

which from Equations (3-13) and (3-14) implies that

$$\alpha = \frac{16\epsilon}{r_0^4}\left\{\int_0^{r_0} r\psi\,dr - \frac{\psi_0 r_0^2}{2}\right\} \tag{3-17}$$

This result can also be obtained from the analysis thus far presented in this section by observing that the current corresponding to $\Delta\varphi = 0$ is purely convection (no conduction) and consequently can be expressed by

$$i = 2\pi n \int_0^{r_0} \rho u r\,dr \tag{3-18}$$

where ρ is given by Equation (3-4) and u by the first term of Equation (3-9). Carrying out the required integration leads to an expression for i which, when divided by the volume flow rate corresponding to $\Delta\varphi = 0$ yields the same result as expressed by Equation (3-17).

Recapitulating the results to this point, the electrokinetic convertor operating in the pumping mode is governed by the following equations

$$\Delta p = \alpha \Delta \varphi - R v \tag{3-13}$$

$$i = C \Delta \varphi + \alpha v \tag{3-14}$$

where

$$R = \frac{8 \mu l}{r_0^2 A} \tag{3-19}$$

and α and C are as defined by Equations (3-17) and (3-15) respectively.

3-3 The Generation Mode

In the pumping mode considered above, through the tube bank the pressure increases in the direction of fluid flow and the voltage decreases in the direction of the current. In the generation mode to be considered now, if the flow is maintained in the same direction as in the pumping mode the pressure will decrease rather than increase and if the current is maintained in the same direction as in the pumping mode the pressure will decrease rather than increase and if the current is maintained in the same direction the voltage will increase rather than decrease. If we redefine Δp and $\Delta \varphi$ as this pressure drop and voltage rise respectively, Equations (3-13) and (3-14) as applied to the generation mode in this new notation become

$$\Delta p = \alpha \Delta \varphi + R v \tag{3-20}$$

$$i = - C \Delta \varphi + \alpha v \tag{3-21}$$

or, as rearranged to interchange inputs and outputs

$$\Delta \varphi = \frac{\beta}{\alpha(1+\beta)} \Delta p - \frac{1}{C(1+\beta)} i \tag{3-22}$$

$$v = \frac{1}{R(1+\beta)} \Delta p + \frac{\beta}{\alpha(1+\beta)} i \tag{3-23}$$

where

$$\beta = \frac{\alpha}{RC} \tag{3-24}$$

and α, R, and C are as defined previously. Equations (3-22) and (3-23) constitute the governing equations for the electrokinetic convertor in the generation mode.

3-4 Simplified Equations

The coefficient of Δp in Equation (3-22) is recognized as the so-called streaming potential S. Its classical value, as implied by Helmholtz, is given by

$$S = \frac{\epsilon(-\psi_0)}{\mu\sigma} \tag{3-25}$$

(ψ_0 will be negative for a positive charge density) which experiments[3] have shown to be valid in capillaries of radii down to about 10^{-5} m. Finer tubes would be all but impossible to obtain anyway.

Equation (3-25) can be derived from the theory in this section as follows. First, if we assume that ψ is very nearly zero everywhere but quite near the tube wall, Equation (3-17) implies that

$$\alpha = \frac{\pi\epsilon(-\psi_0)}{r_0^2} \tag{3-26}$$

Next, if we neglect the contribution of surface conductance to C (as a consequence of r_0 being not too small), Equations (3-26), (3-15), and (3-19) inserted into Equation (3-24) results in

$$\beta = \frac{\pi\epsilon^2\psi_0^2}{\mu\sigma r_0^2} \tag{3-27}$$

Finally, if we assume that β is much less than unity (this will be verified later), the streaming potential becomes β/σ which from Equations (3-26) and (3-27) is the same as the value given by Equation (3-25). We will consider that the validation afforded Equation (3-25) by experiments justifies the assumptions in the derivations with follow.

Equations (3-22) and (3-23), which govern the generation mode, now become

$$\Delta\varphi = S\Delta P - \frac{i}{C} \tag{3-28}$$

$$v = \frac{\Delta P}{R} + Si \tag{3-29}$$

The flow rate, according to these equations, for a fixed Δp has its minimum value when $i = 0$ and its maximum when $\Delta\varphi = 0$. The ratio of maximum to minimum v is readily shown to be $1 + \beta$. Thus, by our assumption that β is much less than unity, the flow rate is essentially independent of the current, and Equation (3-29) reduced to

$$v = \frac{\Delta P}{R} \tag{3-30}$$

By a similar argument the current in the pumping mode is essentially independent of the flow, and Equation (3-14) reduces to

$$i = C\,\Delta\varphi \tag{3-31}$$

The final form of the equations governing the operation of the electrokinetic convertor will now be summarized.

The pumping mode:

$$\Delta P = \frac{8\epsilon(-\psi_0)}{r_0^2}\,\Delta\varphi - \frac{8\mu l}{A r_0^2}\,v$$

$$i = \frac{\sigma A}{l}\,\Delta\varphi$$

The generation mode:

$$\Delta\varphi = \frac{\epsilon(-\psi_0)}{\mu\sigma}\,\Delta P - \frac{1}{\sigma A}\,i$$

$$v = \frac{A r_0^2}{8\mu l}\,\Delta P$$

3-5 Convertor Operating Characteristics

In the pumping mode, considering the applied voltage fixed, the following pump characteristics are evident.

zero-flow pressure: $\frac{8\epsilon(-\psi_0)}{r_0^2}\Delta\varphi$

zero-pressure flow: $\frac{A\epsilon(-\psi_0)}{\mu l}\Delta\varphi$

Due to the linearity of the pressure versus flow relationship, the maximum pumping power occurs when the pressure is one half the zero-flow pressure (and consequently the flow is one half the zero-pressure flow).

maximum pumping power: $\frac{2A\epsilon^2\psi_0^2}{\mu l r_0}(\Delta\varphi)^2$

The maximum pumping efficiency is the maximum pumping power divided by the product of voltage and current.

maximum pumping efficiency: $\frac{2\epsilon^2\psi_0^2}{\mu\sigma r_0^2}$

In the generation mode, considering the applied pressure fixed, the following generator characteristics are evident.

zero-current voltage: $\frac{\epsilon(-\psi_0)}{\mu\sigma}\Delta P$

zero-voltage current: $\frac{A\epsilon(-\psi_0)}{\mu l}\Delta P$

and by arguments similar to those advanced for the pumping mode

maximum generating power: $\frac{A\epsilon^2\psi_0^2}{4\mu^2\sigma l}(\Delta P)^2$

maximum generating efficiency: $\frac{2\epsilon^2\psi_0^2}{\mu\sigma r_0^2}$

It is noteworthy that the maximum pump efficiency is identical to the maximum generator efficiency.

3-6 Numerical Results

To obtain numerical values for the pump and generator characteristics it is necessary to specify the working fluid. Data on ψ_0 is readily available only for water and aqueous solutions. It appears[3] that ψ_0 can approach -0.20 volts for pure water in equilibrium with atmospheric carbon dioxide (in which case the ions are H^+, and HCO_3^-) and is somewhat less for aqueous solutions. Furthermore, additives (such as salt) to pure water tend to decrease ϵ and increase σ and μ resulting in the efficiency having its greatest value for pure water. For pure water: $\epsilon = 7 \times 10^{-10}$ coul/volt m $\sigma = 10^{-4}$ mho/m, $\mu = 10^{-3}$ newt sec/m^2. If we specify that $\psi_0 = -0.20$ volts and $r_0 = 10^{-5}$ m, the smallest value permitted by this theory, β works out to be 0.01568 which indeed is much smaller than unity. We will employ these data in the illustrative examples to follow.

3-7 Illustrative examples

Consider an electrokinetic convertor of the following geometry: $a = 10^{-2}$ m, $\delta = 10^{-2}$ m. The open volume of the tube bank is thus 100 cm^3.

In the pumping mode consider an applied voltage differential of 10^3 volts. The following pump characteristics follow.

zero-flow pressure: 11.2×10^3 newt/m^2 (about 0.1 atm)

zero-pressure flow: 14×10^{-5} m^3/sec (0.14 litres/sec)

maximum pumping power: 0.392 watts

electrical current: 0.1 amp

electrical power input: 100 watts

maximum efficiency: 0.392%

In the generation mode consider an applied pressure differential of 10^5 newt/m^2 (about 1 atm). The following generator characteristics follow.

zero-current voltage: 140 volts

zero-voltage current: 0.014 amp

maximum electrical power: 0.49 watts

fluid flow rate: 12.5×10^{-4} m^3/sec (1.25 litres/sec)

pumping power input [illegible] watts

maximum efficiency: 0.392%

The Reynolds number corresponding to this flow rate is only 2.50 thus assuring laminar flow in the tube bank.

3-8 Conclusions

The characteristics of a steady state electrokinetic energy convertor in both the fluid pumping and electrical generation modes of operation have been determined. For pure water the maximum conversion efficiency in either direction is found to be 0.392%. A tube bank of 100 cm^2 "open" cross-sectional area and 1.0 cm length subject to an applied voltage of 1000 volts is capable of pumping 0.07 litres per second at about 0.05 atm pressure at this efficiency. The same unit subject to an applied pressure of about 1 atm is capable of generating 0.49 watts at 70 volts at this same efficiency.

We are presently undertaking an experimental investigation of this phenomenon.

References

1. H. L. F. Helmholtz, "Studien ... elektrische Grenzschicten," Annalen der Physik und Chemie von G. Wiedemann, Band 7 (1879), z. 337.

2. I. Prigogine, Thermodynamics of Irreversible Processes, Second, Revised Edition, Interscience Publishers, a division of John Wiley & Sons, New York, (1961).

3. I. B. Oldham, F. J. Young, and J. F. Osterle, "Streaming Potential in Small Capillaries," Journal of Colloid Science, Vol. 18, pp. 328-336, (1963).

Nomenclature

A = open cross-sectional area of tube bank, m^2

C = electrical conductance of fluid, mhos

E = electric field, volts/m

i = electrical current, amps

ℓ = length of tube bank, m

n = number of capillary tubes in tube bank

p = fluid pressure, newt/m^2

Δp = pressure differential across tube bank, newt/m^2

r = radial position in tube, m

r_o = tube radius, m

R = viscous resistance of fluid, newt sec/m^5

S = streaming potential, volt m^2/newt

u = fluid velocity, m/sec

v = fluid flow rate, m^3/sec

x = axial position in tube, m

α = induction coefficient defined by Equation (14), amp sec/^{3}

β = dimensionless parameter defined by Equation (24)

ϵ = permittivity of fluid, coul/volt m

μ = fluid viscosity, newt sec/m^2

ρ = charge density, coul/m^3

σ = fluid electrical conductivity, mhos/m

σ_o = surface electrical conductivity, mhos

ψ = electrical potential, volts

$\Delta\psi$ = voltage differential across tube bank, volts

ψ' = component of ψ as defined by Equation (3), volts

ψ'_o = value of ψ' at tube wall

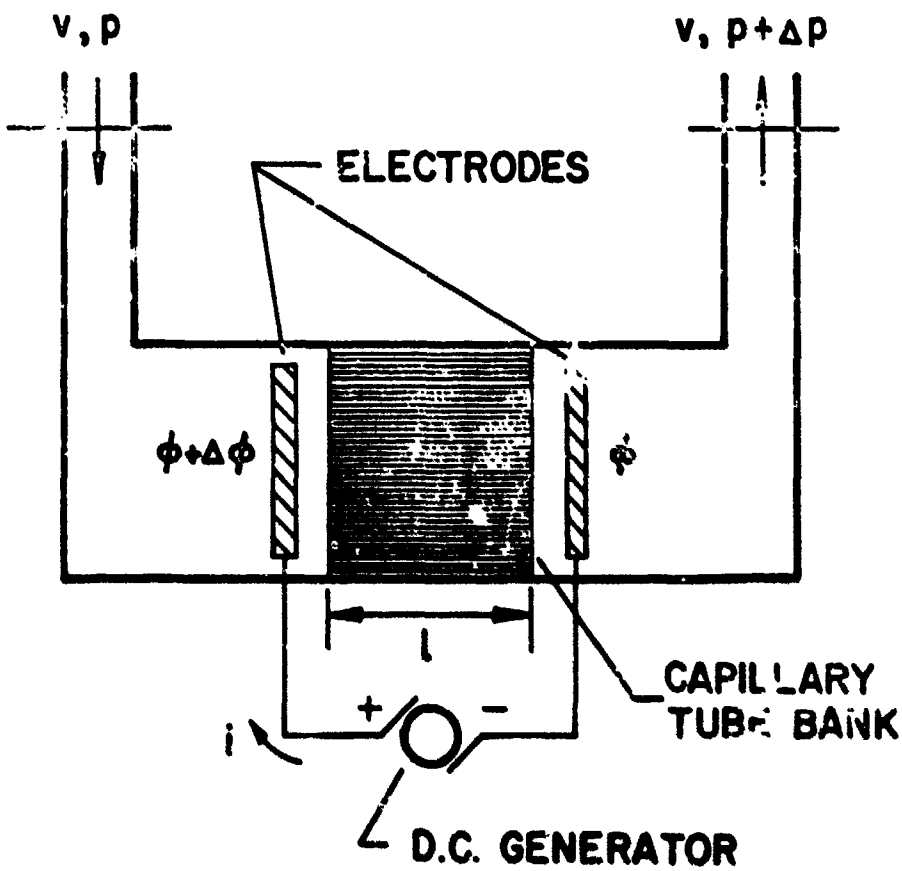

Figure 3-1. The Electrokinetic Convertor

Section 4

ACOUSTIC PUMPING

4-1 Introduction

The effect of acoustic pumping as defined by a steady uni-directional flow developed by a purely oscillatory source of energy has been reported and investigated for many years. One of the first to report on this phenomena was Lord Rayleigh in his classic book Theory of Sound[1]. Lord Rayleigh investigated motion of dust particles in a Kundt's tube and streaming phenomena at the mouth of a Helmholtz resonator.

Following the development of quartz and other piezoelectric oscillators of high power capability, reports began to appear concerning the "Quartz Wind", a steady flow of fluid directed away from the face of the oscillating crystal. This effect which is noticeable only at very high sound intensities has been analyzed with variable success by several investigators since C. Eckart's[2] paper on the subject in 1948. Notable papers on the subject are by Nyborg[3], Westervelt[4], Medwin[5], and Johnsen[6].

Another source of steady flow generated by an oscillating source is the secondary fluid motions set up by interaction of an oscillating sound field and a rigid boundary. Within this class of problems lie Lord Rayleigh's original remarks concerning Kundt's Tubes and Helmholtz Resonators. With the development of the boundary layer theory the interaction of a sound field with the boundary layer was investigated by Schlicting[7] and others for certain specific cases. Medwin[5] developed a generalized theory of streaming phenomena which includes both Quartz Wind and Boundary Layer effects; however, the equations developed have little value insofar as calculating specific quantities for practical cases.

Piercy[8] describes an application of the Quartz Wind phenomena which approaches closely our present topic of acoustic pumping. He proposed a system whereby the streaming velocity generated by a traveling sound wave would permit him to calculate sound absorption coefficients of a fluid contained in the system. The device described in his paper would, if suitably optimized, work quite well as an acoustic pump whose principle effect would be to pump the contained fluid. This particular device was chosen as the primary effort of the current investigation. Analysis has progressed to the point where optimization can be achieved. A model has been constructed and will be used to verify the analysis and optimization.

Dauphinee[9] describes a device specifically designated as an acoustic pump constructed from a standard radio loudspeaker. This device works on the same principle as the streaming from a Helmholtz Resonator, as described by Lord Rayleigh's original paper. It could be described as a vectored momentum pump since the fluid is ejected in a directed jet but sucked in from the surrounding still air. The simplicity, low cost, and surprising effectiveness of this device suggested that it be adopted as a secondary effort in the acoustic pumping program. A model was constructed and tested, verifying the original work by Dauphinee. An analysis has been started.

It should be emphasized that effects other than simple transport of fluid can be obtained from acoustic streaming phenomena. When discontinuities in density occur in the fluid (e.g., a suspended solid particle or gas bubbles) preferential streaming occurs. The discontinuity in density results in a force acting on the interface causing the particle or bubble to move. For this reason a "bubbly" liquid has a high sound absorption and exhibits higher streaming velocities by several orders of magnitudes. This effect could be utilized, for example, in separating a vapor from a liquid phase under zero gravity conditions.

4-2 The Piercy Pump

The device devised by Piercy and Lamb[8] to measure sound absorption is sketched in Figure 4-1a. The modified construction resulting from the current analysis is sketched in Figure 4-1b. The analysis of the action of the pump which follows is derived in part from Piercy[8], Nyborg[3], and in part is original to this investigation.

The piezoelectric crystal at the left of the long tube sends a directed beam of sound axially down the tube. It will be shown later that the optimum frequency is sufficiently high that little diffraction occurs beyond the first few centimenters. The beam exhibits little divergence. The sound beam then almost, but not quite, fills the tube with traveling sound waves, which to a first approximation may be treated as plane waves.

The continuity equation within the sound wave is given by

$$\frac{\partial \rho}{\partial t} + \nabla \cdot \rho u = 0 \tag{4-1}$$

where ρ = density of fluid and u = velocity of fluid. The momentum equation is

$$\rho \frac{\partial u}{\partial t} + \rho u \cdot \nabla u = -\nabla P + (\lambda + \tfrac{4}{3}\mu)\nabla(\nabla \cdot u) - \mu \nabla \times \nabla \times u \tag{4-2}$$

where P = static pressure
μ = dynamic shear viscosity
λ = dynamic volume viscosity

Equations (4-1) and (4-2) are linearized by assuming

$$\rho = \rho_0 + \rho_1 e^{j\omega t} + \rho_2 e^{2j\omega t} + \dots$$
$$u = u_0 + u_1 e^{j\omega t} + u_2 e^{2j\omega t} + \dots$$
$$P = P_0 + P_1 e^{j\omega t} + P_2 e^{2j\omega t} + \dots$$
$$j = \sqrt{-1} \qquad e = 2.7183\dots$$

we will further assume that $\rho_c \gg \rho_i$ and that $\nabla \rho_i \ll \nabla \cdot U_i$ and ∇P_i. These are standard assumptions in acoustic work and are justified by experimental observations.

There will result, when these assumptions are applied to Equations (4-1) and (4-2), a set of equations, two for each order of $\jmath\omega t$.

For example the zero order equations are (neglecting terms of order > 1):

$$\nabla \cdot u_0 = 0 \tag{4-3}$$

$$\rho_0 u_0 \cdot \nabla u_0 = -\nabla P_0 + \mu \nabla^2 u_0 - \rho_0 u_1 \cdot \nabla u_1 \tag{4-4}$$

The first order equations are:

$$\jmath\omega \rho_1 + \rho_0 \nabla \cdot u_1 = 0 \tag{4-5}$$

$$\jmath\omega \rho_0 u_1 + \rho_0 u_0 \cdot \nabla u_1 + \rho_0 u_1 \cdot \nabla u_0 = -\nabla P_1 + (\lambda + \tfrac{1}{3}\mu)\nabla(\nabla \cdot u_1) + \mu \nabla^2 u_1 \tag{4-6}$$

The second set of equations, combined with a valid equation of state, yield the usual acoustic solutions. If $\lambda = \mu = 0$, an ideal fluid results, giving as a solution undamped sound waves. Doppler shifts in frequency result if $u_0 \neq 0$. Normally the assumption is made that $u_0 = 0$ for acoustic work.

The first set of equations is of interest if the primary purpose is to induce streaming in the fluid. u_0 is the streaming velocity which we seek. The term on the left of Equation (4-4) is the spatial acceleration of the fluid.

Only steady state is considered, therefore, the temporal acceleration is zero. The first term on the right is the spatial variation in static pressure. The second term is the viscous drag. The third term represents a body force in the fluid generated by the first order sound field.

The body force is generated by the non-linear response of the fluid to an imposed periodic force. Forces of this type are common in non-linear systems (e.g., rectifiers, gas tubes) and result in energy transfer between harmonics of the fundamental mode. Thus, if a pure tone is sounded at a point in a non-linear fluid, harmonics of higher and higher order will be generated, until the sound is finally absorbed. Because high frequencies are absorbed faster than low frequencies, at steady state a nonlinear wave form is developed. Energy is also transferred from higher harmonics to lower and in particular to zero frequency or D.C. Thus, in a nonlinear circuit D.C. current will result from an imposed a.c. supply.

Now in the Piercy Pump we assume the sound field to be composed of plane waves. This requires that the beam of sound does not contact the wall of the tube. Further, inside the long tube we consider only steady flow in the axial direction. Now Equations (4-3) and (4-4) become:

$$\frac{dU_0}{dx} = 0 \tag{4-7}$$

$$0 = -\frac{dP_0}{dx} + \frac{\mu}{r}\frac{d}{dr}\left(r\frac{dU_0}{dr}\right) - \rho_0 U_1 \cdot \frac{dU_1}{dx} \tag{4-8}$$

Now we take a well known solution to the first order equations for plane waves in an absorbing medium

$$U_1 = U e^{-\alpha x} e^{i(\omega t - \beta x)} \tag{4-9}$$

where U = rms velocity amplitude at source (x = 0)
α = absorption coefficient of fluid
ω = frequency of wave
k = wave number

Now $$\frac{dU_1}{dx} = -\alpha U e^{-\alpha x} e^{i(\omega t - kx)}$$

and $$U_1 \frac{dU_1}{dx} = -\alpha U^2 e^{-2\alpha x}\left[e^{2i(\omega t - kx)} + 1\right]$$

We ignore the double frequency component as it does not contribute to the streaming and obtain the result

$$\frac{dP_0}{dx} - \rho_0 \alpha U^2 e^{-2\alpha x} = \frac{\mu}{r}\frac{d}{dr}\left(r\frac{dU_0}{dr}\right) \tag{4-10}$$

Now the static pressure P_0 does not vary with r and the streaming velocity does not vary with x under the assumption we have made. Integration with respect to r yields

$$\frac{d}{dr}\left(r\frac{dU_0}{dr}\right) = \left(\frac{dP_0}{dx} - \rho_0 \alpha U^2 e^{-2\alpha x}\right)\frac{r}{\mu}$$

$$\frac{dU_0}{dr} = \left(\frac{dP_0}{dx} - \rho_0 \alpha U^2 e^{-2\alpha x}\right)\frac{r}{2\mu} + \frac{A}{r}$$

$$U_0 = \left(\frac{dP_0}{dx} - \rho_0 \alpha U^2 e^{-2\alpha x}\right)\frac{r^2}{4\mu} + A \ln r + B$$

The constants of integration A and B can be found by noting that $\frac{dU_o}{dr} = 0$ at $r = 0$ and $U_o = 0$ at $r = r_o$ or the radius of the tube. Then the solution is:

$$U_o = \frac{r^2 - r_o^2}{4\mu}\left[\frac{dP_o}{dx} - \rho_o \alpha U^2 e^{-2\alpha x}\right] \tag{4-11}$$

To determine $\frac{dP_o}{dx}$ define $\Delta P = \int_o^L \left(\frac{dP_o}{dx}\right) dx$ where L is the length of the tube. Now because U_o is not a function of x as we have assumed, then the expression $\left[\frac{dP_o}{dx} - \rho_o \alpha U^2 e^{-2\alpha x}\right]$ is not a function of x. Now

$$\int_o^L \left[\frac{dP_o}{dx} - \rho_o \alpha U^2 e^{-2\alpha x}\right] dx = L\left[\frac{dP_o}{dx} - \rho_o \alpha U^2 e^{-2\alpha x}\right]$$

also $$\int_o^L \left[\frac{dP_o}{dx} - \rho_o \alpha U^2 e^{-2\alpha x}\right] dx = \Delta P - \frac{1}{2}\rho_o U^2 (1 - e^{-2\alpha L})$$

$$L\left[\frac{dP_o}{dx} - \rho_o \alpha U^2 e^{-2\alpha x}\right] = \Delta P - \frac{1}{2}\rho_o U^2 (1 - e^{-2\alpha L})$$

Then the velocity is given by

$$U_o = \frac{(r_o^2 - r^2)}{4\mu L}\left[\frac{1}{2}\rho_o U^2 (1 - e^{-2\alpha L}) - \Delta P\right] \tag{4-12}$$

The volume flow rate is $Q = \int u_o \cdot dA = 2\pi \int_o^{r_o} r u_o \, dr$

$$Q = \frac{\pi r_o^4}{8\mu L}\left[\frac{1}{2}\rho_o U^2 (1 - e^{-2\alpha L}) - \Delta P\right] \tag{4-13}$$

This result leads one immediately to

$$\Delta P = \frac{1}{2}\rho_o U^2 (1 - e^{-2\alpha L}) - \frac{8\mu L}{\pi r_o^4} Q \tag{4-14}$$

Equation (4-14) is basic to the Piercy Pump, describing the relation between the output $Q\Delta P$ and the input $\frac{1}{2}\rho_o U^2$. This latter term represents the acoustic energy put into the system and the product $Q\Delta P$ represents the output pumping energy.

The above derivation has been highly idealized in several respects, one major one being the implicit assumption of laminar flow. All idealization may now be discarded, however, by a purely empirical approach based on the ideal results. Thus, write instead of equation (4-14)

$$\Delta P = \frac{I_o}{C_o}\left(e^{-2\alpha l_o} - e^{-\alpha(l_o + L)}\right) - f\frac{L}{2r_o}\rho_o \frac{Q^2}{2A^2} \tag{4-15}$$

where ΔP and Q are as defined before

and $I_o = \frac{1}{2}\rho_o C_o U^2$ = acoustic intensity

A, r_o, ℓ_o and L as defined by Figure 4-1b

C_o = velocity of sound in fluid

f = pipe friction factor as defined by Moody

The actual optimization of the design will be done using Equation (4-15) since it is the more general of the two. Equation (4-15) reduces to Equation (4-14) for the special case of laminar flow when ℓ_o cannot physically be zero since no pumping will occur if the left end of the pipe is sealed off. The static pressure would be higher at the open end than at the closed end resulting in only slight circulating back flow between walls and sound beam, as in Eckart's paper[7].

Now Equation (4-15) will be further modified by the substitutions:

$$L = \beta \ell_o$$
$$\alpha = \alpha' \nu^2$$
$$A = \pi r_o^2$$

where β is a pure numeric defined by $\beta = L/\ell_o$

α' is the so-called reduced absorption coefficient of the fluid

ν is the frequency of the sound wave in cycles per second

The reduced absorption α' is available in standard references on acoustics for a wide range of fluids. The absorption is proportional to the square of the frequency. The fact that this is not entirely true is noted by specifying the reduced absorption as a weak function of frequency. For many common fluids, e.g., air and water, $\alpha' \approx$ const.

Now

$$\Delta P = \frac{I_o}{C_o} e^{-2\alpha' \ell_o \nu^2} \left(1 - e^{-2\alpha' \ell_o \beta \nu^2}\right) - \frac{f \ell_o \beta}{4\pi^2 r_o^5} \rho Q^2 \qquad (4\text{-}16)$$

Inspection of this equation for possible optimizing parameters shows that the frequency ν, the flow rate Q, and the length ratio β are the only parameters which might be adjusted for optimum performance.

The output of the pump is defined as the product of head and flow or

$$W_o = Q \Delta P$$

Now $W_o = W_o(\nu, Q, \beta)$ and the optimum value of each parameter is obtained when

$$dW_o = \frac{\partial W_o}{\partial \nu} d\nu + \frac{\partial W_o}{\partial Q} dQ + \frac{\partial W_o}{\partial \beta} d\beta = 0$$

To solve this equation each variable will be eliminated in turn by setting its partial derivative equal to zero.

We will optimize first with respect to v^2 rather than v since the frequency appears only as a square in the equation. The result of this operation is

$$\frac{\partial W_o}{\partial v^2} = 0 = -1 + e^{-2\alpha' \ell_o v^2 \beta} + \beta e^{-2\alpha' \ell_o v^2 \beta}$$

which yields as the optimum frequency

$$\hat{v} = \sqrt{\frac{\ln(1+\beta)}{2\alpha' \ell_o \beta}} \tag{4-17}$$

Substituting this into the expression for W_o yields

$$W_o = Q\beta \left[\frac{I_o}{c_o} g(\beta) - f \frac{\ell_o}{4\pi^2 r_o^4} \rho_o Q^2 \right] \tag{4-18}$$

where $g(\beta) = \left(\frac{1}{1+\beta}\right)^{(1+\frac{1}{\beta})}$

This expression is now to be optimized for the flow rate Q, thus:

$$\frac{dW_o}{dQ} = 0 = \frac{I_o}{c_o} g(\beta) - 3 f \frac{\ell_o}{4\pi^2 r_o^4} \rho_o Q^2$$

or the optimum flow rate is

$$\hat{Q} = \pi r_o^2 \sqrt{\frac{4}{3}\left(\frac{1}{f}\right)\left(\frac{r_o}{\ell_o}\right)\left(\frac{I_o}{\rho_o c_o}\right) g(\beta)} \tag{4-19}$$

Note here that $I_o = \frac{1}{2} \rho_o c_o U^2$ where U = maximum velocity amplitude of wave at the crystal face. Then the optimum flow rate may also be expressed by

$$\hat{Q} = \pi r_o^2 U \sqrt{\frac{2}{3}\left(\frac{1}{f}\right)\left(\frac{r_o}{\ell_o}\right) g(\beta)} \tag{4-20}$$

When Equation (4-20) is substituted into (4-18) we obtain

$$W_o = \pi r_o^2 \rho_o U^2 \beta \left[g(\beta)\right]^{\frac{3}{2}} \sqrt{\frac{2}{3}\left(\frac{1}{f}\right)\left(\frac{r_o}{\ell_o}\right)} \tag{4-21}$$

The function $\beta[g(\beta)]^{3/2}$ has a maximum which can most easily be found by numerical calculation. The function has a rather flat maximum of about 0.2, near $\beta = 5$. Thus, the length of tube, L, which yields the maximum output is 5 times as long as the distance from the crystal to the tube entrance. This latter distance, ℓ_o, has an optimum value; but it is based on the tube entrance loss which is not covered by this analysis. A reasonable dimension for this distance, ℓ_o, is about equal to the tube radius. This leads to a flow area between crystal and tube mouth equal to twice the flow area in the tube. If this assumption is made, the ratio $r_o/\ell_o = 1$ and we have

$$W_o = \frac{\pi}{5} r_o^2 \rho_o U^3 \sqrt{\frac{2}{27}\left(\frac{1}{f}\right)} \qquad (4\text{-}22)$$

The electrical input to a crystal being driven at its resonant frequency is given by

$$W_i = \frac{I_o A}{C_f}$$

where I_o = acoustic intensity

A = radiating face of crystal

C_f = coupling factor, or electromechanical conversion efficiency.

We now assume that $A = \pi r_o^2$ and note that $I_o = \frac{1}{2}\rho_o C_o U^2$; then the pump efficiency defined by

$$\eta = \frac{W_o}{W_i}$$

is given by

$$\eta = \frac{2}{5}\sqrt{\frac{2}{27}\left(\frac{1}{f}\right)}\; C_f \frac{U}{C_o}$$

or

$$\eta = .109 \frac{C_f}{\sqrt{f}} \frac{U}{C_o} \qquad (4\text{-}23)$$

This last equation tells us that the pumping efficiency of the Piercy Pump is proportional to the electromechanical efficiency of the driving crystal, inversely proportional to the square root of the friction factor (head loss) and proportional to the ratio U/C_o. This latter ratio is always less than 1, in fact the best value attainable as a practical matter is in the neighborhood of .033. It is unlikely that f should ever be much smaller than .01 and values of .4 for C_f are not easily attained. With these assumptions it appears the best practical efficiency for this pump is around 1.1% at the present time.

There is no immediate reason why this performance cannot be improved upon. One simple and effective improvement is to use two tubes with each crystal thus doubling the output and the efficiency. The small value of U/C_o can be improved

upon by perhaps an order of magnitude by various stratagems, such as preloading the crystal to prevent shattering. The ultimate in conversion efficiencies has not yet been reached.

A review of the equations derived for the Piercy Pump and some characteristic results for specific fluids are given below:

I. Zero-flow head (Equation (4-16) with Q = 0)

$$\Delta p = \tfrac{1}{2}\rho_0 U^2 e^{-2\alpha' l_0 \nu^2}\left(1 - e^{-2\alpha' l_0 \beta \nu^2}\right) \tag{4-24}$$

II. Zero-head flow (solve Equation (4-16) for Q with $\Delta p = 0$)

$$Q = \pi r_0^2 U \sqrt{\left(\frac{2r_0}{l_0}\right)\left(\frac{1}{f}\right) e^{-2\alpha' l_0 \nu^2}\left(1 - e^{-2\alpha' l_0 \beta \nu^2}\right)} \tag{4-25}$$

III. Optimum frequency

$$\hat{\nu} = \sqrt{\frac{\ln(1+\beta)}{2\alpha' l_0 \beta}} \tag{4-17}$$

IV. Optimum flow

$$\hat{Q} = \pi r_0^2 U \sqrt{\tfrac{2}{3}\left(\frac{1}{f}\right)\left(\frac{r_0}{l_0}\right)\left(\frac{1}{1+\beta}\right)^{\left(1+\frac{1}{\beta}\right)}} \tag{4-20}$$

V. Optimum ratio of tube length to entrance length

$\beta = 5$ (found numerically)

VI. Optimum efficiency

$$\eta = 10.9\, C_f \sqrt{\left(\frac{1}{f}\right)\left(\frac{r}{l_0}\right)}\,\frac{U}{c_0}$$

Some representative data are:

	air	water	mercury
ρ_0	1.29 kg/m^3	998 kg/m^3	13,596 kg/m^3
C_0	343 m/sec	1497 m/sec	1451 m/sec
α'	2.7×10^{-11} sec^2/m	25×10^{-15} sec^2/m	6×10^{-15} sec^2/m

Assume a pump with dimensions

$\ell_o = r_o = .025$ meters (2" diameter)
$\beta = 5$ ($L \approx 5"$)

Note that the peak velocity at the surface of a vibrating Quartz crystal is about 5 m/sec and that the electromechanical coupling coefficient is around .1 for Quartz. Quartz is chosen for this example because of its high mechanical strength, cheapness and availability. Some of the newer ceramic transducer materials would perhaps be a better choice at the lower frequencies.

Using the above data in the listed set of equations results in the following performance:

	air	water	mercury
Zero-Flow Head	.04 inch water	10.4 psi	142 psi
Zero-Head Flow	116 cfm	1060 gpm	1380 gpm
Optimum Frequency	.515 Mc	16.9 Mc	34.6 Mc
Optimum Flow	29.9 cfm	274 gpm	356 gpm
Power Output	8.28 watts	800 watts	14.52 KW
Power Input	101 watts	400 KW	4840 KW
Efficiency	.082%	.002%	.003%

Two things should be noted from the information supplied. First the high outputs of the heavier liquids are associated with low efficiencies and the (relatively) high efficiencies of gases are associated with low outputs. This is due to the high speed of sound in liquids which reduces acoustic energy input. Secondly note that the absorption of the fluid does not affect the efficiency or output of the pump if the pump is operated at the optimum frequency for the particular fluid being handled. However, if the pump is not operated at optimum frequency, the output and efficiency are reduced accordingly. Note also that the optimum frequency is a function of pump dimensions (ℓ_o) and can be varied. The smaller ℓ_o is, the greater the output and efficiency.

4-3 Helmholtz Resonator Pump

This device, described by Dauphinee[9], is an application of a very old effect, noted by Rayleigh and others previously. If an oscillating pressure can be established in a closed region connected to a steady pressure region with a tube or nozzle, a net flow away from the nozzle will occur. This effect is manifested in a large number of ways, one very common one being the circulation set up by a Hi-Fi speaker operated at high volume. The grill cloth acts as a multiple nozzle and the low frequency components act on the surrounding air to induce circulation. The hydrodynamic oscillator (toy boat engine) is

another old but valid example of this principle. In this case net thrust is produced by the oscillating water column, in precisely the same manner as the acoustic pump.

Figure 4-2 shows a sketch of the acoustic pump as described by reference (9). This pump uses a radio loudspeaker as the cavity because it is simple, cheap and readily available. Any cavity whose total volume can be readily varied at a suitable frequency can be used to pump fluid. The cavity may be filled with the fluid to be pumped or with another fluid. The fluid to be pumped fills the nozzle or orifice (a tube or nozzle is not essential). The oscillating pressure in the cavity causes flow oscillation in the nozzle. At the nozzle exit there is a directed flow away from the tube but flow toward the tube tends to come from the still fluid surrounding the pulsed jet issuing from the nozzle. The jet may be contained in a second tube as shown. The pulses issuing from the nozzle entrain fluid from the surrounding region and smooth out the flow leaving the secondary tube. The net result of this operation is a low head high flow rate characteristic similar to a small propeller fan.

The analysis of this pump is, at the same time, simple and complex. It is a simple problem to develop equations permitting the design of a pump to produce a given output. It is quite difficult to develop the actual flow field which describes the pump operation. The analysis is based on the same resonant cavity analysis of Helmholtz. The fluid in the nozzle is assumed incompressible and oscillates back and forth essentially as if it were a solid piston. The fluid in the cavity and/or the diaphragm provides a damping force. The analysis then becomes that of a simple mass on a spring with friction. This model will permit determination of the dimension of the pump and the driving frequency to produce maximum output.

The difficulty arises in trying to calculate output at high amplitudes of vibration. The equations governing the operation are essentially nonlinear and cannot be linearized at finite amplitude. The problem is complicated by the fact that for reasonable output the flow is turbulent and rotational. The device is incidentally a vortex generator quite capable of blowing excellent smoke rings.

Measured values of efficiency lie in the range of .5 to 2% and output of up to 100 cfm at .1 inch head have been observed. The pump has been used according to reference (9) to circulate air at liquid air temperatures with somewhat higher efficiency. The advantage of this type of pump at low temperatures is obvious since there is no lubriction problem. This pump should also be useful in handling very pure fluids where contamination is a problem. Its characteristics are approximately those of a propeller fan, low head high volume delivery, when pumping gaseous fluids. Its efficiency and output are presumably less when handling liquids although this point will require checking. No attempts to pump liquid have been made yet.

References

1. Lord Rayleigh, Theory of Sound, Dover Publications, New York (1945).
2. C. Eckart, Physics Review, Vol. 75, p. 68 (1948).
3. W. L. Nyborg, Journal Acc. Society of America, Vol. 25, p. 68 (1953).
4. P. Westervelt, Journal Acc. Society of America, Vol. 25, p. 60 (1953).
5. Meawin and Ingunick, Journal Acc. Society of America, Vol. 25, p. 538 (1953).
6. Johnsen and Tjotta, Acustica, Vol. 7, p. 7 (1957).
7. H. Schlichting, Physik Z, Vol. 33, p. 327 (1932).
8. Piercy and Lamb, Proc. Royal Society, Vol. A226, p. 43 (1954).
9. Dauphinee, Research (Gb), Vol. 13, p. 300 (1960).

Nomenclature

A = flow area of tube, cm^2

C_f = electromechanical coupling factor of transducer

C_o = adiabatic speed of sound in fluid, cm/sec

f = Moody friction factor for pipe flow

I_o = acoustic intensity of radiating face, $watts/cm^2$

k = wave number of acoustic radiation, cm^{-1}

L = length of tube, cm

ℓ_o = distance from radiating face to tube mouth, cm

P = pressure in fluid, $dynes/cm^2$

Q = volume flow rate thru pump, cc/sec

Q = optimum volume flow rate, cc/sec

r = radial coordinate in tube, cm

r_o = radius of tube wall, cm

v = general fluid velocity, cm/sec

V = rms velocity of transducer face, cm/sec

W_o = power output of pump, watts

W_i = power input to pump, watts

x = axial coordinate in tube, cm

α = acoustic absorption coefficient of fluid, cm^{-1}

α' = reduced absorption coefficient of fluid, sec^2/cm

β = ratio of tube length to ℓ_o (above)

ΔP = pressure head of pump, $dynes/cm^2$

η = efficiency

λ = coefficient of volume viscosity, poise

μ = coefficient of shear viscosity, poise

ν = frequency of acoustic radiation, sec^{-1}

ν = optimum frequency of radiation, sec^{-1}

ρ = density of fluid, gm/cc

ω = angular frequency of acoustic radiation, sec^{-1}

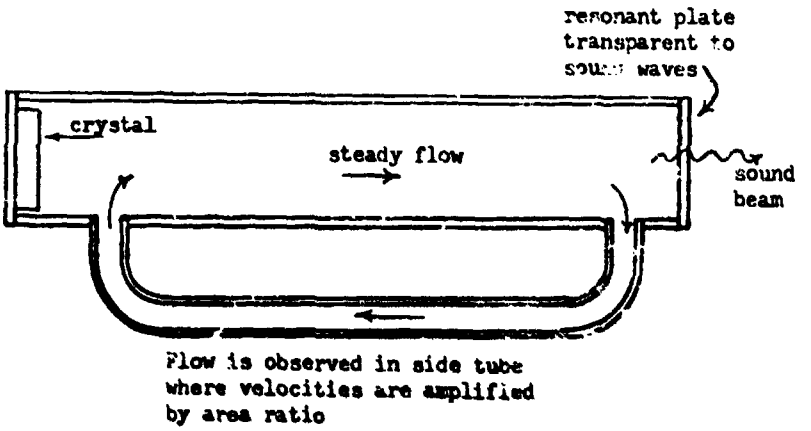

Figure 4-1a. Piercy's Absorption Measuring Device

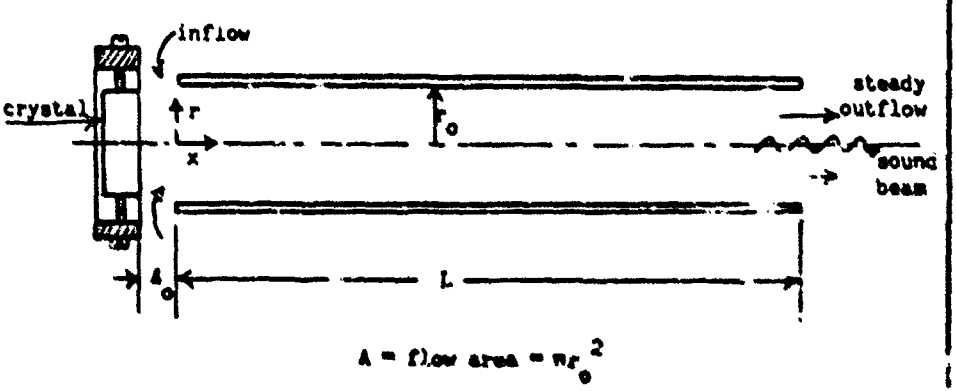

A = flow area = πr_o^2

Figure 4-1b. Piercy Pump as Described in This Report

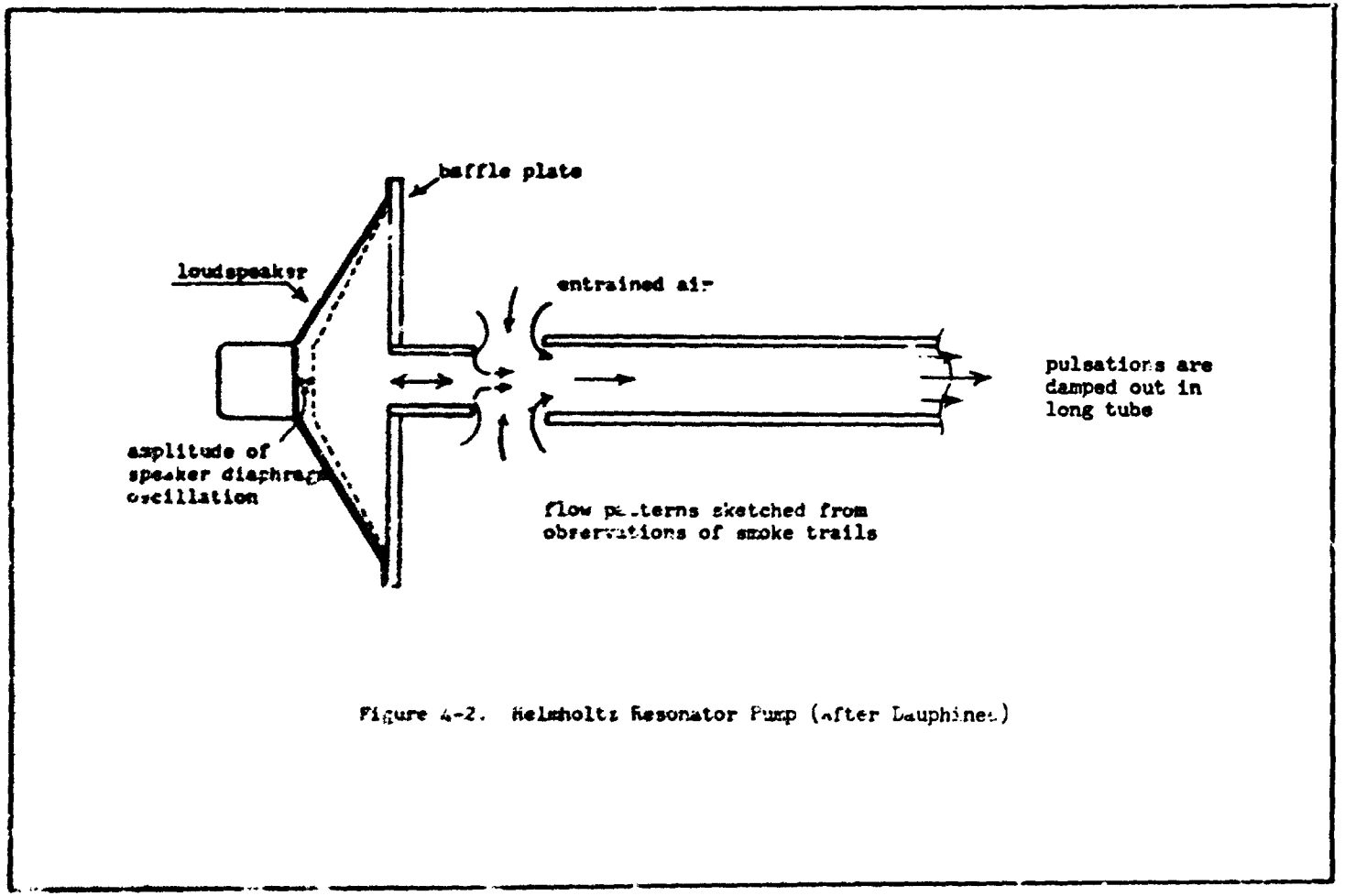

Figure 4-2. Helmholtz Resonator Pump (after Dauphinee)

Section 5

THE WINSLOW EFFECT VALVE

5-1 Introduction

The Winslow effect is a phenomenon observed in liquids by which the flow of a liquid can be restricted by applying an electric field perpendicular to the direction of flow. The effect is most pronounced when the fluid is an emulsion, although there is some indication that it would also hold to some extent for true solutions (where there is thorough mixing on a molecular level). The principle of operation is the following: The application of an electric field across the liquid causes particles of higher dielectric constant (such as finely divided particles, molecules, etc.) to form chains along E lines since this is a lower energy state for these particles. These chains tend to impede the flow of the remaining fluid and thus effectively increase the viscosity of the fluid.

The method which was proposed to use this effect in a pumping system is shown in Fig. 5-1

The signal generator at the left provided both the driving power for the transducer (a barium titanate crystal) and properly phased control voltages to the insulated plates which were to act as valves by means of the Winslow effect. The device was to be rectangular in cross section for ease in evaluating the fields. However, due to problems in assembly and in properly spacing the insulated parts, this design was replaced by the following (see Fig. 5-2):

This is a simplified sketch. The actual device consists of seven concentric thin-wall brass tubes. The center tube is 1/4" dia. and the diameters increase in increments of 1/4" to the largest, which is 1-3/4" dia. The wall thickness of all the tubes is .035". This leaves .090" spacing between all adjacent tubes. The first, third, fifth, and seventh tubes are 12" long and are electrically connected together to form the ground of the system. The second, fourth and sixth tubes are each in two sections, each section 5" long. Tubes number 2, 4 and 6 on the left are electrically connected together to form one "valve" and likewise on the right. Holes are drilled in appropriate places in all the tubes to allow for fluid flow and for action of the transducer. The outside tube is equipped with special fittings to accept the transducer and with inlet and outlet ports for the fluid. The end caps are machined 1/2" plexiglass and are clamped onto the ends by means of four 12"-long, threaded 5/16" bars. Electrical connections to the electrodes are made through the end caps.

Since the transducer is designed for use at audio frequencies and since the fluid probably would not be able to follow vibrations beyond a few thousand cycles per second, a standard audio oscillator and amplifier were used. Connections were made into the power output stage of the amplifier since the voltage waveforms which appeared there were ideally suited to the operation of the electrodes in the pump.

The voltages obtained in the amplifier produced an E field on the order of 10,000 volts/inch in the fluid.

The fluid used was the one recommended by W. M. Winslow[1] as the one which he found to give the best results, activated silicagel powder in kerosene. The mixture turned out to be a very thick, soupy liquid which caused considerable difficulty in handling. It would flow only very slowly through a 3/8" glass pipe twenty inches long. It took over an hour to fill the pump with the liquid. The power source was then connected, but even when turned up to full output, no motion of the fluid was observed. However, it was also noted that no sound was coming from the transducer. This indicated that either, (1) the transducer was defective, or (2) the transducer was operating as it should but its displacement was of too small an amplitude to be heard or to have any effect on the fluid.

In order to get a displacement of the order of magnitude which was required, it seemed that it would be necessary to use some other driving system. The method decided upon was the following: A thin copper diaphragm was soldered across the transducer opening. The center of this diaphragm was connected by a rigid link to the center of a loudspeaker cone, so that, when the speaker was driven by the amplifier, it would cause the diaphragm to vibrate and move the fluid. The pump was refilled and connected to the amplifier. This time the vibrations were audible, but still the fluid would not move.

It is difficult to explain why the device would not work satisfactorily since according to several references[1,2,3] the effect does exist and is measurable. The difficulty seems to be in the fluid used, since the fluids used by Winslow are of low viscosity and, indeed, he recommends low viscosity fluids. However, the only fluid which he recommends specifically, the one used, turned out to have a high viscosity. This high viscosity, in addition to causing high resistance to motion of the fluid, also allows the entrapment of small air bubbles throughout the fluid. These bubbles make the fluid compressible instead of being incompressible, so that the changes of pressure induced into the fluid are absorbed by the air bubbles and are not transmitted throughout the fluid. Thus, even though the particular arrangement which was tried did not work, there is a good chance that, with a better fluid, the same pump and driving system will give useful results.

If the experiment had operated satisfactorily, the following tests were planned:

First: Measurement of the effect of driving voltage (on the transducer and/or on the electrodes) on output pressure difference.

Second: The effect of phase differences between the transducer voltage and the electrode voltage.

Third: The relationship between pressure and flow rate.

Fourth: The effect of driving frequency on pressure and flow rate.

References

1. W. M. Winslow, Journal of Applied Physics, Vol. 20, p. 1137 (1949).

2. C. F. Hix, Jr. and R. P. Alley, "Physical Laws and Effects," John Wiley (1958).

3. Hans E. Hollmann, Journal of Applied Physics, Vol. 21, p. 402 (1950).

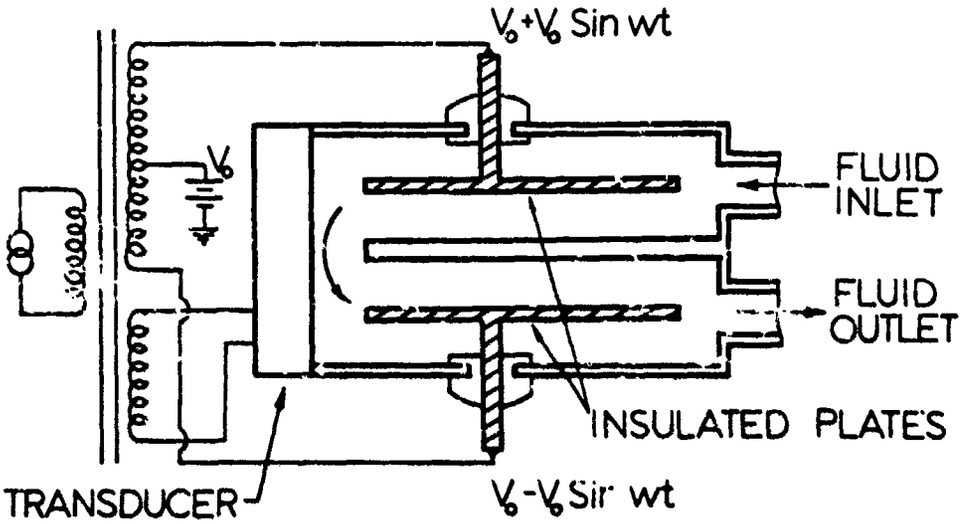

Figure 5-1. Winslow Effect Device No. 1

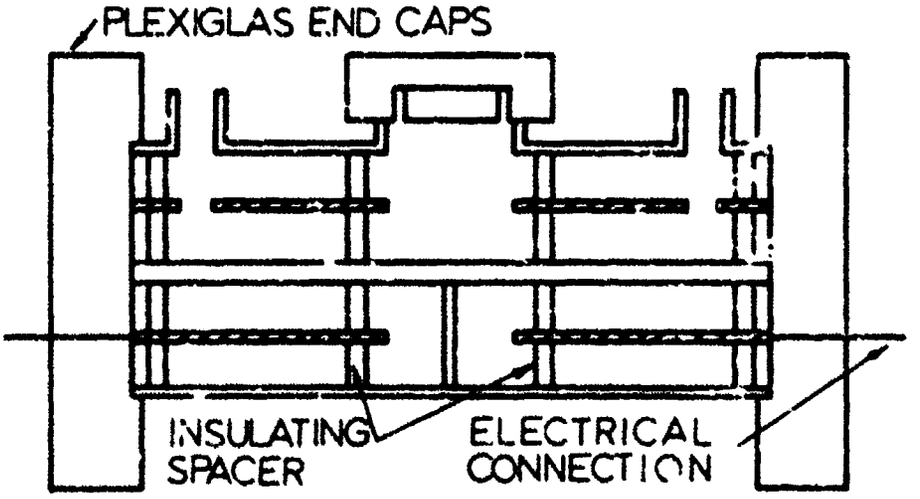

Figure 5-2. Winslow Effect Device No. 2

Section 6

ELECTROMAGNETIC INDUCTION PUMPING

6-1 Introduction

The induction pump is closely related to the ordinary induction motor. Its greatest advantage over other forms of magnetohydrodynamic pumps arises because no electrodes are necessary. In this pump a travelling magnetic field interacts with the current it induces in the fluid and a body force results which has a component in the direction of the desired motion of the fluid. Induction pumps have been used to pump coolants in nuclear reactors[1]. In the study by Blake several geometries are considered and some experimental data are presented.

A detailed study based on the equations derived by Harris[2] treats the effect of magnetic field fringing caused by pole piece separation[3]. It is concluded that fringing reduces the efficiency as much as do laminar skin-friction losses. However, it is assumed that flux penetration is complete and later it is concluded that electrical skin effects are negligible. Clearly, induction devices will not work at zero frequency because no fields currents can be induced. At very high frequencies all the induced fields and currents will be restricted to regions in the fluid where no motion can take place because of the no-slip boundary condition. Since at both ends of the frequency spectrum no force exists to do pumping, there must exist an optimum frequency for induction pumping.

6-2 The Slug Flow Model

Since the flow is turbulent the simplest model of the induction pump assumes a flat velocity profile. Furthermore, skin friction between the container walls and fluid are neglected. The geometry used in this investigation is shown in Fig. 6-1. The polyphase windings are arranged so that at $x = \pm x_0$, H_y, the magnetic field in the y direction, is given by

$$H_y(x = \pm x_0, z, t) = H_0 \cos(\omega t - Ky) \tag{6-1}$$

Neglecting heating effects, the motion of the slug of fluid is given by the Maxwell equations and Newton's laws of motion. The Maxwell equations are

$$\nabla \times \vec{E}^* = -\mu_0 \frac{\partial \vec{H}^*}{\partial t} \tag{6-2}$$

$$\nabla \times \vec{H}^* = \vec{J}^* \tag{6-3}$$

$$\nabla \cdot \vec{H}^* = 0 \tag{6-4}$$

where

$$\vec{J}^* = \sigma (\vec{E}^* + \mu_0 \vec{V}^* \times \vec{H}^*) \tag{6-5}$$

and, $\vec{E}^*$, $\vec{H}^*$, $\vec{J}^*$, μ_0, σ, and v^* are the electric field, magnetic field, current density, permeability of free space, conductivity and velocity of the metal, respectively. Newton's Law of motion is

$$\rho \frac{\partial V_x^*}{\partial t} = -\frac{\partial P^*}{\partial y} + \frac{\mu_0}{2x_0} \int_{-x_0}^{x_0} (\vec{J}^* \times \vec{H}^*)_y \, dx \tag{6-6}$$

Here ρ is fluid density, P^* is pressure, and $(\vec{J}^* \times \vec{H}^*)_y$ is the y component of the electromagnetic body force. By combining (6-2), (6-3) and (6-5) there results a wave equation in magnetic field.

$$\nabla^2 \vec{H}^* + \mu_0 \sigma \nabla \times (\vec{V}^* \times \vec{H}^*) = \mu_0 \sigma \frac{\partial \vec{H}^*}{\partial t} \tag{6-7}$$

Since the mechanical relaxation time for liquid metals is of the order of $\rho x_0^2/2\pi\mu$ (here μ is the viscosity), it is seen that this relaxation time is much greater than the electrical period of the lowest frequency used in the polyphase coil. Thus we are interested only in the time averages of velocity and pressure. Then, for steady pumping, (6-6) becomes

$$\frac{\partial P}{\partial y} = \frac{1}{T} \int_0^T \frac{\mu_0}{2x_0} \int_{-x_0}^{x_0} (J^* \times \vec{H}^*)_y \, dx \, dt \tag{6-8}$$

where P is the time averaged pressure and T is the electrical period. The magnetic wave equation becomes

$$\nabla^2 \vec{H}^* + \mu_0 \sigma \nabla \times (V_y \, j \times \vec{H}^*) = \mu_0 \sigma \frac{\partial \vec{H}^*}{\partial t} \tag{6-9}$$

Here j is a unit vector in the y direction.

If, in the alternating current steady state, it is assumed that the time variation is sinusoidal, then a phasor solution is possible in which $j\omega$ replaces $\partial/\partial t$. Also, since the excitation is of the form $H_0 R_e e^{j\omega(t - z/v)}$ where H_0 is the linear current density per unit y dimension of the exciting winding, then

$$\vec{H}^* = [H_x(x)\hat{\imath} + H_y(x)\hat{\jmath}]\, e^{j(\omega t - ky)} \tag{6-10}$$

Upon substituting the phasor quantities into Maxwell's equations, we obtain

$$\left(\frac{d^2}{dx^2} - K^2\right)(H_x\hat{\imath} + H_y\hat{\jmath}) + \mu_0\sigma\left(jK\hat{\imath} + \hat{\jmath}\frac{d}{dx}\right)V_y H_x = j\omega\mu_0\sigma(H_x\hat{\imath} + H_y\hat{\jmath}) \tag{6-11}$$

$$J_z = \frac{dH_y}{dx} + jKH_x \tag{6-12}$$

an

$$\frac{dH_x}{dx} - jKH_y = 0 \tag{6-13}$$

Equation (6-8) becomes

$$\frac{\partial P}{\partial y} = \frac{\mu_0}{2x_0} \mathrm{Re} \int_{-x_0}^{x_0} J_z \bar{H}_x\, dx \tag{6-14}$$

where Re denotes the real part of and $\bar{H}_x$ is the complex conjugate of H_x. The y component of (6-12) must be combined with (6-13) in order to eliminate dH_x/dx. There results

$$\left(\frac{d^2}{dx^2} - \beta^2\right) H_y = 0 \tag{6-15}$$

where

$$\beta^2 = K^2 + j\omega\mu_0\sigma\left(1 - \frac{KV_y}{\omega}\right)$$

The solution to (6-15) which satisfies the boundary condition on $H_y(x = \pm$

$$H_y = \frac{H_0 \cosh \beta x}{\cosh \beta x_0} \tag{6-16}$$

Hy is obtained directly from (6-13) and is

$$H_x = \frac{j K H_o \sinh \beta x}{\beta \cosh \beta x_o} \tag{6-17}$$

From (6-13)

$$J_z = \frac{H_o (\beta^2 - K^2) \sinh \beta x}{\beta \cosh \beta x_o} \tag{6-18}$$

By the use of (6-17), (6-18) and suitable hyperbolic identities

$$\mathrm{Re}\, J_z \bar{H}_x = \frac{\mu_o^2 H_o^2 \omega \sigma K (1 - \frac{KV_x}{\omega})}{\sqrt{K^4 + [\sigma \mu_o \omega (1 - \frac{KV_x}{\omega})]^2}} \quad \frac{\cosh 2\beta_r x - \cos 2\beta_i x}{\cosh 2\beta_r x_o + \cos 2\beta_i x_o} \tag{6-19}$$

where βr and βi are the real and imaginary parts of β respectively. Integrating (6-19) yields

$$\mathrm{Re} \int_{-x_o}^{x_o} J_z \bar{H}_x dx = \frac{\mu_o^2 H_o^2 \omega \sigma K (1 - \frac{KV_x}{\omega})}{\sqrt{K^4 + [\sigma \mu_o \omega (1 - \frac{KV_x}{\omega})]^2}} \quad \frac{\frac{1}{\beta_r} \sinh 2\beta_r x_o - \frac{1}{\beta_i} \sin 2\beta_i x_o}{\cosh 2\beta_r x_o + \cos 2\beta_i x_o} \tag{6-20}$$

where

$$\beta = \frac{1}{x_o \pi_3 \sqrt{2\pi_1}} \left\{ \sqrt{\sqrt{\pi_1^4 + (\pi_2 \pi_3)^4} + \pi_1^2} + j \sqrt{\sqrt{\pi_1^4 + (\pi_2 \pi_3)^4} - \pi_1^2} \right\} \tag{6-21}$$

Let $x_o \pi_3 \beta \sqrt{2\pi_1} = b$ and rearrange (6-20) which becomes

$$\pi_4 = \frac{2 x_o \frac{\partial P}{\partial y}}{\mu_o^2 H_o^2} = \frac{\pi_3 \pi_2 \sqrt{2\pi_1}}{\sqrt{\pi_1^2 + \pi_2^2 \pi_3^2}} \cdot \frac{\frac{1}{b_r} \sinh 2b_r x_o - \frac{1}{b_i} \sin 2b_i x_o}{\cosh 2b_r x_o + \cos 2b_i x_o} \tag{6-22}$$

where $\pi_1 = (X \cdot V_p \mu_0 \sigma)^{-1}$ $V_p = \omega/k$, $\pi_2 = 1 - V_y/V_p$ and $\pi_3 = V_p/\omega x_0$. In (6-22) we have expressed the ratio of driving pressure gradient to maximum magnetic force as a function of slip and frequency. Frequency is contained in all the parameters. If the phase velocity is fixed at a certain value, varying π_1 is equivalent to adjusting x_0 or σ, π_2 to Vy and π_3 to frequency.

The ratio π_4 has been maximized for various values of π_2. The necessary values of π_1 and π_3 are given on Table 6-1 which follows:

π_4	π_2	π_1	π_3	$(2\pi_1\pi_3)^{-\frac{1}{2}}$
0.7[illegible]	0.1	0.025	0.45	6.67
0.714	0.3	0.075	0.45	3.85
0.714	0.5	0.125	0.45	2.98
0.714	0.7	0.175	0.45	2.52
0.711	0.9	0.195	0.40	2.54

Table 6-I - Optimum Values for Induction Pump

The electrical skin depth δ is defined as $\delta = (2/\omega\mu_0\sigma)^{-\frac{1}{2}}$. Under this definition

$$\frac{x_0}{\delta} = (2\pi_1\pi_3)^{-\frac{1}{2}} \tag{6-23}$$

and Table 6-1 shows that for optimum ratio of pressure gradient to applied magnetic force the ratio of pump width ($2x_0$) to skin depth is not zero as some investigators assume. Instead it varies from about 13.3 at 0.1 slip to 5 at 0.7 slip. Of course, these figures are subject to modification in order to include velocity profile effects.

6-3 The Laminar Flow Model

The effects of the velocity profile can be included by adding a viscous term to (6-6). The resulting equation is

$$\rho \frac{\partial V_y^*}{\partial t^*} = -\frac{\partial P^*}{\partial y^*} + \mu \frac{\partial^2 V_y^*}{\partial x^{*2}} + \mu_0 (J^* + H^*) \tag{6-24}$$

The equations governing the flow are (6-24), (6-2), (6-3'), (6-4) and (6-5). However, these equations are rather nonlinear and probably cannot be linearized because the nonlinearity is an essential factor in the optimum flow profile. Rather than solve the nonlinear problem it is possible to replace it with a large number of linear problems. One such scheme considers the fluid to comprise a plurality moving plates. The plates move at slightly different velocities

under the propulsion of the $(\bar{J} \times \bar{B})$ force and exert forces on each other which are proportional to their velocity differences. If a sufficient number of plates are taken the nonlinear problem is the same as the manifold plate model. This is to be a topic of future investigation.

6-4 Conclusion

For a slug model it has been shown that skin effect cannot be completely neglected. This is certainly a reasonable result because the x component of magnetic field and the z component of current density produce the body force. Both of these quantities are induced effects whose strength tends to increase as the skin effects develop. So in order to optimize the design of an electromagnetic pump, the skin effect must be included.

References

1. L. R. Blake, "Conduction and Induction Pumps for Liquid Metals," Proceedings of the I.E.E., 104A, 49-65 (1957).

2. L. P. Harris, "Hydromagnetic Channel Flows" (Book), Technology Press of M.I.T. (1960).

3. J. M. Lyons and D. L. Turcotte, "A Study of Magnetohydrodynamic Induction Devices," ASTIA, AD 272 082 (1962).

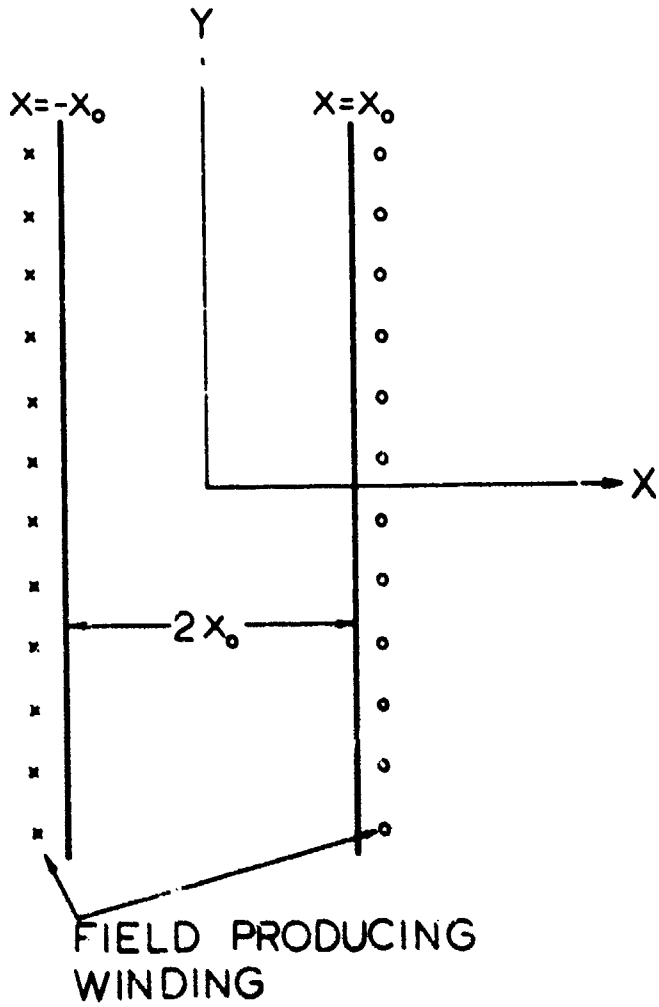

Figure 4-1. Coordinate system for the induction fan.

Section 7

THE SUBSONIC ION MOTOR

7-1 Introduction

In searching the literature for new ways to influence the flow of fluids the contract investigators encountered a brief report[1] concerning a motor apparently driven by ions. This report described a rotor which, when situated in a high electric field would rotate with a large angular velocity. Seeing in this report the possibility of developing a self-contained dielectric pump, the investigators began a preliminary analytical study. The results of this study which will be summarized in the last part of this section, were not encouraging; it is the intent of the investigators to abandon further work in this area with the writing of this section.

7-2 Description of the Apparatus

In 1956 Bemoto[2] gave more information on the phenomenon which he first described in 1955, and he presented experimental evidence later in the same year[3]. The device he used for his experimental work consisted of a pair of electrodes located astride a hollow glass tube filled with a liquid dielectric which served as the rotor, immersed in a bath of liquid dielectric. A schematic of the arrangement is shown in Figure 7-1.

It is observed that when a dielectric cylinder of high permittivity and resistivity is placed between two metal electrodes which are immersed in a polar liquid dielectric of low permittivity it begins to rotate upon application of a high DC potential to the electrodes. The direction of rotation is random and the device continues to rotate in the direction in which it first started. In addition, it was noted that the starting voltage and angular velocity for a given voltage are not reproducible experimental parameters. These preliminary results indicate that the phenomenon is, to a certain extent, statistical in nature.

The two most important requirements for the rotor are a high resistivity to prevent the conduction of charges from the ion layer which forms on the cylinder surface and a high dielectric constant in order to increase the distortion of the electric field between the cylinder and the electrodes. Some solids at low electric field strengths have dielectric constants as high as several thousand but a more typical value for a solid is 3 to 10. However, a high dielectric constant rotor can be fabricated by sealing a liquid such as water (dielectric constant about 80) in a glass rotor.

The physical requirements for the dielectric medium are not completely understood. Bemoto, based on his experimental work, concluded that polar liquids having dielectric constants between acetone (21. and chloroform (5), having resistivities between 10^8 and 10^{11} ohm-cm, can be used successfully.

7-3 The Mechanism of Rotation

When a high potential difference is applied between the parallel electrodes, ions carrying both positive and negative charge are transferred between the electrodes giving rise to a conduction current. Because of the polarization of the cylinder the ions form a layer around the surface of the cylinder, positive for the side facing the positive electrode and negative for the side facing the negative one. As long as the interaction between the ion layer and the electric field remains small, the resulting torque on the cylinder is not sufficient to cause rotation.

However, if the interaction between the field and the ion layer is sufficiently strong and it is no longer co-linear, the cylinder will begin to rotate. Rotation may be initiated by designing an asymmetric field into the device or by supplying a small initial torque to the rotor. Once rotation is begun it will continue provided the current is maintained to keep up the production of ions. The rotor accelerates because of the shift and growth of the ion layer in the downstream direction; this action, in turn, causes an increase in driving torque. Steady rotation is attained when the driving torque is equal to the viscous drag acting on the cylinder.

Figure 7-2 illustrates the charge disposition at any time after the cylinder has attained a steady angular velocity. Consider an arbitrary point Y on the surface of the cylinder. When point Y moves to position P, it starts to accumulate positive charge until a maximum is attained at position m. As point Y moves beyond position m, it starts to lose positive charge until it reaches point P' where it starts to pick up negative charge, attaining the maximum negative charge at position m'.

The ions are considered to have a no slip motion while they are sitting on the cylinder surface. The rate of deposit and withdrawal of ions, and their distribution is believed to depend on the permittivity and resistivity of the cylinder, the field strength, and the angular velocity of the cylinder.

7-4 The analysis

First we consider the overall effectiveness and efficiency of the ion motor. The effectiveness of the motor is the maximum possible output power divided by the power supplied. Since the only portion of the power which can be used for pumping is that due to convection by the ion transfer mechanism described in the previous part, we write

$$\eta_e = \frac{I_c V}{I V} = \frac{I_c}{I} \tag{7-1}$$

where I_c is the convection current and I is the total current due to convection and the initial conduction current. The conversion of $I_c V$ to mechanical power is governed by a mechanical efficiency given by

$$\eta_m = \frac{\omega T}{I_c V} \tag{7-2}$$

Thus the overall efficiency for the rotor-electrode combination is

$$\eta_{all} = \eta_e \eta_m = \frac{I_c V}{I V} \cdot \frac{\omega T}{I_c V} = \frac{\omega T}{I V} \tag{7-3}$$

We now consider the problem of evaluating the electric fields and charge densities required for calculation of the torque and angular velocity of the device. In this section we will merely summarize our results, since they are obtained from a straightforward application of the mathematics of electric fields.

Neglecting end effects, the uniform electric field between a pair of parallel electrodes for a cylindrical boundary as illustrated in Figure 7-3 is

$$\vec{E} = (V/\ell)(\cos\theta\,\vec{a}_\theta - \sin\theta\,\vec{a}_r) \tag{7-4}$$

The distorted electric field inside* and outside the rotating dielectric cylinder is calculated by solving Laplace's equation in cylindrical coordinates for the potential distribution and then finding the gradient of this potential field. Taking into account the electric field induced by the ion layer, the electric field inside the cylinder is

$$\vec{E}_1 = \frac{2K_1}{K_1+K_2} E(\cos\theta\,\vec{a}_\theta - \sin\theta\,\vec{a}_r) \tag{7-5}$$

and outside the cylinder it is

$$\vec{E}_1 = \vec{E}_{1\theta} + \vec{E}_{1r} = \left[\frac{2K_2}{K_1+K_2} E\cos\theta - \frac{\sigma}{\epsilon_1}\right]\vec{a}_\theta - \frac{2K_1}{K_1+K_2} E\sin\theta\,\vec{a}_r \tag{7-6}$$

Considering a control surface on the cylinder and applying the principle of conservation of charge, the differential equation for the charge distribution of the ion layer is

$$\frac{d\sigma}{d\theta} + \frac{\sigma}{\omega\rho\epsilon_1} = \frac{2E}{\omega(K_2+K_1)}\left[\frac{K_2}{\rho_1} - \frac{K_1}{\rho_2}\right]\cos\theta \tag{7-7}$$

*The subscript 1 refers to the dielectric medium while the subscript 2 denotes the rotor.

Neglecting the terms containing the dielectric constant of the medium as being small in comparison with the dielectric constant of the rotor, the particular solution to Equation (7-7) is

$$\sigma_{part} = \frac{\epsilon E \epsilon_0}{(\omega t_{r_1})^2 + 1} \left[\cos\theta + \omega t_{r_1} \sin\theta \right] \tag{7-8}$$

$$= \frac{\epsilon E \epsilon_0}{(\alpha_1^2 + 1)^{1/2}} \cos(\theta - \varphi_1) \tag{7-9}$$

where $\varphi_1 = \tan^{-1} \alpha_1$.

The interactions of the ion layer with the applied field produces the driving torque which is

$$T = \int_0^{2\pi} r \cdot E \sigma b r d\theta = \frac{\pi b r^2 \epsilon E^2 \epsilon_0 \omega t_{r_1}}{(\omega t_{r_1})^2 + 1} \tag{7-10}$$

The convection current is obtained by integrating Equation (7-8) for the charge transferred per unit time, which is

$$I_c = \frac{2\pi r b \epsilon E \epsilon_0 \omega}{\left[(\omega t_{r_1})^2 + 1\right]^{\frac{1}{2}}} \tag{7-11}$$

The frictional torque for a cylinder of radius r rotating in a concentric cylinder of radius $\ell/2$ is given by the well-known expression

$$T_f = \frac{4\pi r^2 \ell^2 \omega \mu b}{\ell^2 - 4r^2} \tag{7-12}$$

Upon equating Equations (7-10) and (7-12) the steady state angular velocity may be obtained as

$$\omega = (t_{r_1})^{-1} \left\{ \left[\epsilon/\mu \right] \left[E^2 \epsilon_0 t_{r_1} \left(\tfrac{1}{4} - (r/\ell)^2 \right) \right] - 1 \right\} \tag{7-13}$$

The results of calculations made with these equations are given in Table 7-1. In general the performance of the ion motor is seen to be poor, as conventional motors offer overall efficiencies in excess of ninety per cent. To convert the mechanical efficiency given in Table 7-1 to the overall efficiency given in Equation (7-1) would require knowledge of the effectiveness; this

quantity may not be evaluated without experimental determination of I, the total current. Table 7-1 also indicates that while the input power is small, the output torque and power are quite limited.

References

1. Inosuke Sumoto, "An Interesti[illegible]menon Observed on Some Dielectrics," Journal of the Physics Society of Japan, Vol. 10, p. 494 (1955).

2. Inosuke Sumoto, "On the Rotary Motion of Dielectrics in the Static Electric Field," Applied Physics, Japan, Vol. 25 (1956).

3. Inosuke Sumoto, "On the Rotary Motion of Dielectrics," Research Institute Report, Japan, Vol. 32, No. 3 (1956).

Nomenclature

a_n = unit vector in the normal direction

a_t = unit vector in the tangent direction

b = length of cylinder, m

E = electric field, volts/m

$\mathcal{E}$ = field distortion constant, $2K_2K_1/(K_2 + K_1)$

I_c = convection current, amps

I = total current, convection plus conduction, amps

K = dielectric constant

ℓ = distance between electrodes, m

r = radius of cylinder, m

t = time, seconds

t_r = relaxation time, $\rho\epsilon$, seconds

T = torque, dyne-cm

V = potential difference, volts

α = relaxation angle, ωt_r, radians

γ = point of interest on rotor

ϵ = permittivity, farad/m

ϵ_o = permittivity of free space, farad/m

η_e = effectiveness of motor, $I_cV/(IV)$, per cent

η_m = mechanical efficiency, $\omega T/(I_cV)$, per cent

η_{all} = overall efficiency, $\omega T/(IV)$, per cent

θ = angle measured from the uniform field line, radians

μ = viscosity, poise

π = 3.141...

ρ = resistivity, ohm-m

σ = charge density of ion layer, coulomb/m^3

φ = $\tan^{-1} \sigma$

ω = angular velocity, rod/sec

Subscripts

1 = the medium

2 = the rotor

n = normal

t = tangent

Table 7-I

The Theorctical Performance of an Ion Motor as a Function of Angular Velocity

ω	100	200	300
α_1 rad.	0.44	0.88	1.32
T dyne-cm	1180	1650	1620
I_c amp.	24.2×10^{-9}	39.5×10^{-9}	47.5×10^{-9}
ωT watts	.0118	.033	.0486
$I_c V$ watts	.0482	.079	.095
η_m %	24.5	41.5	51.2

$\ell = 0.02\,m$ $\qquad$ $\rho_1 = 10^9\,\Omega m$

$r = 0.008\,m$ $\qquad$ $K_1 = 5$

$b = 0.08\,m$ $\qquad$ $K_2 = 80$

$V = 2 \times 10^4$ volts

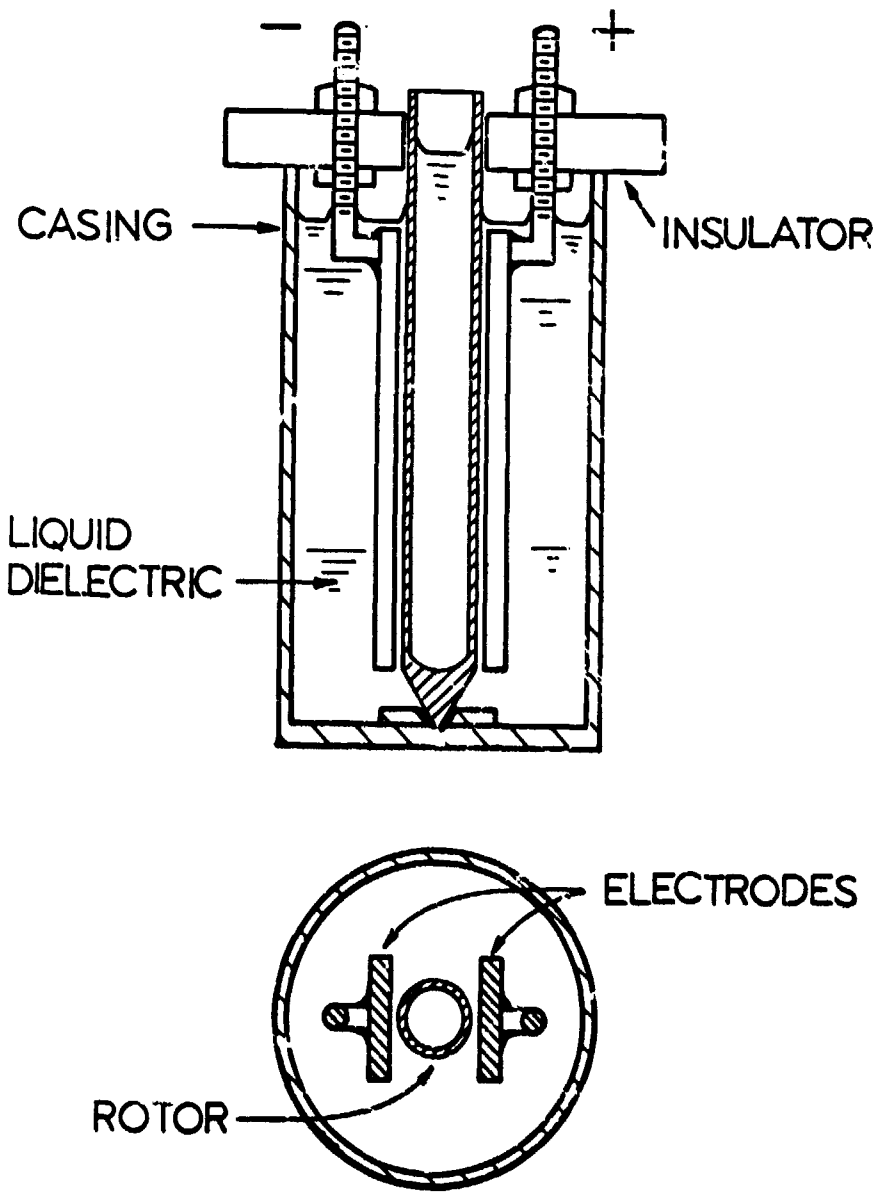

Figure 7-1. Schematic of the Sumoto Ion Motor

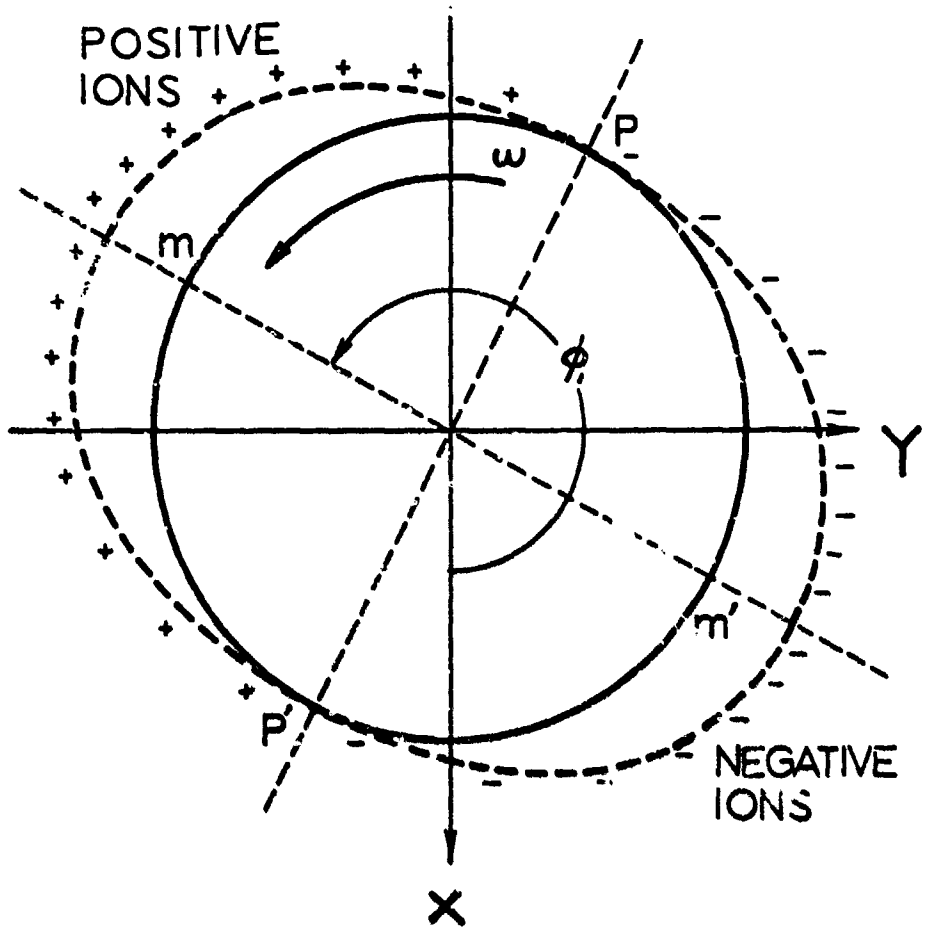

Figure 7-2. The Charge Disposition at any Time after the Cylinder has Attained a Steady Angular Velocity

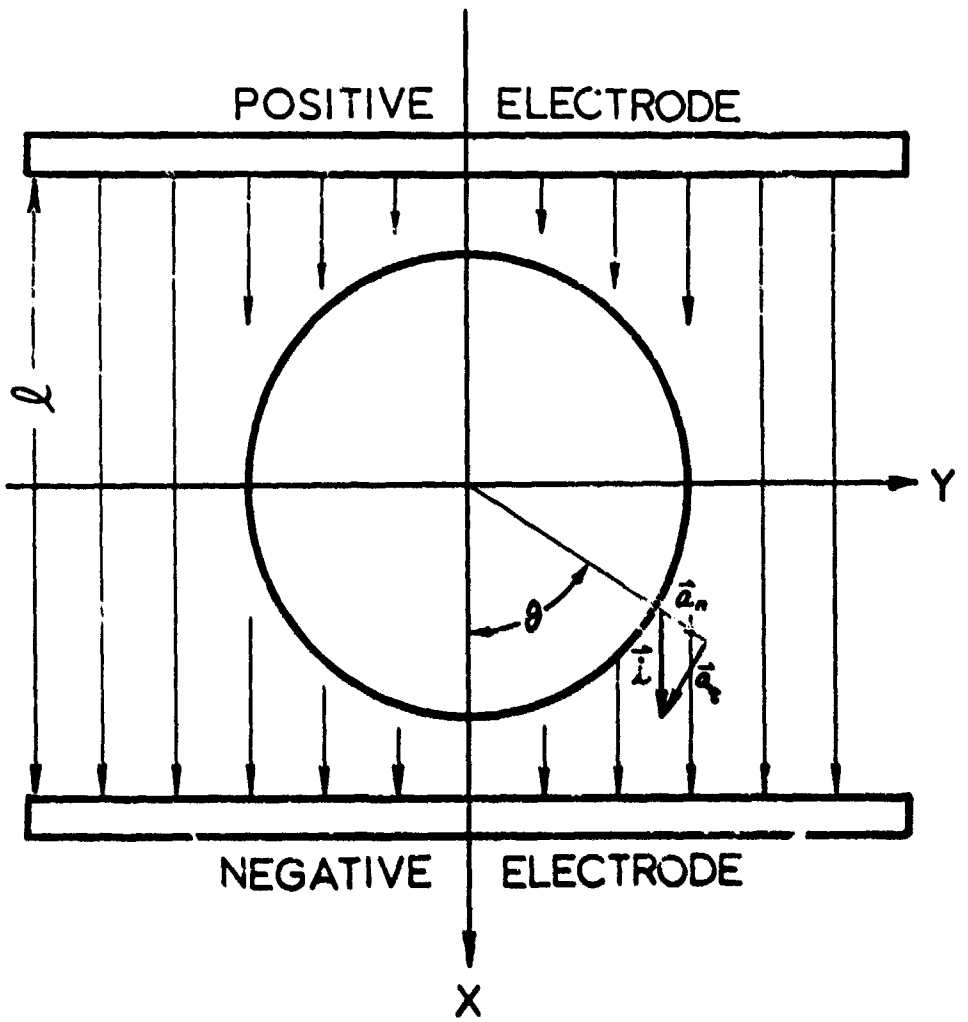

a_n : UNIT NORMAL VECTOR
a_t : UNIT TANGENTIAL VECTOR

Figure 7-3. The Location of the Unit Vectors on a Cylindrical Boundary Inserted Between Plane Parallel Electrodes

Section 8

INFLUENCE OF A MAGNETIC FIELD ON THERMOELECTRIC COOLING

8-1 Introduction

The recent literature[1,2,3,4] indicates a growing interest in applying magnetic fields to certain semiconductors in order to enhance their usefulness in thermoelectric cooling devices. The technique of applying magnetic fields to semiconductors was originally conceived as a means of learning more about the solid state parameters of a material. The most recent work, however, has been directed toward finding a way of improving the figure of merit of a material in order to improve its thermoelectric usefulness.

In order to place the work done on this contract in proper perspective, we will briefly review the principles of thermoelectric refrigeration.

8-2 Thermoelectric Refrigeration

When the ends of two dissimilar materials are joined together and an electric current is passed through the junction, it is found that heat may be pumped from a low temperature reservoir to a high temperature one. It is observed that the heat removed is proportional to the current, the constant of proportionality being the Peltier coefficient for the combination of materials that make up the junction. The Peltier coefficient is defined as

$$\pi = Q/I \quad \text{watts/amp} \tag{8-1}$$

From the second Kelvin relation the Peltier coefficient may be defined in terms of the Seebeck coefficient as

$$\pi = \alpha T \tag{8-2}$$

The performance index which indicates how well a refrigeration device is working is measured by the coefficient of performance, β, and is defined as

$$\beta = Q_c/P \tag{8-3}$$

In order to find the coefficient of performance in terms of material properties, we will analyze the model illustrated in Figure 8-1. Our model is assumed to consist of two cylinders of semiconducting material; in one leg charge is transported by electrons and is designated as an n-type material, in the other, charge is transported by holes* and is designated as a p-type material. We will make the following assumptions about our model:

*A hole is a concept used to describe where an electron is not. See any standard reference on semiconductors for a more complete explanation.

1. Heat transfer takes place to and from the reservoirs only, which are maintained at temperatures T_h and T_c.

2. The device is perfectly insulated except for the ends in contact with the reservoirs.

3. The junction resistance is negligible compared with the bulk resistance of the arms.

4. The arms are of constant cross section along their length.

5. The electrical resistivity, ρ, thermal conductivity, λ, and Seebeck coefficient, α, of the materials making up the couple are constant.

The energy that is removed from the cold reservoir is the sum of three separate terms as follows:

1. The Joule heat delivered to each of the two reservoirs per unit time is

$$\frac{1}{2} I^2 R = \frac{1}{2} I^2 \left[\frac{\rho_n L_n}{A_n} + \frac{\rho_p L_p}{A_p} \right] \tag{8-4}$$

2. The rate of transport of zero-current heat between the two reservoirs is $K\Delta T$ where K is the thermal conductance

$$K\Delta T = (\lambda_n A_n / L_n + \lambda_p A_p / L_p)\Delta T \tag{8-5}$$

3. The rate of Peltier heat absorbed at each reservoir is simply

$$-\pi I_{pn} = -T\alpha I_{pn} \tag{8-6}$$

where I_{pn} is the current flowing from the p arm to the n arm at the junction in question.

In order to evaluate the energy removed from the cold reservoir and to find the coefficient of performance of the device, the three terms must be summed. Since in our model the current flows from the n arm to the p arm at the cold junction, the sign is reversed from that given in equation (8-6). Thus the heat removed is that which is pumped out by the Peltier effect minus that which flows back into the junction by simple conduction and the Joulean heat, thus

$$Q_c = \alpha T_c I - \frac{1}{2} I^2 R - K\Delta T \tag{8-7}$$

The voltage which must be overcome by the power source is the sum of the Seebeck voltage set up by the temperature difference the Peltier effect establishes, and the IR drop across the element, thus

$$V = \alpha \Delta T + IR \tag{8-8}$$

and the power input is simply VI

$$P = \alpha I \Delta T + I^2 R \tag{8-9}$$

From Equation (8-3) we may now find the coefficient of performance by using Equations (8-9) and (8-7) to yield

$$\beta = \frac{f T_c - \frac{1}{2} f^2 - KR \Delta T / \alpha^2}{f \Delta T + f^2} \tag{8-10}$$

where we have defined a new variable, $f = IR/\alpha$

The smaller the product KR, the larger will be the coefficient of performance. If we form the KR product we obtain

$$KR = [\lambda_n \gamma_n + \lambda_p \gamma_p][\rho_n / \gamma_n + \rho_p / \gamma_p] \tag{8-11}$$

where $\gamma_n = A_n/L_n$ and $\gamma_p = A_p/L_p$.

By taking the derivative of KR with respect to γ_n/γ_p and setting the result equal to zero, we find the value that minimizes KR

$$\gamma_n/\gamma_p = (\rho_n \lambda_p / \rho_p \lambda_n)^{\frac{1}{2}} \tag{8-12}$$

The value of KR when γ_n/γ_p has the value given in Equation (8-12) is

$$(KR)_{min} = [(\rho_n \lambda_n)^{\frac{1}{2}} + (\rho_p \lambda_p)^{\frac{1}{2}}]^2 \tag{8-13}$$

Using this value of KR in Equation (8-10) yields

$$\beta = \frac{f T_c - \frac{1}{2} f^2 - \Delta T / Z}{f \Delta T + f^2} \tag{8-14}$$

where

$$Z = \frac{\alpha^2}{\left[(\rho_n \lambda_n)^{\frac{1}{2}} + (\rho_p \lambda_p)^{\frac{1}{2}}\right]^2} \tag{8-15}$$

is called the figure of merit of the couple which will produce the maximum coefficient of performance.

We may now find the value of f which maximizes β, by taking the derivative of Equation (8-14) with respect to f and setting the result equal to zero. The results of this operation are

$$f_{opt} = \frac{\Delta T}{(1 + Z\bar{T})^{\frac{1}{2}} - 1} \tag{8-16}$$

and thus the optimum current to be supplied to the device is

$$I_{opt} = \frac{\alpha \Delta T}{R\left[(1 + Z\bar{T})^{\frac{1}{2}} - 1\right]}$$

The maximum value of the coefficient of performance may be found by substituting Equation (8-16) into Equation (8-14)

$$\beta_{max} = \frac{T_c}{\Delta T}\left[\frac{(1 + Z\bar{T})^{\frac{1}{2}} - T_H/T_c}{(1 + Z\bar{T})^{\frac{1}{2}} + 1}\right] \tag{8-17}$$

The maximum temperature difference can be found by setting the derivative with respect to the current I, of the heat pumping rate [Equation (8-7)] equal to zero to obtain the current which maximizes the heat pumping rate

$$I = \alpha T_c / R$$

This result may be substituted into Equation (8-7) which may then be set equal to zero to obtain the maximum temperature difference with the optimum current flowing

$$\Delta T = \alpha^2 T_c^2 / (2RK)$$

which can be further maximized by using the minimum value of the RK product in the above equation to yield

$$\Delta T_{max} = \frac{1}{2} T_c^2 Z \tag{8-18}$$

It is observed from the above discussion and Equations (8-17) and (8-18) that the larger the figure of merit Z, the greater will be the coefficient of performance, and the maximum temperature difference of a thermoelectric refrigerator. Ure[1], and also Smith and Wolfe[2] have demonstrated that substantial improvements in the figure of merit can be made by application of a magnetic field. It is the purpose of this investigation to explore further the dependence of certain semiconductor's properties on the magnetic flux density.

8-3 The Apparatus

Because there does appear to be some hope in improving the performance of thermoelectric devices by application of magnetic fields, it was decided to construct an apparatus that would let us make measurements to test this hypothesis. The apparatus we designed was to be one which was simple to build and simple to operate. It was designed to collect data which by application of Harman's technique[6] would allow one to find:

1. the Hall voltage,
2. the resistance of the element,
3. the thermal conductivity,
4. the Seebeck coefficient,
5. the Peltier temperature effects.

Thus, once a test sample is installed in the apparatus, a considerable amount of information about the test element may be found.

Figure 8-2 shows a drawing of the vacuum chamber arrangement which holds the specimen. The vacuum chamber is designed to fit between the poles of a permanent magnet*. The vacuum chamber can be evacuated to a pressure of about 10^{-4} mm. Hg, which permits measurements to be made up to temperatures near 375°K using only the Joulean heat of the element. By sealing off the vacuum connections, it is possible to fill the test chamber with a liquified gas in order to make measurements below room temperature.

The current leads to the semiconductor also support the element mechanically, so that the only conductive heat losses from the elements outside of the current leads are the thermocouple leads.

The thermocouples consist of 0.005 in. diameter chromel and constantan wires insulated with 0.001 in. of Teflon. This combination of materials was selected because it offers good resistance to heat transfer. Initially, all leads were connected to the element by means of a silver-conductive epoxy; this material proved to be completely unsatisfactory as its resistance was as much as 50 times that of the test element and fell considerably short of having the properties claimed by the manufacturer. Test elements are now being nickel plated and connections to the elements will be made with soft solder in the

*It can also be used with an electromagnet, but we decided to keep the arrangement as simple as possible initially and use a permanent magnet that was already on hand.

usual fashion. All thermocouple leads are electrically connected to the semiconductor and can also be used for voltage measurements.

A jig has been constructed to hold the semiconductor while the leads are attached. A schematic of the test sample and the leads which are attached to it are shown in Figure 8-3. After the leads are attached, the distance between 4 and 5 must be measured accurately using an optical comparator. This measurement is known as L' and is used in making the resistance calculations. The test rig has built into it an aligning disc which is used to position the semiconductor so that the width dimension is parallel to the magnetic flux lines. The thermocouple and current leads are led out of the vacuum chamber by means of Stupakoff connectors.

The vacuum chamber is then mounted inside of a plywood box which has a peg board front; the front of the box serves as a switching area for connecting instrumentation. The box also tends to isolate the experimental arrangement from drafts.

8-4 The Data Analysis

Early in our work we devised a scheme which is a modification of the one given by Harman[8] to yield the information which is required to detect the influence of the magnetic field on the material properties. We are primarily interested in detecting changes in the figure of merit of a single material which is defined as

$$Z = \alpha^2 / \rho \lambda \tag{8-19}$$

Let us consider the model depicted in Figure 8-4 where (s) denotes the semiconductor and (m) the current leads.

The total energy flux into the cold junction can be written as

$$q_{cs} = \frac{\alpha_s T_c I}{A_s} - \lambda_s \left.\frac{dT}{dx}\right|_{x_s - L/2} \tag{8-20}$$

and similarly for the hot junction

$$q_{hs} = \frac{\alpha_s T_h I}{A_s} - \lambda_s \left.\frac{dT}{dx}\right|_{x_s + L/2} \tag{8-21}$$

Fourier's law of heat conduction, says that in the steady-state the heat out of the element must equal the heat into the element plus the heat generated in the element

$$\lambda_A \frac{d^2T}{dx^2} + \frac{I^2 \rho_A}{A_A^2} = 0 \tag{8-22}$$

with the boundary conditions

$$T = T_c \text{ at } x = -L/2$$
$$T = T_H \text{ at } x = +L/2$$

we find as a solution to Equation (8-22) and its boundary conditions

$$T = -\frac{I^2 \rho_A x^2}{2 A_A^2 \lambda_A} + \frac{T_H - T_c}{L} x + \frac{T_H + T_c}{2} + \frac{I^2 \rho_A L^2}{8 A_A^2 \lambda_A} \tag{8-23}$$

and at $x = -L/2$

$$\frac{dT}{dx} = + \frac{I^2 \rho_A L}{2 A_A^2 \lambda_A} + \frac{T_H - T_c}{L} \tag{8-24}$$

and at $x = +L/2$

$$\frac{dT}{dx} = - \frac{I^2 \rho_A L}{2 A_A^2 \lambda_A} + \frac{T_H - T_c}{L} \tag{8-25}$$

Substituting Equation (8-24) into (8-20) we obtain

$$q_{cA} = \frac{\alpha_A T_c I}{A_A} - \frac{I^2 \rho_A L}{2 A_A^2} - \frac{\lambda_A}{L} (T_H - T_c) \tag{8-26}$$

and substituting Equation (8-25) into (8-21) one finds

$$q_{HA} = \frac{\alpha_A T_H I}{A_A} + \frac{I^2 \rho_A L}{2 A_A^2} - \frac{\lambda_A}{L} (T_H - T_c) \tag{8-27}$$

A similar set of equations can be developed for the current leads to yield

$$q_{c_m} = \frac{\alpha_m T_c I}{A_m} + \frac{I^2 \rho_m \ell_m}{2 A_m^2} - \frac{\lambda_m}{\ell_m} (T_c - T_a) \tag{8-28}$$

and

$$q_{Hm} = \frac{\alpha_m T_H I}{A_m} + \frac{\lambda_m}{l_m}(T_H - T_a) - \frac{I^2 \rho_m l_m}{2 A_m^2} \tag{8-29}$$

Applying the conservation of energy to each junction, that is

$$q_{Hm} = q_{Hs}$$

and

$$q_{cm} = q_{cs}$$

we obtain for the hot junction

$$\left(\frac{\alpha_m}{A_m} - \frac{\alpha_s}{A_s}\right) T_H I - \frac{I^2}{2}\left(\frac{\rho_m l_m}{A_m^2} + \frac{\rho_s L}{A_s^2}\right) + \frac{\lambda_m}{l_m}(T_H - T_a) + \frac{\lambda_s}{L}(T_H - T_c) = 0 \tag{8-30}$$

and for the cold junction

$$\left(\frac{\alpha_m}{A_m} - \frac{\alpha_s}{A_s}\right) T_c I + \frac{I^2}{2}\left(\frac{\rho_m l_m}{A_m^2} + \frac{\rho_s L}{A_s^2}\right) - \frac{\lambda_m}{l_m}(T_c - T_a) + \frac{\lambda_s}{L}(T_H - T_c) = 0 \tag{8-31}$$

Combining Equations (8-30) and (8-31) yields

$$\left(\frac{\alpha_m}{A_m} - \frac{\alpha_s}{A_s}\right)(T_H + T_c) I + \left(\frac{\lambda_m}{l_m} + \frac{2\lambda_s}{L}\right)(T_H - T_c) = 0 \tag{8-32}$$

If the current leads are made of a common material, then the thermal conductivity of that material is generally known. However, an experimentally determined value can be found by biasing the sample with an AC voltage, in which case $T_H = T_c$ and Equation (8-28) becomes

$$q_m = \frac{I^2 \rho_m l_m}{2 A_m^2} - \frac{\lambda_m}{l_m}(T - T_a) \tag{8-33}$$

and Equation (8-26) becomes

$$q_s = -\frac{I^2 \rho_s L}{2 A_s^2} \tag{8-34}$$

since conservation of energy requires $q_s = q_m$, we obtain

$$\frac{I^2 \rho_m l_m}{2 A_m^2} - \frac{\lambda_m}{l_m}(T - T_a) = \frac{-I^2 \rho_s L}{2 A_s^2}$$

or

$$\lambda_m = \frac{l_m I^2}{2}\left[\frac{R}{(T - T_a)}\right] \tag{8-35}$$

where

$$R = \frac{\rho_m l_m}{A_m^2} + \frac{\rho_s L}{A_s^2} \tag{8-36}$$

Thus, to find the thermal conductivity of the lead material requires that we know the electrical resistivity of the semiconductor as a function of temperature.

We may now find the thermal conductivity of the semiconductor from Equation (8-32) as

$$\lambda_s = -\frac{I L}{\Delta T}\frac{(T_h + T_c)}{2}\left[\frac{\alpha_m}{A_m} - \frac{\alpha_s}{A_s}\right] - \frac{L}{2}\frac{\lambda_m}{l_m} \tag{8-37}$$

but $(T_H + T_c)/2 = \bar{T}$ and α_m will be negligible in comparison with α_s, so Equation (8-37) may be approximated by

$$\lambda_s \approx \frac{\alpha_s I L \bar{T}}{A_s \Delta T} - \frac{L}{2}\frac{\lambda_m}{l_m} \tag{8-38}$$

which is the same as Harman's result except for the lead terms.

In order to determine the thermal conductivity by Equation (8-38) it is necessary to know α_s and ρ_s. The latter quantity can be determined by AC measurements but the former requires both AC and DC measurements. These measurements

are made using the combination thermocouple and voltage pickups. Figure 8-5 illustrates the experimental arrangement which is used in determining the Seebeck coefficient and electrical resistivity of the sample. We use the subscripts cr to denote a chromel and co to denote a constantan thermocouple.

By impressing an AC voltage on the sample the temperature of the sample will remain uniform. The voltage drop in the sample in the length L' is then measured with leads $(4\text{-}5)_{co}$ or $(4\text{-}5)_{cr}$

$$V_{L'} = (V_{4-5})_{co} = (V_{4-5})_{cr}$$

and

$$V_L = (V_{3-8})_{co} = (V_{3-8})_{cr}$$

Then at the measured temperature the electrical resistivity is

$$\rho_s = \frac{V_{L'} A_s}{I L'} \tag{8-39}$$

By impressing a DC voltage on the sample the Seebeck coefficient can be measured. The Seebeck coefficient is defined as

$$\alpha = \frac{V_\alpha}{\Delta T}$$

where

$$V_\alpha = \pm \left[\tfrac{1}{2}(V_L^+ + V_L^-) - V_L\right] + \alpha_t \Delta T \tag{8-40}$$

and

$V_L^+ = (V_{3-8})_{co} = (V_{3-8})_{cr}$ with the current in the positive direction.

$V_L^- = (V_{3-8})_{co} = (V_{3-8})_{cr}$ with the current in the negative direction.

$V_L = (V_{3-8})_{co} = (V_{3-8})_{cr}$ measured with the AC voltage impressed on the sample.

α_t = the Seebeck coefficient of the thermocouple lead used for the voltage drop measurement.

$\Delta T = (T_H - T_c)$ the measured temperature difference caused by the DC current.

In order to maintain consistency, it is necessary to measure all voltage drops with thermocouple leads of the same material - that is all voltage measurements must be made with either chromel or constantan leads, for example

$$V_\alpha = \pm\left[\frac{1}{2}\left(V^{+}_{L(co)} + V^{-}_{L(co)}\right) - V_{L(co)}\right] + \alpha_t \Delta T$$

The sign of the Seebeck coefficient depends on whether or not the Seebeck coefficient is plus or minus. Note that the average DC voltage drop must be found by taking readings with the current going in both directions in order to eliminate the thermal EMF induced by the Peltier effect at the junctions. V_L is the voltage drop measured under AC conditions at the average temperature of the element, $\frac{1}{2}(T_H + T_c)$.

The figure of merit can now be calculated from the thermal conductivity, Seebeck coefficient and electrical resistance of the element. This analysis has neglected radiation and conduction heat transfer to and from the element. Harman[6] has indicated, however, that such effects are generally considered to be negligible at or below room temperature.

8-5 Results

As of the date of this report, final reassembly of the apparatus is nearing completion. Problems associated with the silver conductive epoxy resin caused delays not anticipated in the original scheduling of the experimental work. Preliminary work done on samples before the epoxy problem became critical indicate that changes in properties caused by application of the magnetic field will be significant.

References

1. R. W. Ure, Jr., "Theory of Materials for Thermoelectric and Thermomagnetic Devices," Proceedings of the IEEE, Vol. 51, pp. 699-713 (1963).

2. G. E. Smith and R. Wolfe, "Thermoelectric Properties of Bismuth-Antimony Alloys," Journal of Applied Physics, Vol. 33, pp. 841-846 (1962).

3. R. Wolfe and G. E. Smith, "Experimental Verification of the Kelvin Relation of Thermoelectricity in a Magnetic Field," Physical Review, Vol. 129, pp. 1086-1087 (1963).

4. R. Wolfe, G. E. Smith and S. E. Haszko, "Negative Thermoelectric Figure of Merit in a Magnetic Field," Applied Physics Letters, Vol. 2, pp. 157-159 (1963).

5. R. A. Smith, Semiconductors (Cambridge: Cambridge University Press, 1959).

6. T. C. Harman, J. H. Cahn and M. J. Logan, "Measurements of Thermoelectric Properties by Using the Peltier Heat" in Thermoelectricity, ed. P. H. Egli (New York: John Wiley & Sons, Inc., 1960).

Nomenclature

A = area, cm^2

B = magnetic flux density, gauss

f = IR/α, degrees C

I = current, amperes

K = thermal conductance, watts/°C

ℓ = lead length, cm

L = sample length, cm

L' = distance between thermocouples 4 and 5, cm

P = power input, watts

q = heat transfer density, watts/cm^2

Q = heat transfer, watts

R = electrical resistance, ohms

T = temperature, degrees K

$\bar{T}$ = average temperature, $\frac{1}{2}(T_H + T_C)$, degrees K

V = voltage

x = coordinate

Z = figure of merit, $(\text{degrees K})^{-1}$

α = Seebeck coefficient, volts/°C

β = coefficient of performance

γ = ratio of area to length, cm

λ = thermal conductivity, watt/cm-°C

π = Peltier coefficient, watts/amp

ρ = electrical resistivity, ohm-cm

Subscripts

a = ambient

c = cold

co = constantan

cr = chromel

H = hot

m = current lead

max = maximum

min = minimum

n = due to electrons

opt = optimum

p = due to holes

s = sample

t = thermocouple

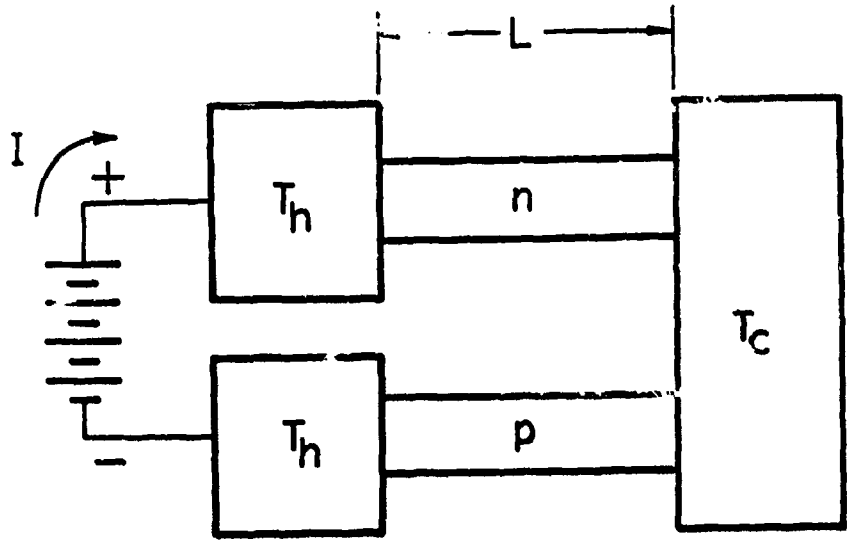

Figure 8-1. A Thermoelectric Refrigerator

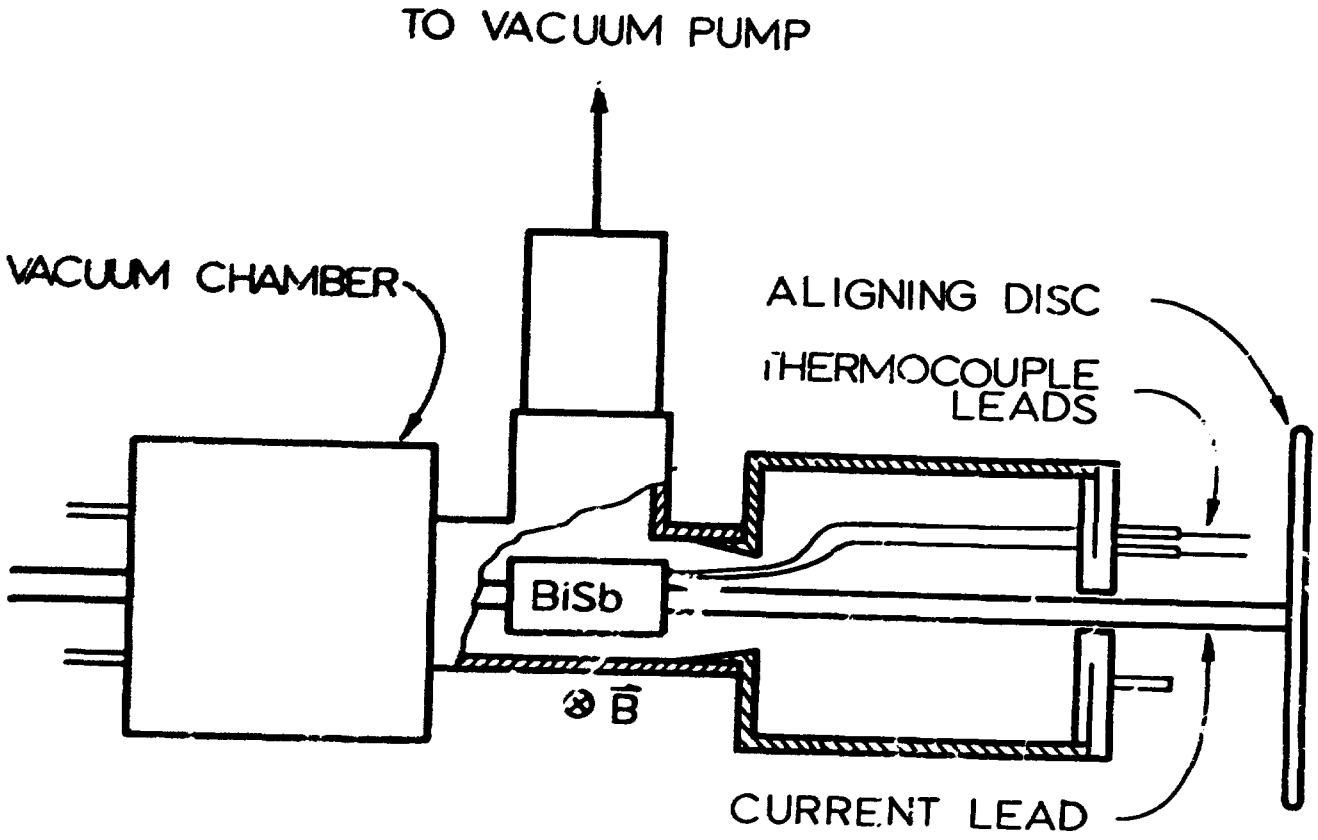

Figure 8-2. A Schematic of the Vacuum Chamber Arrangement for Finding the Effect the Magnetic Field has on the Properties of a Semiconductor

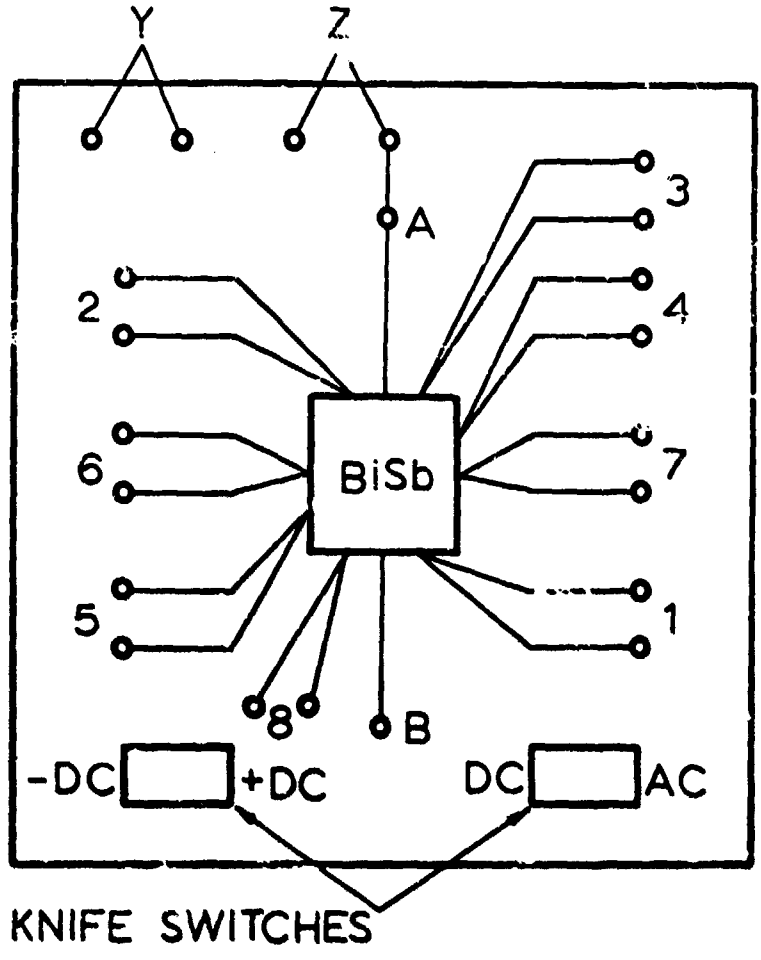

Y : CONNECTOR FOR EXTERNAL RESISTANCE

Z : CONNECTOR FOR AMMETER

A, B : VOLTAGE DROP CONNECTORS

1-8 : CHROMEL CONSTANTAN THERMOCOUPLES

Figure 8-3. A Schematic of the Test Element Showing the Location of the Thermocouple Connections and Current Leads

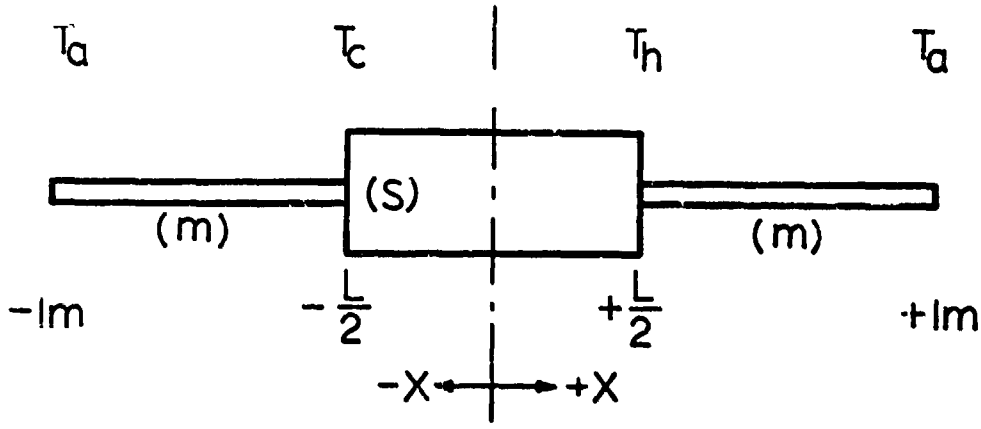

Figure 8-4. A Pictorial Representation of the Mathematical Model Used in Deriving the Property Relationships

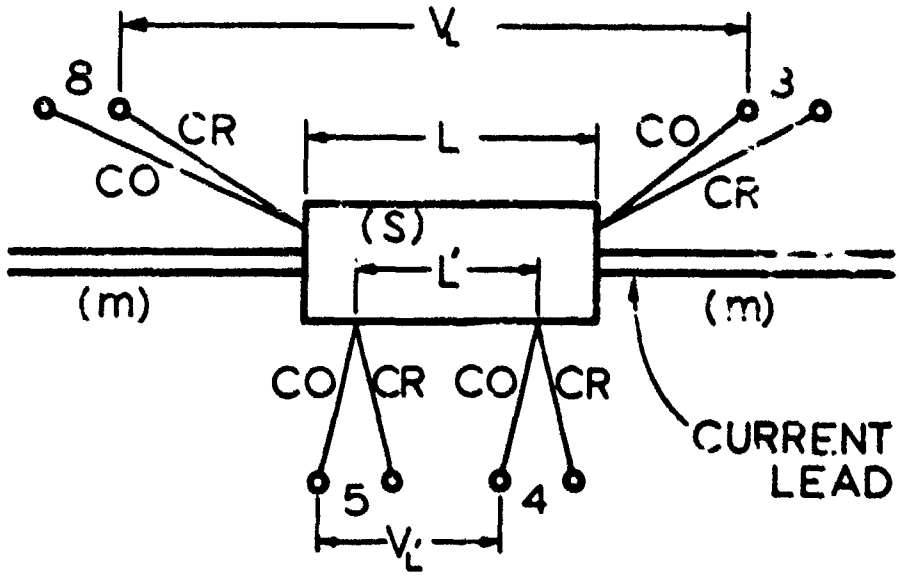

Figure 8-5. The Experimental Arrangement Used for Measuring the Seebeck Coefficient and Electrical Resistivity of the Sample

Section 9

DECONTAMIN... BY DIELECTROPHORESIS

9-1 Introduction

Interest in finding ways to remove contaminating particles, on the order of 25 microns in diameter, from fluids used in various systems has grown to considerable proportions in the last few years. This growth is due, to a large extent, to the growing complexity and sensitivity of systems to contaminants which a few years ago were considered tolerable. In trying to find ways to remove these unwanted materials from a fluid, investigators have sought means of applying body forces to the fluid-contaminant mixture, which would result in a greater force being exerted on the contaminating particles than on the fluid and would, therefore, continuously reduce the concentration of contaminant.

There are two electrical forces which can be used to achieve this goal; electrophoresis which is discussed in Volume III, "Ion Drag Pressurization," and dielectrophoresis which will be considered in this section. The dielectrophoretic force would be of use in removing matter which polarizes when situated in a dielectric fluid. Pohl[1] has set forth in a very clear manner the difference between dielectrophoresis and electrophoresis. We briefly summarize his work here.

Dielectrophoresis arises because of the tendency of polarized material to move into regions of high field strength. Its salient features are as follows:

1. It produces particle motion independent of the direction of the field, therefore, AC or DC voltages may be employed.

2. It is most readily observable in coarse suspensions - that is with particle diameters greater than 2 microns.

3. It requires highly divergent fields.

4. It requires high electric field strengths with fields greater than 2000 volts/cm.

5. It would be most apparent in fluids with low viscosity.

6. It generally requires a large difference ($K_2 - K_1 \approx 2 - 100$) in dielectric constants between the solvent and the solute.

7. It will deposit weights of heavy contaminants in direct proportion to the voltage applied in equal times of deposition.

Electrophoresis arising from the electrostatic attraction of charged particles for charged electrodes, on the other hand, is characterized by the following features:

1. It produces particle motion which is dependent on the direction of the field. Reversal of the field reverses the direction of travel of the particles.

2. It is observable with particles of any molecular size.

3. It operates in either uniform or divergent fields.

4. It requires relatively low voltages.

5. It requires a relatively small charge per unit volume of particles.

Most of the work using dielectrophoresis has been concerned with the separation of powders of different dielectric constants and with some batch separation of liquids[1,2,3,4]. It is our intent, initially, to analytically explore the feasibility of using dielectrophoresis to remove contaminants as small as 25 microns from a fluid; this work would be followed by simple experiments designed to verify our analysis.

9-2 Results of the Preliminary Work

Since beginning work on this subject in April of this year, we have begun analytical examinations of the following problems:

1. A determination of the gradient of a non-uniform electric field between concentric cylinders, divergent concentric cones, concentric spheres and divergent plates. These problems are important because the dielectrophoretic force depends on the gradient of the electric field rather than the field strength itself.

2. The force acting on a spherical particle in a non-uniform electric field.

3. The dynamics of a particle in a hydrostatic field.

4. The motion of a particle in a force field consisting of an electric force and viscous drag force. The results of this analysis is a second order, third degree differential equation, requiring in all likelihood, a numerical solution.

5. A consideration of the magnitude of the Magnus effect in various contaminant-fluid mixtures in order to determine under which conditions must this force be taken into account in dielectrophoretic separation.

9-3 Work Proposed for the Next Year

In the next phase of our work we hope to complete the analytical work started and discussed in Section 9-2. In addition we hope to design an experimental apparatus which would allow us to begin the verification of theoretical work done by others in this area.

References

1. H. A. Pohl, "Some Effects of Nonuniform Fields on Dielectrics," Journal of Applied Physics, Vol. 29, pp. 1182-1188 (1958).

2. H. A. Pohl, "Nonuniform Field Effects in Poorly Conducting Media," Journal of the Electrochemical Society, Vol. 107, pp. 386-390 (1960).

3. H. A. Pohl and J. P. Schwar, "Particle Separation by Nonuniform Electric Fields in Liquid Dielectrics, Batch Methods," Journal of the Electrochemical Society, Vol. 107, pp. 383-385 (1960).

4. H. A. Pohl and C. E. Plymale, "Continuous Separations of Suspensions by Nonuniform Electric Fields in Liquid Dielectrics," Journal of the Electrochemical Society, Vol. 107, pp. 390-396 (1960).

Section 10

ATTENUATION OF PRESSURE SURGES BY TAPERED PIPES

10-1 Abstract

A tapered pipe changes the magnitude of impressed pressure of volume flux pulses, much as an electrical transformer. It also distorts the pulse shape depending on the geometry of the taper.

In this section an analysis is made of the propagation of a short pulse of volume flux through an inviscid liquid that is initially flowing at a constant rate. Such a pulse would result in practice if a valve at the discharge end of the tapered section were suddenly closed then suddenly opened. It is shown that a correctly oriented taper can reduce the resulting surge pressures.

10-2 Introduction

If a valve at the end of a pipe through which fluid is flowing is suddenly closed, a pressure wave is produced which propagates upstream. The magnitude of this pressure wave may be very great and cause damage to pipe and fittings. This can be a particularly serious problem in pipelines used to transport cryogenic liquids because metals may be brittle at low temperatures and subject to fracture.

The purpose of this section is to analyse the effect of tapering a section of the pipe in order to reduce the magnitude of the surges. At this time only surges (or "pulses") of short duration will be considered; we hope to carry out an analysis of long duration pulses at a later date. The present work will apply to pressure pulses that result when a valve is suddenly closed and suddenly reopened after a short interval. Paynter and Ezekiel[1] made an approximate analysis of the tapered pipe by breaking it into several uniform sections, but the present analysis is more exact and shows that the shape (or distortion) of the pulses depends on the particular way the pipe is tapered.

The liquid is assumed to be inviscid. (We hope to remove this assumption in subsequent work.) The analysis also assumes one-dimensional flow, which restricts it to tapered pipes in which the changes in the lateral dimension are small compared to the corresponding changes in length[2]. A rigid pipe is also assumed.

10-3 Basic Equations

The flow of a compressible inviscid fluid is completely described by the following equations:

Euler $$\rho \frac{D\vec{W}}{Dt} = -\nabla p \qquad (10\text{-}1)$$

Continuity

$$\nabla \cdot \rho \vec{w} + \frac{\partial \rho}{\partial t} = 0 \tag{10-2}$$

State

$$K = \rho \frac{\partial P}{\partial \rho} \tag{10-3}$$

where w is the fluid velocity, ρ is density, t is time, p is pressure, and K is the isothermal bulk compression modulus.

The usual acoustic approximation will be made; i.e., the convective acceleration is negligible compared to the local acceleration and the variations in density are small[3]. For liquids these assumptions are valid for all reasonable fluid velocities (say, less than 40 ft/sec) and pressure pulses on the order of thousands of pounds per square inch[4]. With these assumptions the axial component of the Euler Equation (10-1) becomes

$$\frac{\partial P}{\partial x} = -\rho_o \frac{\partial u}{\partial t} \tag{10-4}$$

where x is the axial coordinate (Figure 10-1), ρ_o is the mean density and u is the x-component of the fluid velocity. Since one-dimensional (plane) flow has been assumed, p and u are functions only of x and t. Averaging Equation (10-4) across an arbitrary cross section of area A(x) thus gives

$$\frac{\partial P}{\partial x} = -\frac{\rho_o}{A(x)} \frac{\partial \bar{q}}{\partial t} \tag{10-5}$$

where $\bar{q}(x,t)$ is the volume flux at x, given by

$$\bar{q} \equiv \int_A u \, dA \tag{10-6}$$

Averaging the continuity Equation (10-2) over a cross section of the channel, and utilizing the equation of state (10-3) to eliminate density gives

$$\frac{\partial \bar{q}}{\partial x} = -\frac{A(x)}{K} \frac{\partial P}{\partial t} \tag{10-7}$$

Equations (10-5) and (10-7) are the basic equations describing pulse behavior. Their derivation is discussed in greater detail in Appendix I.

Initially, the liquid in the pipe will be assumed to be flowing at a constant rate q_o in the negative x direction (toward the valve). The pressure in the pipe will be assumed to be constant, with a magnitude p_o. p will henceforth be regarded as the difference between the actual pressure and p_o.

It will be convenient to define a new variable

$$\bar{q}(x,t) = \bar{q}(x,t) + q_o \tag{10-8}$$

Since $\bar{q}(x,0) = -q_o$ the initial conditions for q and p are

$$q(x,0) = 0 \tag{10-9a}$$

$$p(x,0) = 0 \tag{10-9b}$$

The boundary condition at $x = 0$ is that the flow is suddenly stopped for a short time τ and then allowed to resume at its initial rate. Thus

$$q(0,t) = \begin{cases} 0 & t = 0 \\ q_o & 0 < t < \tau \\ 0 & \tau < t \end{cases} \tag{10-10}$$

The second boundary condition is that at $x = L$ the tapered pipe is terminated by a very long rigid tube having a constant cross-sectional area A(L). This boundary condition is utilized in terms of the acoustic impedance at $x = L$.

10-4 Solution of Equations

Equation (10-8) is substituted in Equations (10-5) and (10-7) and the Laplace transform is taken of the resulting equations in conjunction with the initial conditions (10-9). These operations give

$$\frac{dP}{dx} = -\ell s Q \tag{10-11}$$

$$\frac{dQ}{dx} = -cs P \tag{10-12}$$

where P(x,s) and Q(x,s) are the Laplace transforms of p(x,t) and q(x,t), and

$$\ell \equiv \frac{\rho_o}{A(x)} \tag{10-13}$$

$$C \equiv \frac{A(x)}{K} \tag{10-14}$$

The Laplace transform of the boundary condition at x = 0, Equation (10-10), is

$$Q(0,s) = \frac{q_{ie}}{s}\left(1 - e^{-s\tau}\right) \tag{10-15}$$

At x = L, the boundary condition is shown in Appendix II to be

$$Z(L,s) = \sqrt{\ell'/c'} \tag{10-16}$$

where Z(L,s) is the acoustic impedance at x = L, and

$$\ell' \equiv \frac{\rho_o}{A(L)} \tag{10-17}$$

$$C' \equiv \frac{A(L)}{K} \tag{10-18}$$

The most convenient form of the differential equations is obtained by differentiating and combining Equations (10-11) and (10-12), giving

$$\ell^2 C s^3 P + \dot{\ell} s \dot{P} - \ell s \ddot{P} = 0 \tag{10-19}$$

$$\ell C^2 s^3 Q + C s \dot{Q} - C s \ddot{Q} = 0 \tag{10-20}$$

where

$$\cdot \equiv \frac{d}{dx}$$

A solution will first be obtained for Q and then the inverse Laplace transform found. Using this solution for Q in conjunction with the acoustic impedance a solution for P and its inverse follows easily.

(a) Volume Flux

Following Stapelfeldt[5] a solution for Q of the form

$$Q = C\, e^{-\Gamma(x,s)} \tag{10-21}$$

is assumed, which when substituted in Equation (11-20) gives

$$C s \dot{\Gamma}^2 + \dot{C} s \dot{\Gamma} - C s \ddot{\Gamma} = \ell C^2 s^2 \tag{10-22}$$

This is a Riccati differential equation in $\dot{\Gamma}$ which may be solved in terms of the power series

$$\dot{\Gamma} = b_1 s + b_0 + b_{-1}\frac{1}{s} + \cdots \tag{10-23}$$

Substituting Equation (10-23) into Equation (10-22) and equating coefficients of like powers of s gives

$$b_1 = m\sqrt{\ell C}$$

$$b_0 = \frac{1}{4}\left(\frac{\dot{\ell}}{\ell} - \frac{\dot{C}}{C}\right)$$

$$b_{-1} = \frac{m}{\sqrt{\ell C}}\left[\frac{7}{32}\frac{\dot{C}^2}{C^2} - \frac{5}{32}\frac{\dot{\ell}^2}{\ell^2} - \frac{1}{16}\frac{\dot{\ell}\dot{C}}{\ell C} + \frac{1}{8}\left(\frac{\ddot{\ell}}{\ell} - \frac{\ddot{C}}{C}\right)\right] \tag{10-24}$$

where $m = \pm 1$. $m = +1$ corresponds to a wave traveling in the +x direction and $m = -1$ corresponds to a wave traveling in the -x direction.

Since C is an arbitrary constant it is permissible to take

$$\Gamma = \int_0^x \frac{d\Gamma}{d\xi}\, d\xi \tag{10-25}$$

Thus,

$$\Gamma = ms\int_0^x \sqrt{\ell C}\, d\xi + \frac{1}{4}\int_0^x \left(\frac{\dot{\ell}}{\ell} - \frac{\dot{C}}{C}\right) d\xi + \frac{1}{s}\int_0^x b_{-1}\, d\xi + \cdots \tag{10-26}$$

From the boundary condition at x = 0, Equation (10-15)

$$C = \frac{q_0}{s}\left(1 - e^{-s\tau}\right), \tag{10-27}$$

and

$$Q^+(x,s) = \frac{q_0}{s}\left(1-e^{-s\tau}\right)e^{-s\int_0^x \sqrt{\ell c}\, d\xi - \frac{1}{4}\int_0^x \left(\frac{\dot{\ell}}{\ell} - \frac{\dot{c}}{c}\right) d\xi - \frac{1}{s}\int_0^x b_{-1}^+ d\xi + \cdots} \tag{10-28}$$

where the superscript + indicates m = +1.

The acoustic impedance Z is defined by

$$Z(x,s) \equiv \frac{P(x,s)}{Q(x,s)} \tag{10-29}$$

Differentiating Z and utilizing Equations (10-11) and (10-12) gives

$$\frac{dZ}{dx} = cs\,Z^2 - \ell s, \tag{10-30}$$

which is a Riccati differential equation. For a solution let

$$Z = f_0 + \frac{f_{-1}}{s} + \frac{f_{-2}}{s^2} + \cdots \tag{10-31}$$

Inserting this series in Equation (10-30) and equating coefficients of like powers of s yields

$$Z = m\sqrt{\frac{\ell}{c}} + \sqrt{\frac{\ell}{c}}\left\{\frac{1}{4\sqrt{\ell c}}\left[\frac{\dot{\ell}}{\ell} - \frac{\dot{c}}{c}\right]\right\}\frac{1}{s} + \cdots \tag{10-32}$$

where m = +1 gives the impedance for a wave traveling in the +x direction and m = -1 is that for a wave traveling in the -x direction.

The equations for Q and Z are employed to determine the volume flux at x = L. Note that

$$Q(L,s) = Q^+(L,s) \times \frac{Q(L,s)}{Q^+(L,s)} \tag{10-33}$$

The quantity $Q(L, s)/Q^+(L, s)$ can be expressed in terms of the terminal acoustic impedance $Z(L, s)$ as follows: At $x = L$

$$Z(L,s) = \frac{P(L,s)}{Q(L,s)} = \frac{P^+(L,s) + P^-(L,s)}{Q^+(L,s) + Q^-(L,s)} \tag{10-34}$$

where the superscript denotes a wave traveling in the -x direction (m = -1). Also

$$Z^+(L,s) = P^+(L,s)/Q^+(L,s) \tag{10-35}$$

$$Z^-(L,s) = P^-(L,s)/Q^-(L,s) \tag{10-36}$$

Combining Equations (10-34), (10-35) and (10-36) gives

$$\frac{Q(L,s)}{Q^+(L,s)} = \frac{Z^-(L,s) - Z^+(L,s)}{Z^-(L,s) - Z(L,s)} \tag{10-37}$$

In terms of the series solution for $\phi(x, s)$, Equation (10-32)

$$\frac{Z^-(L,s) - Z^+(L,s)}{Z^-(L,s) - Z(L,s)} = \frac{2\sqrt{\frac{\rho}{c}}}{\sqrt{\frac{\rho}{c}} + Z}\bigg|_{x=L} + \left\{ \frac{\frac{1}{2c}\sqrt{\frac{\rho}{c}}\left[\frac{\dot{\rho}}{\rho} - \frac{\dot{c}}{c}\right]}{\left(\sqrt{\frac{\rho}{c}} + Z\right)^2}\bigg|_{x=L} \right\} \frac{1}{s} + \cdots \tag{10-38}$$

From Equations (10-28), (10-33), (10-37) and (10-38), then,

$$Q(L,s) = 2\rho_0 \left\{ \frac{\sqrt{\frac{\rho}{c}}}{\sqrt{\frac{\rho}{c}} + Z}\bigg|_{x=L} \right\} \times$$

$$\left\{ \frac{(1 - e^{-sT})}{s} e^{-s\int_0^L \sqrt{\rho c}\, dx} - \frac{1}{4}\int_0^L \left(\frac{\dot{\rho}}{\rho} - \frac{\dot{c}}{c}\right) dx - \frac{1}{s}\int_0^L b_{-1}^+ \, dx \right\} \times$$

$$\left\{ 1 + \frac{\frac{1}{4c}\left(\frac{\dot{\rho}}{\rho} - \frac{\dot{c}}{c}\right)}{\left(\sqrt{\frac{\rho}{c}} + Z\right)}\bigg|_{x=L} \frac{1}{s} \right\} \tag{10-39}$$

Considerable simplification of the equation is possible. Note that

$$\left.\frac{\sqrt{\frac{\ell}{c}}}{\sqrt{\frac{\ell}{c}}+2}\right|_{x=L} = \frac{\sqrt{\frac{\ell'}{c'}}}{\sqrt{\frac{\ell'}{c'}}+\sqrt{\frac{\ell'}{c'}}} = \frac{1}{2} \tag{10-40}$$

$$e^{-s\int_0^L\left(\frac{\dot{\ell}}{\ell}-\frac{\dot{c}}{c}\right)dx} = \left[\frac{\sqrt{\frac{\ell}{c}}\Big|_{x=0}}{\sqrt{\frac{\ell}{c}}\Big|_{x=L}}\right]^{\frac{1}{2}} = \left[\frac{A(L)}{A(0)}\right]^{\frac{1}{2}} \tag{10-41}$$

and

$$\frac{1}{\ell c} = \frac{K}{\rho_0} = a^2 = \text{constant}\ , \tag{10-42}$$

where a is the velocity of wave propagation. With the introduction of Equations (10-40), (10-41) and (10-42), Equation (10-34) becomes

$$Q(L,s) = \frac{q_0}{2}\left[\frac{A(L)}{A(0)}\right]^{\frac{1}{2}}\left[e^{-\frac{sL}{a}} - e^{-s\left(\tau+\frac{L}{a}\right)}\right]f(s) \tag{10-43}$$

where

$$f(s) = \frac{1}{s}e^{-\frac{\ell}{s}} + \frac{a}{4}\frac{\dot{\ell}}{\ell}\Big|_{x=L}\frac{1}{s^2}e^{-\frac{\ell}{s}} \tag{10-44}$$

and

$$\ell = a\int_0^L\left(\frac{1}{4}\frac{\ddot{\ell}}{\ell} - \frac{1}{8}\frac{\dot{\ell}^2}{\ell^2}\right)dx \tag{10-45}$$

The inverse Laplace transform of equation (10-43) is

$$q(L,t) = \frac{q_0}{2}\left[\frac{A(L)}{A(0)}\right]^{\frac{1}{2}}\left[F_{\frac{1}{2}}(t) - F_{\tau+\frac{L}{a}}(t)\right] \tag{10-46}$$

where

$$F_{\bar{\omega}}(t) = \begin{cases} 0 & 0 < t < \bar{\omega} \\ F(t-\bar{\omega}) & t > \bar{\omega} \end{cases} \tag{10-47}$$

and

$$F(\rho) = \mathcal{L}^{-1}\left\{f(s)\right\} \tag{10-48}$$

From Churchill[6]

$$\mathcal{L}^{-1}\left\{f(s)\right\} = J_0(2\sqrt{\rho s}) + \frac{a}{4}\frac{\dot{\rho}}{\rho}\Big|_{x=L}\left(\frac{s}{\rho}\right)^{1/2} J_1(2\sqrt{\rho s}) \tag{10-49}$$

where J_0 and J_1 are Bessel functions of order zero and one. For small ζ, corresponding to short pulses, the Bessel functions may be expanded in a power series and only the significant terms retained. Thus,

$$F(s) \doteq 1 - s\left(1 - \frac{a}{4}\frac{\dot{\rho}}{\rho}\Big|_{x=L}\right) \tag{10-50}$$

The quantity $\left(1 - \frac{a}{4}\frac{\dot{\rho}}{\rho}\Big|_{x=L}\right)$ in Equation (10-50) characterizes the distortion present in the pulse. Of significant interest from the viewpoint of an electrical analogue is that the distortion indicated by Equation (10-50) corresponds to the "initial slope criterion" that has been used to evaluate tapered electrical transmission lines[7,8].

With the aid of Equation (10-8), Equation (10-46) is put in terms of the volume flow $q(L, t)$, giving

$$\bar{q}(L,t) = q_0\left[\frac{A(L)}{A(0)}\right]^{\frac{1}{2}}\left[F_{\frac{L}{a}}(t) - F_{\tau+\frac{L}{a}}(t)\right] - q_0 \tag{10-51}$$

Equation (10-51) is illustrated in Figure 10-3 for $a(L) > a(0)$.

(b) Pressure

The pressure pulse p(0, t) corresponding to the valve closure may readily be found from

$$P(0,s) = Q(0,s)\, Z(0,s) \tag{10-52}$$

For $t < 2L/a$ there will be no reflections incident at $x = 0$, so $Z(0, s) = Z^{+}(0, s)$, where from Equation (10-32) with $m = +1$,

$$Z^{+}(0,s) = \sqrt{\frac{\rho}{c}}\Big|_{x=0} + \sqrt{\frac{\rho}{c}}\,\frac{1}{4\sqrt{\rho c}}\left(\frac{\dot{\rho}}{\rho} - \frac{\dot{c}}{c}\right)\Big|_{x=0}\frac{1}{s} + \cdots \tag{10-53}$$

Thus, with Equation (10-15)

$$P(0,s) \doteq \frac{g_0}{s}(1 - e^{-s\tau})\left(\frac{1}{s}\sqrt{\frac{\rho}{c}} + \frac{1}{s}\sqrt{\frac{\rho}{c}}\,\frac{1}{4\sqrt{\rho c}}\left[\frac{\dot{\rho}}{\rho} - \frac{\dot{c}}{c}\right] + \cdots\right)\Big|_{x=0} \tag{10-54}$$

Taking the inverse gives

$$P(0,t) \doteq \begin{cases} g_0\dfrac{\sqrt{K\rho_0}}{A(0)}\left(1 + \dfrac{a}{2}\dfrac{\dot{\rho}}{\rho}\Big|_{x=0} t\right) & 0 < t < \tau \\[2ex] g_0\dfrac{\sqrt{K\rho_0}}{A(0)}\left(\dfrac{a}{2}\dfrac{\dot{\rho}}{\rho}\Big|_{x=0}\tau\right) & t > \tau \end{cases} \tag{10-55}$$

At $x = L$ the pressure may be found from

$$P(L,s) = Q(L,s)\, Z(L,s) \tag{10-...}$$

$Q(L, s)$ is given by Equation (10-43) and $Z(L, s)$ by Equation (10-16), (10-17), and (10-18), resulting in

$$P(L,s) = \frac{g_0}{s}\frac{\sqrt{K\rho_0}}{A(L)}\left[\frac{A(L)}{A(0)}\right]^{1/2}\left[e^{-\frac{sL}{a}} - e^{-s\left(\tau + \frac{L}{a}\right)}\right] f(s) \tag{10-57}$$

and the inverse is

$$P(L,t) = \rho_o \left[\frac{K P_o}{A(L)A(0)}\right]^{1/2} \left[F_{\frac{L}{a}}(t) - F_{\tau+\frac{L}{a}}(t)\right] \tag{10-58}$$

The pressure at x = 0 and x = L is illustrated in Figure 10-3

10-5 Distortion

The slanted tops of $\bar{q}(L, t)$ and $p(L, t)$ in Figure 10-2 and 10-3 represent the distortion produced by the tapered section. It is generally only a small change in the pressure, and is not significant where the magnitude of the surge pressure is of prime importance. The distortion can be characterized by the slope of the pulse as given by

$$\lambda = \frac{L}{a} \frac{dF}{d\xi} \tag{10-59}$$

From Equation (10-50)

$$\lambda = -L \int_0^L \left[\frac{1}{4}\frac{\ddot{\rho}}{\rho} - \frac{1}{8}\frac{\dot{\rho}^2}{\rho^2}\right] dx + \frac{L}{4}\frac{\dot{\rho}}{\rho}\Big|_{x=L} , \tag{10-60}$$

and λ can thus be easily calculated for any taper function A(x). For example, if the taper is linear

$$A(x) = A(0)(1+bx) \tag{10-61}$$

and

$$\rho = \frac{\rho_o}{A(0)} \frac{1}{1+bx} \tag{10-62}$$

Thus

$$\lambda = -\frac{bL}{8(1+bL)}(3bL+2) \tag{10-63}$$

10-6 Attenuation of Surge Pressures

Of most importance in the design of liquid transfer lines is the maximum surge pressure that would be transmitted through the line when the flow is suddenly stopped. This would be $p(L, T/a)$, and from Equation (10-57) this is

$$P\left(L, \frac{L}{a}^{+}\right) = \rho_0 \left[\frac{K P_0}{A(L) A(0)}\right]^{1/2} \tag{10-64}$$

and is indicated in Figure 10-3.

It is particularly important to compare the pressure given by Equation (10-64) with the pressure that would be developed if the tapered section were absent and the pipe had a uniform cross-sectional area $A(L)$. For the uniform pipe

$$P_{uniform} = \rho_0 \frac{\sqrt{K P_0}}{A(L)} \tag{10-65}$$

and the ratio is thus

$$\frac{P\left(L, \frac{L}{a}^{+}\right)}{P_{uniform}} = \sqrt{\frac{A(L)}{A(0)}} \tag{10-66}$$

Equation (10-66) makes it evident that if a pipe is to be terminated by a quick-closing valve the surge pressure can be decreased by adding a tapered section that has the larger end at the valve [$A(L) < A(0)$].

It should also be noticed that if surge pressures should be estimated on the basis of a uniform cross-section pipe, the actual pressure would be greater if a valve were joined to the pipe by means of a tapered section and the smaller end were at the valve.

10-7 Discussion

The method outlined here is not adequate to describe the shape of long duration pulses, because these contain low-frequency Fourier components, for which the truncated series solutions in terms of the frequency s are not convergent[10]. However, the initial pressure for long pulses is the same as for short pulses ($T \ll L/a$), so Equation (10-66) is true for any duration of valve closure.

A minor deficiency of the method is that is does not take into account the initial Bernoulli pressure variation in the tapered section. This, however, is negligible in comparison with the surge pressures.

Much work still remains to be done. The effect of friction should be explored. Also, the shape of long pulses should be investigated as well as step changes in flow.

References

1. H. M. Paynter and F. D. Ezekiel, "Water Hammer in Nonuniform Pipes as an Example of Wave Propagation in Gradually Varying Media," Trans. ASME, Vol. 80, pp. 1585-1959 (1958).

2. F. J. Young and B. H. Young, "Impedance of Tapered Structures," The Journal of the Acoustical Society of America, Vol. 33, pp. 1206-1210 (1961).

3. H. W. Liepmann and A. Roshko, "Elements of Gasdynamics," John Wiley and Sons, Inc., New York, p. 67 (1957).

4. R. D. Walker, E. T. Kirkpatrick and W. T. Rouleau, "Viscous Dispersion in Water Hammer," Trans. ASME, Series D, Journal of Basic Engineering, Vol. 82, pp. 759-764 (1960).

5. R. Stapelfeldt, "The Short Pulse Behavior of Lossy Tapered Transmission Lines," doctoral dissertation, Carnegie Institute of Technology, Pittsburgh, Pennaylvania (1960).

6. R. V. Churchill, "Modern Operational Mathematics in Engineering," McGraw-Hill Book Company, Inc., New York (1944).

7. J. Aukel, "Engineering Problems in the Exponential Transmission Line Pulse Transformer Design," doctoral dissertation, Carnegie Institute of Technology, Pittsburgh, Pennaylvania (1953).

8. F. J. Young, E. R. Schatz and J. B. Woodford, "The Optimum Transmission-Line Pulse Transformer," AIEE, Communications and Electronics, July, 1959.

9. G. R. Rich, "Hydraulic Transients," Dover Publications, Inc., New York, (1963).

10. W. H. Skilling, "Electrical Engineering," John Wiley and Sons, Inc., New York (1957).

Nomenclature

$A(x)$	=	cross-sectional area, ft^2
a	=	velocity of wave propagation, Equation (11-42), ft/sec
b	=	slope of linear taper, ft^{-1}
b_1, b_o, b_{-1}	=	coefficients of power series, Equation (11-23)
C	=	constant
c	=	$A(x)/K$, Equation (11-14)
e	=	base of natural logarithms
$F(\zeta)$	=	inverse Laplace transform, Equation (11-48)
$F_{\bar{w}}(t)$	=	inverse Laplace transform, Equation (11-47)
f_o, f_{-1}, f_{-2}	=	coefficients of power series, Equation (11-31)
$\mathcal{J}$	=	integral defined by Equation (11-45)
J_o	=	Bessel function of order zero
J_1	=	Bessel function of order one
K	=	isothermal bulk compression modulus, lb/ft^2
L	=	length of tapered section, ft
ℓ	=	$\rho_o/A(x)$, Equation (11-13)
m	=	± 1
$P(x, s)$	=	Laplace transform of $p(x, t)$
$p(x, t)$	=	pressure; also pressure rise above initial pressure p_o, lb/ft^2
P_o	=	initial pressure, lb/ft^2
$Q(x, s)$	=	Laplace transform of $q(x, t)$
$q(x, t)$	=	$\bar{q}(x, t) + q_o$, Equation (11-8)
$\bar{q}(x, t)$	=	volume flux, ft^3/sec
q_o	=	initial volume flux, ft^3/sec
R	=	radius of pipe, ft
r	=	radial coordinate, ft

s = frequency

t = time, sec

u = x-component of velocity, ft/sec

v = r-component of velocity, ft/sec

$\vec{w}$ = fluid velocity, ft/sec

x = axial coordinate, ft

$Z(x, \cdot)$ = acoustic impedance, Equation (11-29)

$\Gamma(x, s)$ = exponent in solution for Q, Equation (11-21)

ζ = $t - \tilde{\omega}$

λ = slope of pulse, Equation (11-59)

ρ = density, slug/ft^3

ρ_o = mean density, slug/ft^3

τ = duration of valve closure, sec

$\tilde{\omega}$ = a particular value of time, sec

Superscripts

$'$ = value at $x = L$

$+$ = wave traveling in $+x$ direction. Also, a positive incremental amount added to a variable

$-$ = wave traveling in $-x$ direction

Other

$\cdot$ = $\frac{\partial}{\partial x}$

Appendix I

For convenience in developing equations (10-5) and (10-7) the line will be assumed to have a circular cross-section. Thus $A(x) = \pi R^2$, where R is the radius of the cross-section and $dA = 2\pi r dr$, where r is the radial distance.

Averaging Equation (10-4) across the cross-section gives

$$\frac{1}{A(x)} \int_0^R \frac{\partial P}{\partial x} 2\pi r dr = - \frac{\rho_0}{A(x)} \int_0^R \frac{\partial u}{\partial t} 2\pi r dr \tag{10-67}$$

Since $\rho = p(x, t)$, and $R = R(x)$, Equation (10-67) becomes

$$\frac{\partial \bar{p}}{\partial x} = - \frac{\rho_0}{A(x)} \frac{\partial \bar{q}}{\partial t} \tag{10-5}$$

Averaging Equation (10-2) across the cross-section and employing the assumption of small density changes gives

$$\frac{1}{A(x)} \int_0^R \frac{\partial u}{\partial x} 2\pi r dr + \frac{1}{A(x)} \int_0^R \frac{1}{r} \frac{\partial (rv)}{\partial r} 2\pi r dr = - \frac{1}{A(x)} \frac{1}{\rho_0} \int_0^R \frac{\partial \rho}{\partial t} 2\pi r dr \tag{10-68}$$

where v is the radial component of velocity. Carrying out the integrations yields

$$\frac{\partial \bar{q}}{\partial x} - u(R) 2\pi R \frac{dR}{dx} + 2\pi R v(R) = - \frac{A(x)}{\rho_0} \frac{\partial \rho}{\partial t} \tag{10-69}$$

since $\rho = \rho(x, t)$ from the assumption of plane flow. From Figure 10-4, which indicates conditions at the wall ($r = R$), it is evident that

$$\frac{v(R)}{u(R)} = \frac{dR}{dx} \tag{10-70}$$

Substituting this in Equation (10-69) gives

$$\frac{\partial \bar{q}}{\partial x} = - \frac{A(x)}{\rho_0} \frac{\partial \rho}{\partial t} \tag{11-71}$$

From the Equation of state (10-3),

$$\frac{\partial \rho}{\partial t} = \frac{\rho_o}{K} \frac{\partial \bar{P}}{\partial t} \tag{10-72}$$

which when substituted in Equation (10-71) yields the desired Equation (10-7).

Appendix II

For a rigid tube of uniform cross-sectional area A(L) the solutions to Equations (10-11) and (10-12) are

$$P(x,s) = A e^{-s\sqrt{\ell' c'}\, x} + B e^{s\sqrt{\ell' c'}\, x} \tag{10-73}$$

$$Q(x,s) = \sqrt{\frac{c'}{\ell'}} \left[A e^{-s\sqrt{\ell' c'}\, x} - B e^{s\sqrt{\ell' c'}\, x} \right] \tag{10-74}$$

where A and B are constants and $L \leq x < \infty$. For an infinitely long tube there will be no reflections, and B must be zero. Thus, the acoustic impedance is

$$Z(L,s) \equiv \frac{P(L,s)}{Q(L,s)} = \sqrt{\frac{\ell'}{c'}} \tag{10-75}$$

In electric transmission line theory $\sqrt{\ell'/c'}$ is known as the <u>characteristic impedance</u> Z_0.

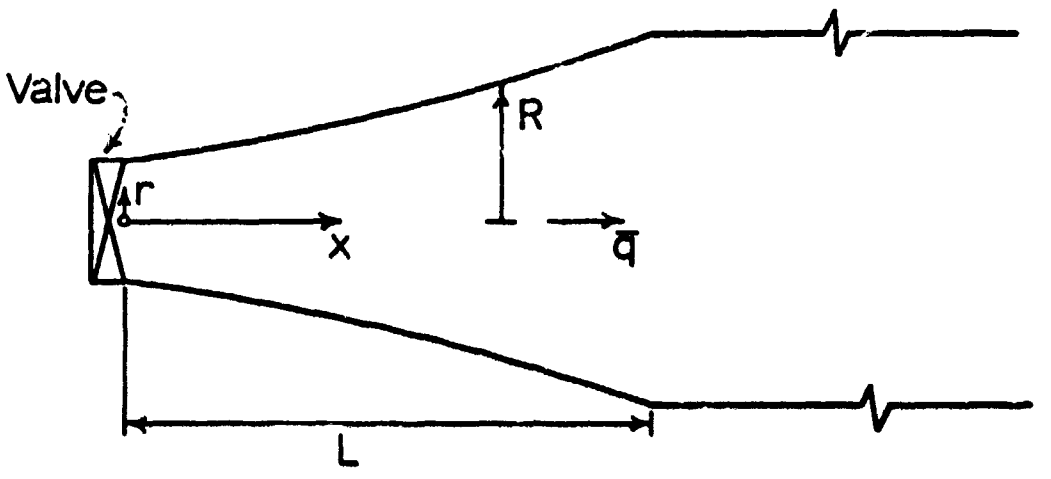

Figure 10-1. Tapered Line, Illustrating Coordinates

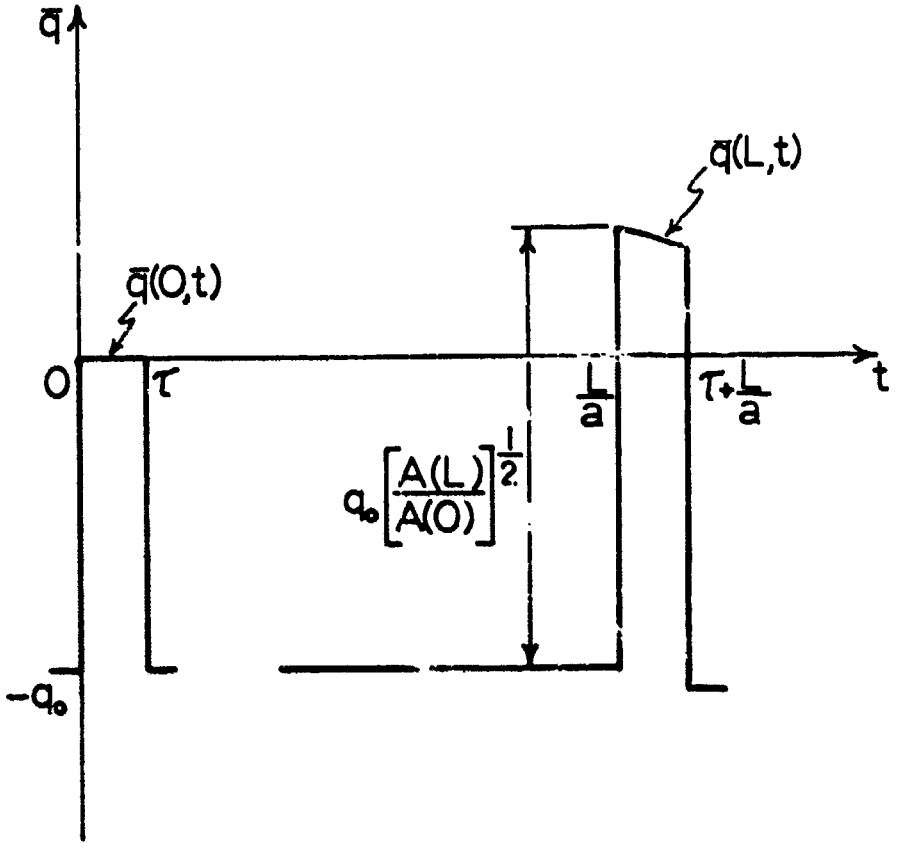

Figure 10-2. Variations of Volume Flux With Time at the Ends of the Tapered Section

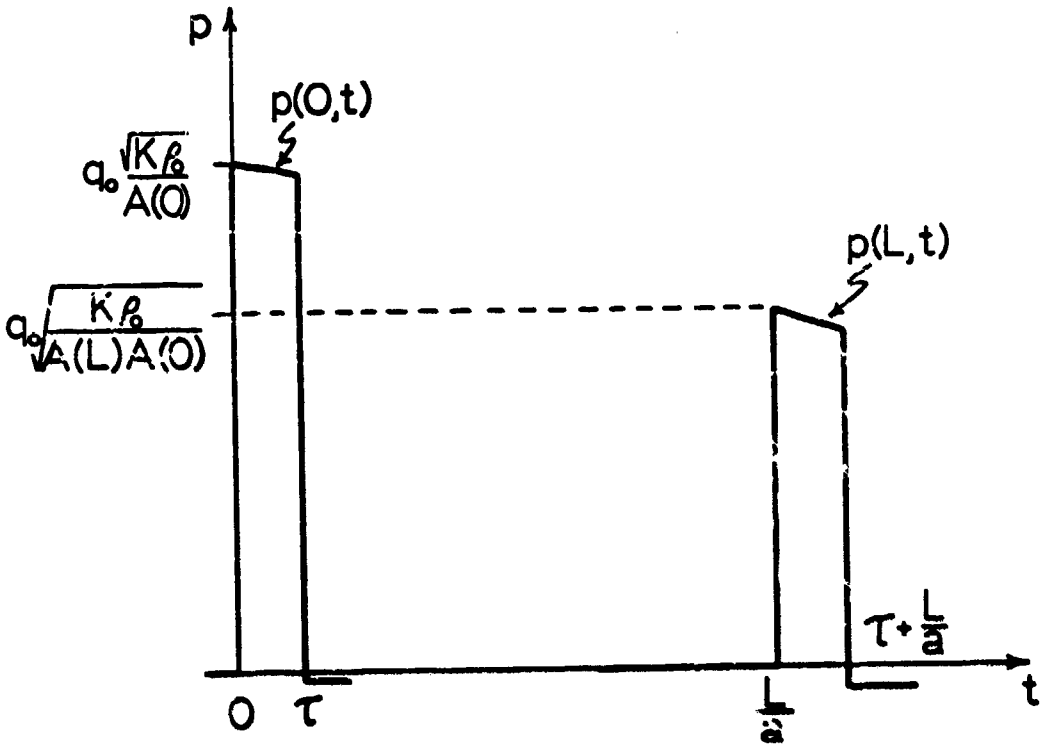

Figure 10-3. Pressure Variations at Each End of the Tapered Section

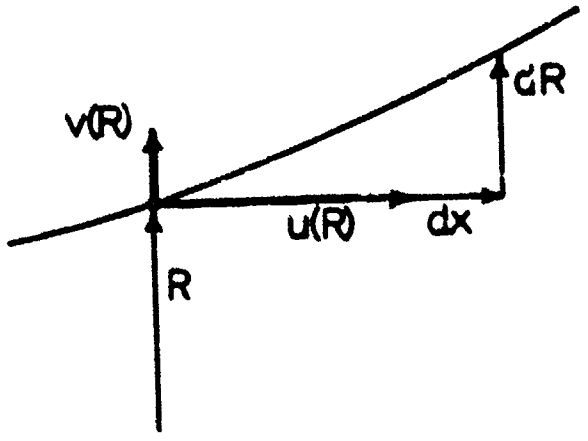

Figure 10-4. Velocity Components at the Wall of the Tapered Line